# A FGF-Hh FEEDBACK LOOP CONTROLS STEM CELL PROLIFERATION IN THE DEVELOPING LARVAL BRAIN OF *Drosophila melanogaster*

A Dissertation

by

ANDREA LYNN BARRETT

Submitted to the Office of Graduate Studies of
Texas A&M University
in partial fulfillment of the requirements for the degree of

DOCTOR OF PHILOSOPHY

December 2007

Major Subject: Biochemistry

# A FGF-Hh FEEDBACK LOOP CONTROLS STEM CELL PROLIFERATION IN THE DEVELOPING LARVAL BRAIN OF *Drosophila melanogaster*

A Dissertation

by

ANDREA LYNN BARRETT

Submitted to the Office of Graduate Studies of
Texas A&M University
in partial fulfillment of the requirements for the degree of

DOCTOR OF PHILOSOPHY

Approved by:

| | |
|---|---|
| Chair of Committee, | Sumana Datta |
| Committee Members, | Arne Lekven |
| | Vlad Panin |
| | Gregory Reinhart |
| Head of Department, | Gregory Reinhart |

December 2007

Major Subject: Biochemistry

# ABSTRACT

A FGF-Hh Feedback Loop Controls Stem Cell Proliferation in the Developing Larval Brain of *Drosophila melanogaster*.

(December 2007)

Andrea Lynn Barrett, B.S., Sam Houston State University

Chair of Advisory Committee: Dr. Sumana Datta

The adult *Drosophila* central nervous system is produced by two phases of neurogenesis: the first phase occurs during embryonic development where the larval brain is formed and the second occurs during larval development to form the adult brain. Neurogenesis in both phases is caused by the activation of neural stem cell division and subsequent progenitor cell division and terminal differentiation. Proper activation of neural stem cell division in the larval brain is essential for proper patterning and functionality of the adult central nervous system. Initiation of neural stem cell proliferation requires signaling from the Fibroblast Growth Factor (FGF) homolog Branchless (Bnl) and by the Hedgehog (Hh) growth factor. I have focused on the interactions between both of these signaling pathways with respect to post-embryonic neural stem cell proliferation using the *Drosophila* larval brain.

Using proliferation assays and quantitative real-time PCR, I have shown that Bnl and Hh signaling is inter-dependent in the 1$^{st}$ instar larval brain and activates neural

stem cell proliferation. I have also shown that overexpression of *bnl* can rescue signaling and neuroblast proliferation in a *hh* mutant. However, overexpression of *hh* does not rescue signaling or neuroblast proliferation in a *bnl* mutant, suggesting that Bnl is the signaling output of the Bnl-Hh feedback loop and that all central brain and optic lobe neural stem cells require Bnl signaling to initiated proliferation.

# DEDICATION

This dissertation is dedicated to my family, who has been an endless source of love, encouragement, and unfaltering support. To my mother, especially, without a doubt I know I could not have done this without her. You have been the best mother two daughters could ever hope for. To my sister, who has been my best friend since the moment we met and she is a true inspiration for how to be a great person. To my brother-in-law, I couldn't have asked for a better person to be in my sister's life. I have never seen her as happy as she is now. All of you are such an important part of my life and I am the person I am today because of you. I could not have asked for a better group of people to call my family. I love you.

# ACKNOWLEDGEMENTS

Most importantly, I am in deep gratitude to Dr. Sumana Datta. I am certain that my life would be completely different if I had not joined her lab as a graduate student. She has been a source of encouragement and support in more ways than can be measured. I thank my committee, Dr. Arne Lekven, Dr. Vlad Panin, and Dr. Gregory Reinhart, for their advice and guidance throughout my graduate career. I want to thank all members of the Datta lab who have made it a great environment in which to work the past 4 years, especially, Anita Hernandez, for her friendship and endless supplies of laughter. Lastly, I want to thank all of my friends, especially Dr. Carrie Langlais and Dr. Michelle Heacock, in the graduate program who have made this experience better than I could have ever imagined.

# TABLE OF CONTENTS

CHAPTER Page

# LIST OF FIGURES

FIGURE Page

# LIST OF TABLES

# CHAPTER I

# INTRODUCTION

For the proper development of any organism, genetic and morphological events must be spatially and temporally regulated. The organism relies heavily on proper gene expression and function to coordinate cells that will eventually generate specific tissues and organs of the body. After development, these same communication processes are needed for maintenance of areas by replacement/repair of cells in tissues or organs that no longer function properly due to injury or mortality. However, strict regulation is needed to prevent aberrant cell growth, which could lead to loss of tissue/organ function or diseases such as cancer. Therefore the study of fundamental signaling molecules and their downstream signaling pathways is paramount to understanding the processes undertaken during development, homeostasis, and repair of an organism. The study of the regulation of stem cell proliferation in development is a key area of research where basic scientific knowledge gained using lower order model organisms can transcend the genomic complexity gap and significantly contribute to overall understanding of stem cell control.

Over the last few decades, the area of stem cell research has garnered a great deal of attention. Many researchers believe that stem cells hold the key to regenerative medicine and cancer therapies. Elucidating the mechanisms that regulate stem cell

---

This dissertation follows the style and format of Developmental Biology.

growth and differentiation into wanted cell types would revolutionize the medical community. The potentials for the use of stem cell directed treatments of diseases like diabetes, Parkinson's disease, and Rheumatoid Arthritis are high and growing exponentially.

In this dissertation, I examine the interactions between specific signaling molecules required for neural stem cell proliferation in Drosophila melanogaster and the significant contribution this study makes to overall understanding of stem cell proliferation control in the central nervous system.

**STEM CELLS**

Over the years, the definition of a stem cell has evolved to encompass specific defining features that include the capacity to self-renew and generate cell lineages that differentiate into a wide variety of cell types. It is still not yet known how stem cells are controlled, how many different types there are, and where they are located in the body. There are three basic types of stem cells that make up the human body: germinal, embryonic, and adult stem cells (Bongso and Richards, 2004). Germinal stem cells give rise to gametes in the human adult reproductive system, i.e. sperm and eggs. Embryonic stem cells are the precursors of all human adult cells and are derived from the inner cell mass of an embryo in the blastocyst stage (Fallon et al., 2000; Stojkovic et al., 2004). Adult stem cells in humans are located in most tissues and are responsible for regenerating those tissues over time or upon injury (Lim et al., 2007; Serakinci and

Keith, 2006). Each of these stem cell categories has varying potentials with regards to proliferation and plasticity/differentiation potential. Stem cells divide in two fashions: symmetrically, where both daughter cells become stem cells or asymmetrically, where one of the daughter cells remains a stem cell and the other daughter begins the process of determination and adopts a different fate (Figure 1.1) (Maric et al., 2007). The differentiation potential of stem cells can be broadly characterized as totipotent, pluripotent, or multipotent. The only stem cells considered to be truly totipotent are the germ line stem cells which have the capacity to generate any cell in the body. Pluripotent stem cells are unable to generate all types of cells in the body but have the capacity to become most cells in the body. Embryonic stem cells, the cells that make up the inner cell mass of the embryo at blastula stage, are considered to be pluripotent. The multipotent stem cell is more restricted in the types of cells it is able to generate but still retains the ability to generate several different types of cell. Adult stem cells are for the most part considered multipotent stem cells (Serafini and Verfaillie, 2006; Shi et al., 2007; Stojkovic et al., 2004).

*Adult stem cells*

Embryonic stem cells present an exciting avenue for cancer therapeutics and regenerative medicine, however they possess several issues, i.e. moral and immunological, that makes their use problematic. Therefore, adult stem cells pose as an attractive alternative to embryonic stem cell research. Adult stem cells were first

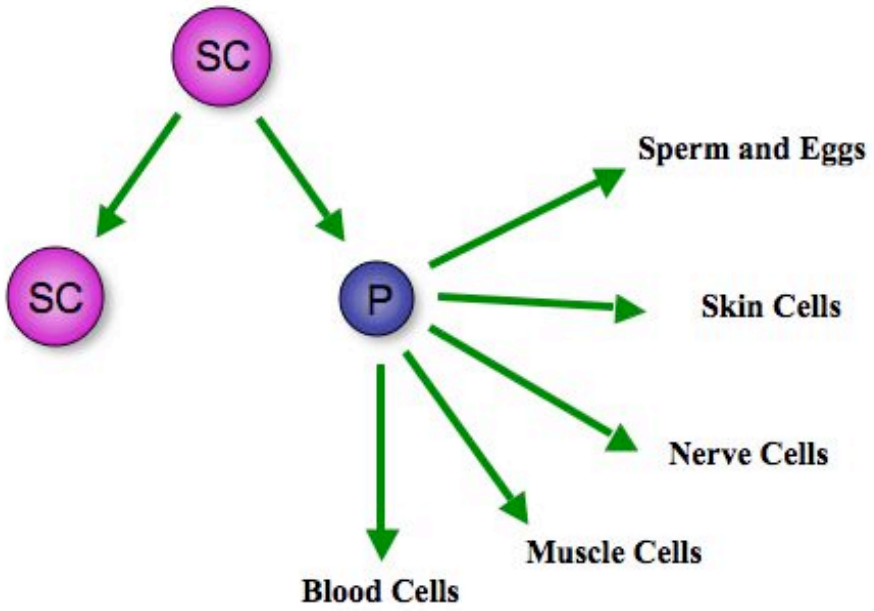


**Figure 1.1. Asymmetric stem cell division.** A stem cell divides asymmetrically generating two daughter cells. One daughter cell is a new stem cell that replenishes the original pool of stem cells and the other daughter cell is a progenitor cell that has the potential to eventually generate any type of terminally differentiated cell in the body.

described in organs with high cell turnover, i.e. blood, skin, and gut (Metcalf, 1993). However, reports have shown that they can also be found in organs without high cell turnover like the central nervous system and heart. Thus far, stem cells have been identified in many organs/tissues and include: hematopoietic stem cells (the best studied to date), neural stem cells, epidermal stem cells, skeletal muscle stem cells, and mesenchymal stem cells.

*Vertebrate neural stem cells*

It was thought for some time that the adult brain was non-neurogenic and was completely formed at the end of embryogenesis. However, it was quickly discovered that several areas of the vertebrate brain contain mitotically active cells. These mitotically active cells were later determined to be neural stem/progenitor cells. To date the most well characterized areas are the subventricular zone (SVZ) of the lateral ventricle and the subgranular zone (SGZ) of the dentate gyrus within the hippocampus (Gage et al., 1995; Reynolds and Weiss, 1992; Vescovi et al., 1993). Both areas contain a subpopulation of cells that are mitotically quiescent but have the capacity to proliferate asymmetrically to generate new progenitor cells that can migrate and differentiate into neuronal/glial cells upon the right stimulation. Other areas of the vertebrate brain, like the cerebellum, striatum, tectum, and the neocortex all contain identifiable neural stem cells. Interestingly, the spinal cord, originally thought to be strictly non-neurogenic, has recently been identified as a neurogenic region of the CNS, albeit at very low levels (Weiss et al., 1996).

In the next chapter section, I will discuss in more detail the events that occur during vertebrate and insect neurogenesis and provide some insight into the potential mechanisms of stem cell generation and control.

## CENTRAL NERVOUS SYSTEM DEVELOPMENT

The central nervous system (CNS) is a very complex structure that is required for proper development of higher multicellular organisms and coordinates essential functions that include sensory mechanisms, movement, and cognition. Therefore, study of the molecular and morphological components required for proper development and function of the central nervous system is an area that has been highly investigated. In this chapter section, the development of the vertebrate central nervous system in *Mus musculus* and the insect central nervous system in *Drosophila melanogaster* will be addressed and a comparative analysis will be given.

### *Vertebrate neurogenesis*

The development of the vertebrate adult central nervous system occurs mostly during the development of the embryo with only a small fraction of neurogenesis occurring during adult life. Neurogenesis begins in the embryo shortly after gastrulation, an early phase of embryogenesis where morphology of the embryo is dramatically restructured by cell migration. One of the first steps in neurogenesis occurs with induction of neural tube formation, a process called neurulation. Along the dorsal surface of the embryo the prospective neuroectoderm is induced by the notochord, a

structure derived earlier from the mesoderm, to thicken and flatten into a structure called the neural plate. The neural plate begins to invaginate at the midline of the neural tube. The neural plate will then begin to round up, detach from adjacent epidermal cells, and form the neural tube, which eventually gives rise to the adult brain and spinal cord (Arendt and Nubler-Jung, 1999; Ford-Perriss et al., 2001; Geldmacher-Voss et al., 2003). During these morphological changes, specification of the neuroectoderm is occurring through specific regional expression of proneural and neurogenic genes. The neuroectoderm is subdivided into three columns on each side of the midline by the columnar genes *nkx 2.2*, *genomic screen homeobox (gsh)*, and *msx*. Expression of these genes gives rise to the medial, intermediate, and lateral regions, respectively. The medial region generates motoneurons and interneurons, while the intermediate region generates only interneurons. The lateral region generates the neural crest where sensory neurons are located (Arendt and Nubler-Jung, 1999; Cornell and Ohlen, 2000). In conjunction with the columnar genes, transcription factors encoded by the *neurogenin* and *atonal* genes establish proneural clusters. Through a process called lateral inhibition, Delta-Notch signaling within the proneural cluster will induce differentiation and segregation of neural stem cells from the rest of the cells within the cluster (Arendt and Nubler-Jung, 1999).

The neural tube is divided into three main layers. The ventricular zone (VZ; adjacent to lumen of the neural tube), contains neural stem cells, called germinal cells, that divide asymmetrically giving rise to undifferentiated neuronal progeny that transiently populate the middle subventricular zone (SVZ). The mantel layer/marginal

zone (MZ; adjacent to body cavity) contains differentiating neurons and axonal outgrowth. Before neural tube closure, the CNS is subdivided along the anterior-posterior axis into four distinct domains: forebrain, midbrain, hindbrain, and spinal cord. As neurogenesis progresses, a series of swellings and constrictions form as the wall of the neural tube grows at the fore-, mid-, and hindbrain regions, which give rise to the adult brain structure. Most cells in the brain and spinal cord continue to actively proliferate throughout embryogenesis but this is limited to the ventricular and subventricular zones (Arendt and Nubler-Jung, 1999; Cayuso and Marti, 2005; Dono, 2003; Ford-Perriss et al., 2001).

For many years it was thought that neurogenesis stopped after embryogenesis. However, this hypothesis was discarded when proliferating cells were identified in regions of the adult brain. To date, neurogenic regions have been identified in two areas of the adult brain, the lateral ventricle and the dentate gyrus within the hippocampus (Cayuso and Marti, 2005; Temple and Alvarez-Buylla, 1999) (Figure 1.2). Other areas in the brain including the neocortex, tectum, striatum, and even the spinal cord have also been shown to have post-natal proliferation, albeit at low levels (Cayuso and Marti, 2005; Dahmane and Ruiz i Altaba, 1999; Dahmane et al., 2001; Dono, 2003; Palma et al., 2005; Stecca and Ruiz i Altaba, 2005; Temple and Alvarez-Buylla, 1999; von Bohlen Und Halbach, 2007). A large amount of work has been published on the subventricular zone (SVZ) of the lateral ventricle and the subgranular zone (SGZ) of the dentate gyrus, both of which show sustained neurogenesis in the adult.

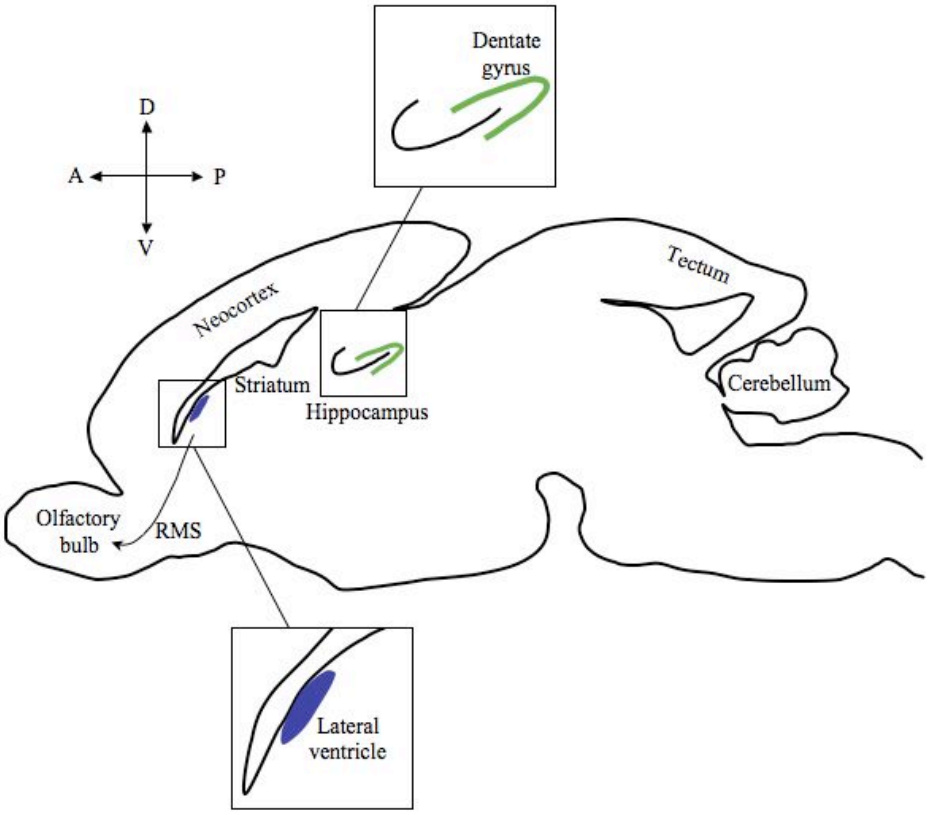


**Figure 1.2. Areas of neurogenesis in the adult mouse brain.** A sagital view of the adult mouse brain with areas of neurogenesis labeled. Two main areas of neurogenesis are the dentate gyrus (in green) of the hippocampus, shown in greater detail in box A, and the subventricular zone (SGZ) of the lateral ventricle (in blue), shown in greater detail in box B. Other areas of neurogenesis, albeit at low levels, are the neocortex, striatum, Tectum, and cerebellum. RMS, rostral migratory system utilized for migration of new neurons to the olfactory bulb from the SVZ.

The SVZ is the region of the adult brain that continually generates new neurons bound for the olfactory bulb and is composed of four basic types of cells: astrocytes, immature precursors, migrating neuroblasts, and ependymal cells (Doetsch et al., 1999; Temple, 1999). Through *in vitro* and *in vivo* studies, it has been shown that astrocytes are neural stem cells that divide asymmetrically to generate immature precursor cells. These precursor cells then give rise to neuroblasts that migrate along the rostral migratory system (RMS) to integrate into the olfactory bulb and differentiate into interneurons (Ahn and Joyner, 2005; Alvarez-Buylla et al., 2002).

The SGZ is a region of the adult brain that generates new interneurons in the hippocampus, which is believed to play a role in memory. Neurogenesis in the dentate gyrus is occurs in five stages. First, neural progenitor cells begin to proliferate, which then allows transient amplifying cells to differentiate into immature neurons. The immature neurons begin to migrate at short distance into the granule cell layer in the dentate gyrus, where it will send dendrites and axonal projections to establish synaptic contacts (von Bohlen Und Halbach, 2007). Study of several neurogenic regions of the vertebrate brain have helped catapult the understanding of the mechanisms utilized in signaling to endogenous neural stem cells.

*Regulation of neural stem cell proliferation in vertebrate nervous system*

Several signaling molecules have been shown to regulate the proliferation of neural stem cells in the vertebrate brain. The signaling molecule, Sonic Hedgehog (Shh), is expressed by Pürkinje cells in the subventricular zone (SVZ). *In vitro*

experiments which exogenous Shh is added to SVZ cultures cells show not only that Shh stimulates overall proliferation but also stimulates an increase in neural stem cell numbers and resulting neuron populations (Palma et al., 2005). In contrast, when Shh signaling is hindered, SVZ cells proliferation decreases. Currently, it was unclear which cells in the SVZ were the Shh receiving cells. However, *in vivo* experiments where neural stem cells in the SVZ and SGZ were labeled at early post-natal time points and their responsiveness followed through long-term fate mapping. Theses studies revealed that neural stem cells in both regions could respond to Shh signaling and can produce multiple lineages of cells for up to one year (Ahn and Joyner, 2005; Palma et al., 2005).

The ultimate goal in studying the mechanisms that control central nervous system development and regulation/maintenance is to be able to manipulate endogenous cells/tissue to either generate more of a specific cell/tissue for the purpose of regeneration or hinder the growth and propagation of disease/damaged tissue. The mammalian vertebrate is a great model system for studying these processes. However, the complexities inherent in a more evolutionarily sophisticated organism make dissecting the inner workings of these processes very difficult. In the next chapter section, I will discuss neurogenesis events in *Drosophila melanogaster* that are similar to those seen in mammals. My research shows that a less complex organism can answer the same basic mechanistic questions about regulation of post-embryonic neural stem cell proliferation.

*Drosophila melanogaster neurogenesis*

The *Drosophila* model system is a very powerful experimental paradigm that is widely utilized. The relatively small size (180 Mb) of the *Drosophila* genome reflects a smaller degree of genetic redundancy than is found in mammals. For example, three FGF like molecules have been identified in *Drosophila* versus 22 in mammalian systems (Gryzik and Muller, 2004; Stathopoulos et al., 2004; Sutherland et al., 1996; Tsang and Dawid, 2004).The extensive knowledge of *Drosophila* biology, development, and the availability of numerous mutants make it an excellent system for the study of signaling pathways and their regulation of neural stem cell proliferation. The relatively short life cycle, marked by distinct morphological stages, allows for quick and efficient experimental analysis.

In comparing development of the central nervous system (CNS) of mammals and *Drosophila*, there are some obvious differences. First, the vertebrate CNS develops on the dorsal side of the embryo while the CNS of *Drosophila* develops on the ventral side. Secondly, a neural tube does not develop in invertebrates. Thirdly, the adult *Drosophila* CNS develops through two temporally regulated neurogenesis phases, embryonic and postembryonic. During embryogenesis, generation of what will become the larval CNS occurs. However, only approximately 10% of cells generated during embryogenesis will become apart of the adult CNS structure. The other 90% is generated during larval and pupal stages (Maurange and Gould, 2005; Truman and Bate, 1988). This is in contrast to development of the adult vertebrate CNS that is almost 100% established upon completion of embryogenesis.

However, there are many striking similarities between vertebrate and invertebrate CNS development. During the *Drosophila* embryonic phase of neurogenesis, expression of vertebrate homologs of the columnar genes (i.e. *ventral nervous system defective* (*vnd*), *intermediate neuroblast defective* (*ind*), and *muscle segment homeobox* (*msh*)) working in concert with segment polarity genes (i.e. *engrailed* (*en*)*, wingless* (*wg*)*, hedgehog* (*hh*)*, and gooseberry-distal* (*gsb-d*)) to divide the ventral and procephalic neuroectoderm into 'neural equivalence groups' (Figure 1.3A). The neural equivalence group consists of five to seven neuroectodermal cells, of which only one will eventually adopt a neuroblast fate (Doe, 1992; Doe, 1996; Egger et al., 2007b; Urbach et al., 2003). The specification of a neuroblast from the equivalence group is first determined by the level of expression of the *achaete-scute (ac/sc)* complex, similar to *neurogenin* and *atonal* in mammals. All cells in the equivalence groups express the *ac/sc* complex, however, the cell that expresses the highest level will begin to adopt a neuroblast fate (Egger et al., 2007b). Neuroblast fate determination occurs through a process called lateral inhibition, where expression of the transmembrane ligand Delta by the presumptive neuroblast causes activation of the Notch receptor in adjacent cells. The activation of the Notch signaling pathway down-regulates expression of proneural genes, effectively blocking those cells from adopting a neuroblast fate, and forcing them to adopt an epidermal fate (Figure 1.3C). Morphological differentiation then occurs when the newly specified neuroblast enlarges and delaminates dorsally in the embryo. After delamination, the neuroblast then begins to divide asymmetrically along the apico-basal axis in a stem cell-like fashion to generate two daughter cells, one being a new

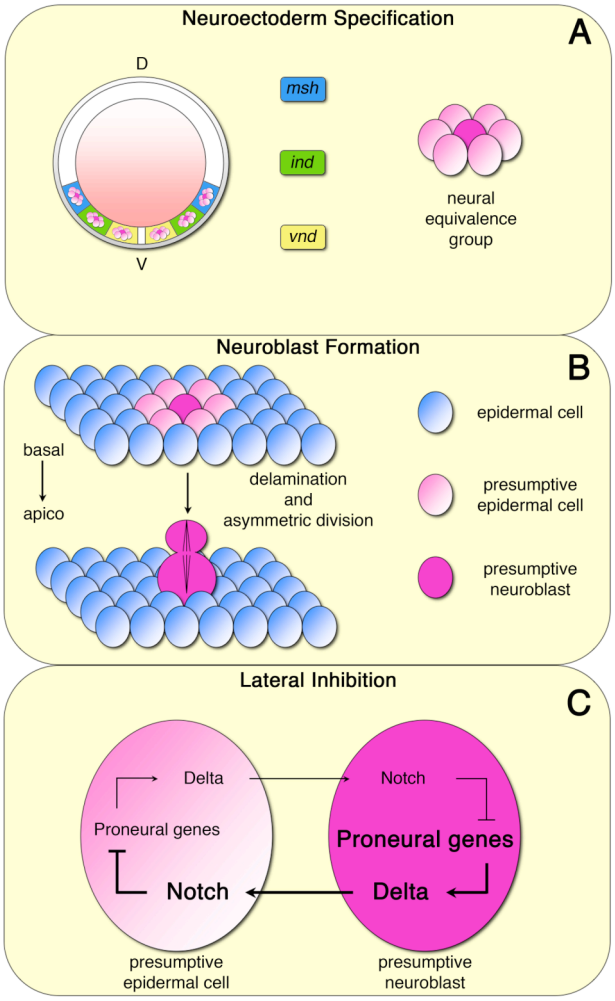


**Figure 1.3. Steps of embryonic neurogenesis in *Drosophila*.** (A) Specification of the neuroectoderm by expression of *ventral nervous system defective* (*vnd*), *intermediate neuroblast defective* (*ind*), and *muscle segment homeobox* (*msh*) in columns parallel and bisymmetrical to the midline along with expression of other genes generates "neural equivalence groups" in a repeated segmental pattern. (B) Formation of the neuroblast occurs when the presumptive neuroblast cell begins to delaminate from the neuroectoderm in the basal direction and begins asymmetric division to generate a progenitor cell that will give rise to two neurons/glia. (C) Schematic of lateral inhibition between a presumptive neuroblast and a presumptive epidermal cell. Where the neuroblast expresses *delta* at a higher level than the epidermal cell, therefore activating the Notch receptor causing an inhibition of proneural gene expression. This process effectively tells the presumptive epidermal cell to not because a neuroblast and adopt the epidermal cell fate.

neuroblast and the other a ganglion mother cell (GMC) (Figure 1.3B). The GMC will then divide symmetrically to generate two progenitor cells that will differentiate into neurons and/or glial cells (Doe, 1996; Hartenstein et al., 1987; Prokop and Technau, 1991). This will generate the central brain (CB), thoracic (Th), and abdominal (Ab) neuroblasts of the CNS. The optic lobe region of the brain, which generates the optic lobe (OL) neuroblasts, derives from an embryonic optic placode that is located dorsolaterally behind the developing brain. Not until all of the neuroblasts in the rest of the CNS are formed (embryonic stage 11) does the optic placode invaginate and fuse to the basal surface of the brain hemisphere (Ebens et al., 1993; Egger et al., 2007a; Green et al., 1993; Hartenstein, 1993). All neuroblasts continue to asymmetrically divide, except for the OL neuroblasts, which divide symmetrically, throughout embryogenesis to generate the larval nervous system. However, in late embryogenesis all but ten neuroblasts, the mushroom body (MB) and ventral lateral (VL) neuroblasts, enter into a state of quiescence until later larval stages (Prokop and Technau, 1991; Truman and Bate, 1988).

The postembryonic phase of neurogenesis begin during the 1$^{st}$ instar larval stage and ends during pupal stage (Ito and Hotta, 1991). For the formation of the adult CNS, resurrection of neuroblast proliferation and asymmetric division is needed to generate the bulk of neuronal cells that encompass the CNS. The reactivation of neuroblast proliferation occurs in a distinct temporal and spatial pattern (Figure 1.4). The first subpopulation of neuroblasts to exit a state of quiescence and begin proliferation and asymmetric division in a stem cell like fashion are the CB neuroblasts during the late 1$^{st}$

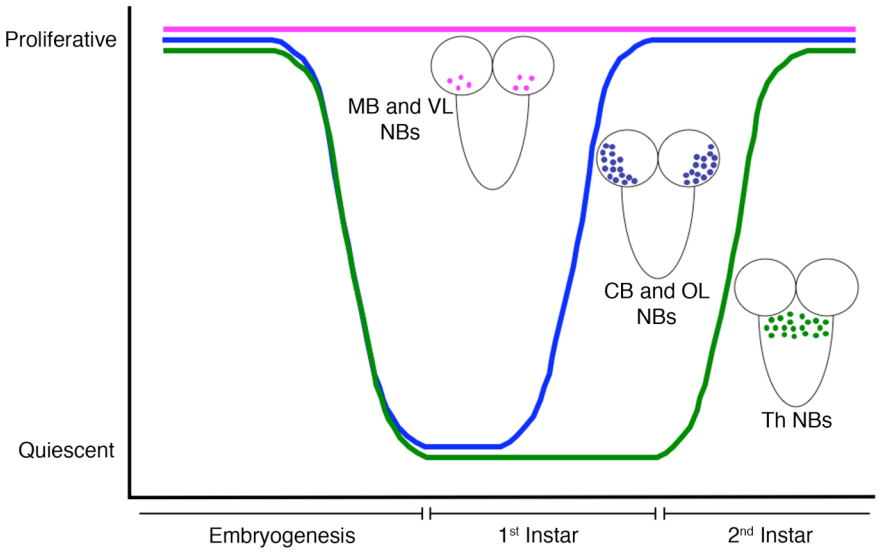


**Figure 1.4. Post-embryonic neuroblast proliferation is spatially and temporally regulated.** Neuroblasts in the larva can be subdivided into 3 main groups based on their temporal reactivation of proliferation. The mushroom body (MB) and ventral lateral (VL) neuroblasts (in pink) remain proliferative throughout embryonic and larval life. The optic lobe (OL) and central brain (CB) neuroblasts (in blue) exit quiescence at mid 1st instar. The thoracic (Th) neuroblasts (in green) exit quiescence at early 2nd instar.

instar larval stage. The next subpopulation of neuroblasts to enter into a proliferative state is the OL neuroblasts. The last subpopulation to exit quiescence are the thoracic neuroblasts, which begin division during the early 2nd instar larval stage. Most of the research done in neural development of *Drosophila* involved investigating neuroblast formation and identification in the ventral and procephalic neuroectoderm region of the CNS. Therefore, little information is known about OL neuroblast formation. It has been reported that the cells in the optic lobe are neuroblasts that divide symmetrically, then later switch to asymmetric division during late 2nd instar. These neuroblasts separate into the inner proliferative center (IPC) and outer proliferative center (OPC) which develops into structures of the adult visual system (Ebens et al., 1993; Egger et al., 2007a; Hofbauer and Campos-Ortega, 1990). However, recently it was shown that the symmetrically dividing cells are neuroepithelial cells that eventually give rise to neuroblasts that will divide asymmetrically (Egger et al., 2007a). The transition from a quiescent to dividing neuroblast in the unique *Drosophila* larval CNS results in an attractive model to study regulation of neural stem cells.

*Regulation of Neuroblast proliferation in Drosophila melanogaster*

Multiple genes have been shown to regulate the re-activation of neuroblast proliferation in the larval CNS, most through the control of the G1-S transition of the cell cycle (Figure 1.5). *terribly reduced optic lobes* (*trol*) is a gene that was initially identified in a screen for abnormal morphology of the larval brain lobe and encodes the Drosophila Perlecan, a heparan sulfate proteoglycan

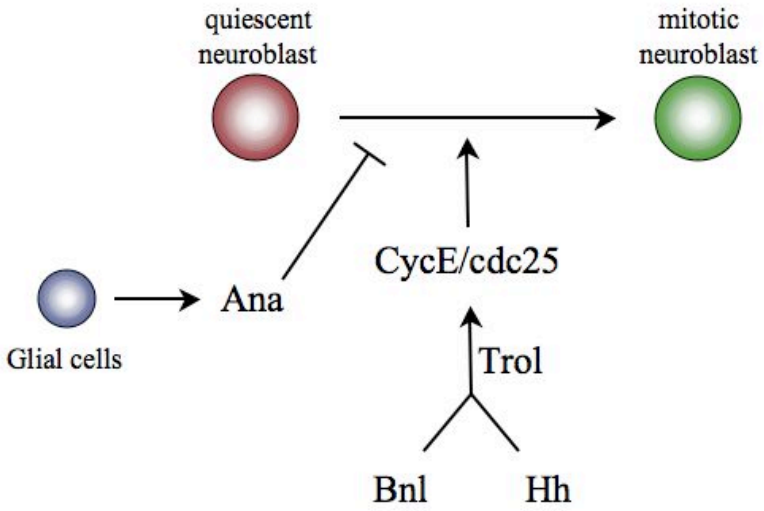


**Figure 1.5. Genes shown to genetically interact in regulation of neuroblast proliferation during larval neurogenesis in *Drosophila*.**

(Datta and Kankel, 1992; Voigt et al., 2002). In *trol* loss-of-function mutants, reactivation of neuroblast proliferation is severely hindered. Proliferation of the OL, CB, and most notably the Th neuroblasts are affected (Datta, 1995). The neuroblast proliferation defect can be rescued by ectopic expression of cyclin E, not cyclin B, suggesting that the neuroblasts are arrested in the G1 phase of the cell cycle. Over expression of *string* (*stg*), which encodes *Drosophila* Cdc25, also rescues the neuroblast proliferation defect in *trol* loss-of-function mutants, strengthening the argument that the neuroblast are G1 arrested (Caldwell and Datta, 1998; Park et al., 2003a). In contrast, *anachronism* (*ana*) loss-of-function mutants show an increase in neuroblast reactivation. This suggests that *ana*, which encodes a glycoprotein that is secreted from neighboring glial cells, is required for maintenance of quiescence (Ebens et al., 1993). Analysis of the *trol/ana* double mutant shows *ana* as epistatic to *trol*; suggesting that Trol is most likely required to repress Ana function or bypass its repressive effect on the cell cycle (Datta, 1995).

It has been widely discussed that components of the extracellular matrix of a cell can interact with other external signaling molecules (i.e. growth factors, receptors). Two genes, *hedgehog* (*hh*) and *branchless* (*bnl*), have been shown the genetically enhance the neuroblast proliferation phenotype in a *trol* mutant background. Through co-immunoprecipitaton studies, it was shown that FGF-2 (human homolog of Branchless) and Hh physically interact with Trol (Park et al., 2003b). This suggests that Hh and Bnl regulate the onset of neuroblast proliferation and their signal is mediated through Trol.

In this section I have given a thorough analysis of development of the central nervous system in both vertebrates and invertebrates. I have discussed the similarities in gene function with regards to regulation of neural stem cell proliferation. I am interested in gaining a better grasp of the mechanism/s utilized by these signaling molecules in regulating neural stem cell proliferation in Drosophila. More specifically, I am interested in understanding the interaction between the Hedgehog and Branchless signaling pathways and how together, they regulate neural stem cell division.

## FIBROBLAST GROWTH FACTOR SIGNALING PATHWAY

The development and complex patterning of the embryo is specified and regulated by a host of different signaling factors. The fibroblast growth factor (FGF) signaling pathway is one of the major signaling pathways that have been shown to be key to several processes during embryonic development. The different processes range from mesoderm induction and tracheal development to limb formation and neural development. The FGF signaling pathway has also been implicated in post embryonic homeostasis, i.e. wound healing, angiogenesis, tumor development and progression (Bottcher and Niehrs, 2005; Powers et al., 2000; Sutherland et al., 1996; Venkataraman et al., 1999).

The FGF ligand is a member of a large family of polypeptide growth factors that have been identified in organisms from nematodes to humans (Ornitz and Itoh, 2001; Thisse and Thisse, 2005). The first FGF molecule, FGF-2 (basic FGF), was identified by Hugo Armelin in 1973 as a mitogen that could stimulate growth in mouse NIH3T3

fibroblasts. To date, 22 FGF family members (FGF1-23) have been identified in mouse and humans. They range from 17 to 34 kDa in molecular weight and share 13-71% amino acid identity. Only three FGFs, Branchless (Bnl), Pyramus (Pyr), and Thisbe (Ths), have been identified in *Drosophila* and are considerably higher in molecular weight, i.e. ~80kDa (Bottcher and Niehrs, 2005; Groth and Lardelli, 2002; Gryzik and Muller, 2004; Ornitz, 2000; Ornitz and Itoh, 2001; Stathopoulos et al., 2004; Sutherland et al., 1996; Thisse and Thisse, 2005). The general FGF protein structure has four domains that include a signal peptide, an amino-terminus, a 120 amino acid highly conserved core region, and a carboxy-terminus (Figure 1.6A). The core region has been shown to be the region for binding to the fibroblast growth factor receptor (FGFR) and heparan sulfate proteoglycans (HSPGs), which are required for receptor activation (Kan et al., 1993; Ornitz, 2000; Venkataraman et al., 1999).

The FGF receptor is a transmembrane protein that is a member of the receptor tyrosine kinase superfamily (RTK) and is structurally composed of three Ig domains, a heparan-binding domain, and a tyrosine kinase domain (Figure 1.6B). The vertebrate FGFs signal through one of four FGF receptors, whereas *Drosophila* FGFs signal through one of only two FGF receptors, i.e. Breathless (Btl) and Heartless (Htl). Activation of the FGF receptor induces signaling through several pathways, which include the phospholipase C gamma (PLC-γ) pathway, phosphatidylinositol-3 kinase (PI3K)/AKT pathway, and the main signaling cascade, the Ras/mitogen activated protein kinase (Ras/MAP kinase) pathway (Bottcher and Niehrs, 2005; Sutherland et al., 1996; Tsang and Dawid, 2004) (Figure 1.7). The PLC-γ pathway involves PLC-γ binding to a

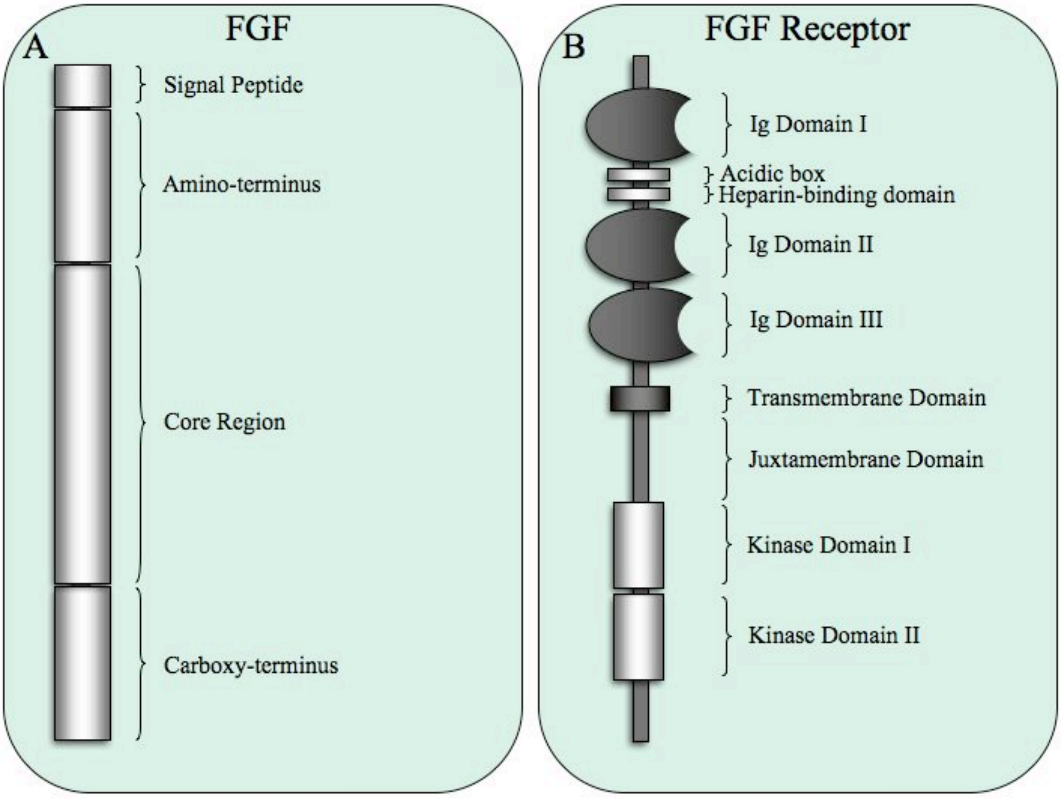


**Figure 1.6. Domain structures of FGF and the FGF Receptor.** (A) FGF contains 4 main domains: signal peptide, amino-terminal domain, core domain for FGFR and heparan sulfate proteoglycan (HSPG) binding, and a carboxy-terminal domain. (B) The FGF Receptor contains 3 Ig domains, alternative splicing of the 3rd Ig domain gives receptor specificity to different FGFs. The acidic box binds bivalent cations and is required for optimal HSPG binding. The heparin-binding domain interacts with the extracellular matrix (ECM). The transmembrane domain maintains conformation for ligand dependent activation. The juxtamembrane domain is required for binding to FRS2. Both kinase domains are the catalytically active portion of the receptor and bind adaptor proteins when activated (Bottcher and Niehrs, 2005).

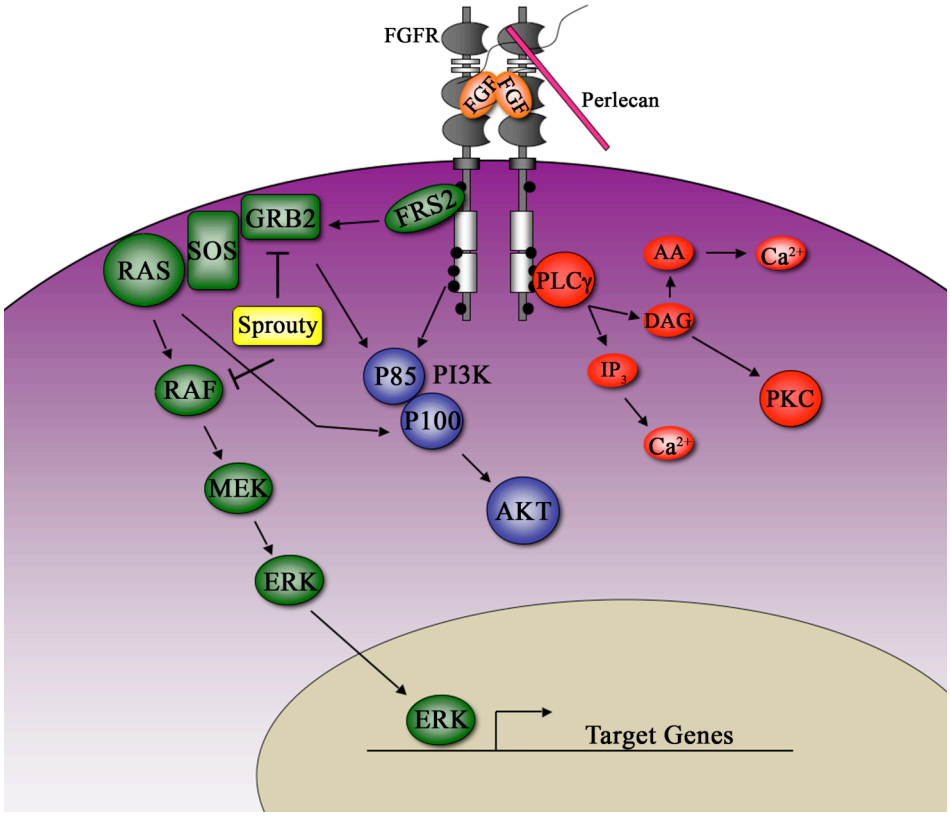


**Figure 1.7. The Fibroblast Growth Factor signaling pathway.** Activation of 3 signaling pathways can occur upon receptor activation. The RAS/MAP Kinase pathway (in green) is main signaling pathway. The other two signaling pathways are the PI3 Kinase/AKT pathway (in blue) and the PLCγ/Ca2+ pathway (in red).

phosphorylated tyrosine on the FGF receptor, where activation causes hydrolysis of phosphoatidylinositol-4,5-diphosphate ($PIP_2$) into inositol-1,4,5-triphosphate ($IP_3$) and diacylglycerol (DAG). $IP_3$ and DAG activate protein kinase C (PKC) and release of $Ca^{2+}$, respectively, which has been implicated in axonal growth in vertebrates. The PI3K/AKT pathway can be activated by several methods, which involve two components of the Ras/MAP Kinase pathway, Grb2 and Ras, which phosphorylates the p85 or p110 subunits of PI3K, respectively. The other method is FGF receptor activation of the p85 subunit. This pathway has been shown to work parallel to the Ras/MAP kinase pathway in mesoderm induction (Bottcher and Niehrs, 2005). The Ras/MAP kinase pathway involves binding and phosphorylation of FGF receptor substrate 2 (FRS2), which recruits the adaptor protein growth factor receptor-bound protein-2 (Grb2) and forms a complex with Son of sevenless (SOS), a guanine nucleotide exchange factor. SOS then activates Ras by GTP exchange and initiates the MAP kinase signaling cascade (Bottcher and Niehrs, 2005; Groth and Lardelli, 2002; Tsang and Dawid, 2004).

## HEDGEHOG SIGNALING PATHWAY

The Hedgehog (Hh) signaling pathway is an essential signaling pathway involved in cell growth, tissue patterning, and cell differentiation during embryonic development. The Hedgehog pathway retains its signaling capacity throughout adult life and in addition to developmental roles been shown to be involved in tissue homeostasis. More recently, the misregulation of Hedgehog signaling has been implicated in a variety

of cancers, including basal cell carcinomas (BCC), medulloblastoma, prostate cancer (PCa), pancreatic cancer, small-cell lung cancer, and breast cancer (Kubo et al., 2004; Lau et al., 2006; Oliver et al., 2005; Shaw and Bushman, 2007; Thayer et al., 2003; Watkins et al., 2003).

The *hedgehog (hh)* gene was first discovered in *Drosophila* in a classic genetic screen looking for defects in segmental patterning (Nusslein-Volhard and Wieschaus, 1980). The *Drosophila hh* gene encodes for a ~ 46 kDa full-length precursor protein that undergoes posttranslational modifications. First, the C-terminal end of the protein is responsible for autoproteolytic cleavage of the precursor protein into two biochemically distinct products, a ~19 kDa segment called HhN (for N-terminal portion) and a ~ 25 kDa segment called HhC (for C-terminal portion) (Lee et al., 1994; Porter et al., 1995). The HhN product, responsible for all biological function, is further modified by addition of a cholesterol moiety during the autocatalytic event. Lastly, addition of a palmitate fatty acid group is achieved by action of an o-acyl transferase encoded by the *rasp/skinny hedgehog (ski)/sightless (sit)* gene in the Golgi complex before secretion (Ho and Scott, 2002; Ingham and McMahon, 2001; Micchelli et al., 2002; Miura and Treisman, 2006; Porter et al., 1996). The modified HhN product is then called HhNp (for processed). HhNp is then secreted from the producing cell by action of a 12 pass-transmembrane protein with a sterol-sensing domain (SSD) called Dispatched. Dispatched is only required in the Hh sending cell and requires the cholesterol moiety on Hh for proper function (Burke et al., 1999). There have been four vertebrate homologs of Hedgehog identified: Tiggywinkle Hedgehog (Twhh), Desert Hedgehog (Dhh), Indian

Hedgehog (Ihh), and Sonic Hedgehog (Shh) which are also posttranslationally processed in the same fashion (Ingham and McMahon, 2001; Pepinsky et al., 1998).

Upon secretion, the Hh ligand participates in short- and long-range signaling. The presence of the cholesterol and palmityl groups, regulates the range of signaling through membrane tethering, multimerization, and trafficking by extracellular protein interactions (Gallet et al., 2003; Lum and Beachy, 2004; Zeng et al., 2001). Hh signaling is mediated through Patched receptor binding. Patched (Ptc) is a 12 pass-transmembrane protein that contains a sterol-sensing domain (SSD) similar to Dispatched (Taipale et al., 2002). In the absence of Hh binding, Ptc acts as a repressor, inhibiting the function of another 7 pass-transmembrane protein, called Smoothened (Smo). This repression allows phosphorylation of the transcription factor Cubitus Interruptus (Ci) by cAMP dependent protein kinase A (PKA) and formation of a cytoplasmic protein complex bound to microtubules, composed of Costal-2 (Cos2), Fused (Fu), Suppressor of Fused (Su(Fu)), and Ci. While in this protein complex, Ci is targeted for partial degradation by an E3-ubiquitin ligase, called Slimb in *Drosophila*. The portion of Ci that is remaining, termed $Ci_R$, translocates to the nucleus, where it acts as a repressor of target gene expression. However, in the presence of ligand, Hh binds to the Ptc receptor, relieving repression of Smo function. The Cos2/Fu/Ci/Su(Fu) protein complex is dissociated by recruitment of Cos2 and Fu to the a cytoplasmic domain of Smo. This effectively bypasses of Ci proteosomal degradation, which in turn allows for an active form of Ci, termed $Ci_A$, to enter the nucleus and turn on expression of specific hh target genes, like *ptc* (Figure 1.8). In vertebrates, there have

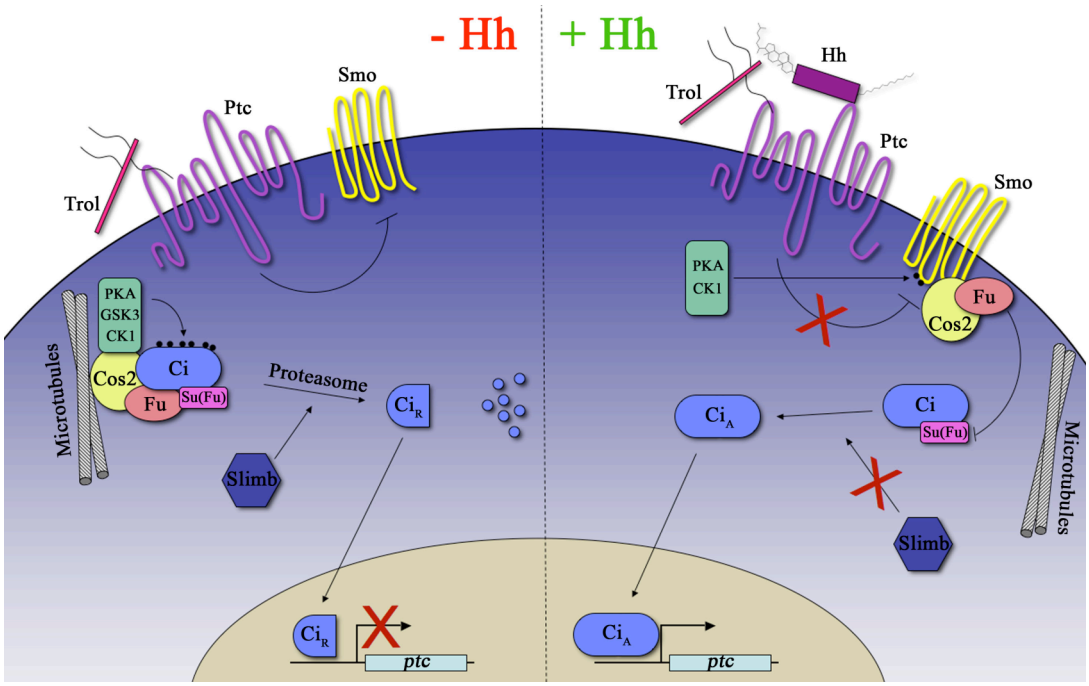


**Figure 1.8. The Hedgehog signaling pathway.** Without Hh activation, the Hh receptor Patched represses the action of Smoothened. This allows for the binding of Ci to the Su(Fu)/Cos2/Fu complex allowing Slimb and PKA to cleave Ci into a repressive form, $Ci_R$, that enters the nucleus and blocks transcription of Hh target genes. With Hh activation, Patched repression is removed allowing Smoothened to interact with Fu. This prevents Ci from binding to the Su(Fu)/Cos2/Fu complex, therefore allowing Ci to enter the nucleus in an activator form, $Ci_A$.

been two *patched* and one *smoothened* gene identified, *patched1*, *patched2* and *smoothened*. There have also been three *ci* family genes identified, called *gli1*, *gli2*, and *gli3*, which exhibit a more complex activator/repressor paradigm than Ci processing in *Drosophila* (Ingham and McMahon, 2001; Jia and Jiang, 2006; Lum and Beachy, 2004; Lum et al., 2003; Nybakken and Perrimon, 2002).

## FIBROBLAST GROWTH FACTOR AND HEDGEHOG SIGNALING INTERACTIONS

Signaling pathways and their roles in development through regulation of cell proliferation, differentiation, survival, and maintenance is a very widely studied area. There are arguably only five main signaling pathways utilized during development of the embryo: the Hedgehog (Hh), Wingless (Wnt), Fibroblast Growth Factor (FGF), Delta/Notch, and Bone Morphogenetic Protein (Bmp) signaling pathways. In studying these signaling pathways, it has become evident that many processes of development require multiple signaling cascades for proper induction, growth, and patterning. Therefore, elucidation of interactions between signaling pathways, is key to understand the complexities of developmental regulation. In this section, I will discuss more specifically about how the FGF and the Hh signaling pathways interact, i.e. dependently or independently, in multiple areas of development.

*FGF and Hh dependent signaling*

Within the past few decades the study of both the FGF and Hh signaling pathways have greatly advanced. The first studies of Hh showed that it was required for proper segmental patterning in *Drosophila* embryos (Nusslein-Volhard and Wieschaus, 1980). Since that time, the number of developmental and non-developmental process es attributed to Hh continues to grow everyday.

Due to cellular diversity generated in a multicellular organism, is not hard to imagine that differing interactions between two signaling pathways in different areas of development would be seen. For example, one of the first interactions established between the Hh and FGF signaling pathways is the positive feedback loop generated during vertebrate limb bud growth and patterning. After induction of the mesenchymal cascade, i.e. expression of the *Gremlin* and *Formin* genes by some unknown mechanism, FGF4 is activated by Gremlin in the apical ectodermal ridge (AER). FGF4 is required for maintenance of Sonic hedgehog (Shh) expression in the posterior limb bud mesoderm called the zone of polarizing activity (ZPA), which is considered to be a signaling center essential for limb patterning. Shh is in turn required for maintenance and propagation of *Formin* and *Gremlin* expression in the ZPA, effectively closing the positive feedback loop (Laufer et al., 1994; Nissim et al., 2006; Niswander et al., 1994; Zuniga et al., 1999). This example shows that maintenance of *Shh* and *fgf* expression is dependent on activity of the opposite signaling pathway. An important factor in this positive feedback loop is that there are intermediate players that mediate the loop.

Shh and FGF signaling through a positive feedback loop is also shown to occur in proliferation induction of stem/progenitor cells of the ciliary body/ ciliary marginal zone (CB/CMZ) of the embryonic chick retina, therefore inducing retinal regeneration if the retina is injured or removed. This particular example shows a more direct interaction of both signaling pathways. If the FGF pathway is inhibited, regeneration stimulated by Shh is also inhibited. The opposite is also true: if the Shh pathway is inhibited, regeneration stimulated by FGF is inhibited. Elucidation of this interaction is taken further by detecting that both FGF and Shh induce Erk phosphorylation, a component of the RAS/MAP Kinase cascade generally employed by FGF signaling. Shh signaling was also determined to up-regulate expression of several members of the FGF signaling pathway (Spence et al., 2007; Spence et al., 2004). These models for FGF and Hh signaling in two very different areas of the body show that pathway inter-dependence can occur in a variety of fashions to elicit the same outcome.

*FGF and Hh independent signaling*

During development of the vertebrate central nervous system, the FGF and Shh signaling pathways are utilized extensively, as evidenced by expression patterns of both growth factor and growth factor receptor. In the developing spinal cord, oligodendrocytes originate from the ventral neural tube at restricted foci. This is influenced by Shh secreted from the notochord and floorplate of the neural tube. Shh induces expression of *Olig1* and *Olig2*, basic helix-loop-helix transcription factors (Chandran et al., 2003). Therefore, you would expect isolated neural stem cells from

this region of the spinal cord to be Shh responsive in formation of oligodendrocytes. However, isolated neural stem cells were shown to respond to FGF2 signaling by forming oligodendrocyte cells. In addition they expressed *Olig2* without stimulation by Hh. Based on these results, Chandran et al hypothesized that FGF2 induced oligodendrocyte formation by stimulating the Shh pathway. To test this, they added cyclopamine, an inhibitor of Hh signaling, to the FGF2 responsive neurosphere culture and assayed for oligodendrocyte formation. In addition, they also isolated FGF2 responsive neural stem cells from Shh null mice and assayed for oligodendrocyte formation. In both cases, oligodendrocyte formation was seen, suggesting that *in vivo* Shh influenced neural stem cells are stimulated in vitro by FGF2 through a Shh independent pathway (Chandran et al., 2003).

Independent signaling of FGF and Shh is also seen in the development of the ventral telencephalon of the vertebrate forebrain. It was known that Shh is expressed in the notochord and ventral area of the neural tube, including the forebrain, and is required for proper development of ventral cell types. When Shh is lost, a ventralizing defect is seen. However, loss of the *Shh* gene and the Shh pathway repressor gene *Gli3* has little effect on the development of the ventral structure of the brain (Gutin et al., 2006). It was thought that another player must be involved in ventralization of the CNS. Because FGFs and FGFRs are known to be extensively expressed throughout the developing vertebrate brain, it was thought that they may be involved in ventral development of the brain. This was shown to be the case because loss of *Fgfr1* or *Fgfr3* in the telencephalon caused loss of ventral differentiated cells (Gutin et al., 2006). Loss of both Fgfr1 and

Fgfr2, mimicked the phenotype of Shh loss. However, expression of Shh and Gli1 are not affected, indicating no Fgfr dependence in the ventral brain. Surprisingly, loss of Gli3 does not rescue the dorsalized phenotype that was seen in the Shh mutant (Gutin et al., 2006). This suggests that both Fgfr and Shh are required for development of the same areas in the ventral region of the vertebrate brain but that the two signaling pathways are independent of one another (Gutin et al., 2006).

Hh and FGF signaling pathway interactions have been extensively studied in many areas of development. However, not much is known about the interactions of these two pathways and neural stem cell proliferation. My dissertation proposes to fill this gap by determining the molecular mechanism of Hh-FGF interaction in the activation of stem cell division in the *Drosophila* central nervous system.

# CHAPTER II

# BRANCHLESS AND HEDGEHOG OPERATE IN A POSITIVE FEEDBACK LOOP TO REGULATE THE INITIATION OF NEUROBLAST DIVISION IN THE *Drosophila* LARVAL BRAIN

## INTRODUCTION

The proper coordination of proliferation and patterning in developing organisms requires the interaction of different signaling systems. Two of these systems, the RAS/MAPK pathway activated by fibroblast growth factor (FGF) and the Hedgehog (HH) pathway, are frequently paired during critical stages of organogenesis. For example, classical developmental paradigms such as limb formation (Campbell, 2002; Martin, 1998; Nissim et al., 2006) and central nervous system patterning (Bertrand and Dahmane, 2006; Park et al., 2003b) require the coordinated actions of both RAS/MAPK and HHs in vertebrates and invertebrates alike. Closer examination of the interplay between the FGF and HH pathways in disparate developmental systems, however, reveals many different mechanisms through which these two pathways interact to regulate developmental events.

The first possibility is that HH and FGF/MAPK signaling operate as two independent pathways. For example, in the mouse ventral telencephalon, FGF signaling is independent of Sonic Hedgehog (SHH) and does not affect expression of either *SHH* itself or its target gene and effector *GLI1* (Gutin et al., 2006). Furthermore, loss of the SHH target and transcription repressor GLI3 does not rescue the *FGFR1*; *FGFR2*

phenotype. Here FGF appears to act later than, but independently of, SHH. Both FGF and SHH can stimulate the production of oligodendrocyte precursors from neural stem cells. Blockage of SHH signaling by addition of cyclopamine or by use of SHH-null stem cells has no effect on FGF2-based oligodendrocyte generation, indicating that the FGF signaling is not dependent on SHH ligand (Chandran et al., 2003) although this does not eliminate the potential for interaction based on intracellular signaling components.

A second possibility is that HH signaling inhibits expression of FGF. This phenomenon has been observed during budding morphogenesis in the mouse lung. *SHH* is expressed in the tips of the distal epithelium in day 11.5 embryonic lung buds (Bellusci et al., 1997; Bellusci et al., 1996). Application of exogenous SHH down-regulates the expression of *FGF10* while culture of the same cells without SHH results in an up-regulation of *FGF10* (Lebeche et al., 1999). Furthermore, in *SHH* knockout mice, *FGF10* shows widespread expression compared to controls (Pepicelli et al., 1998). Analysis of *FGF10* expression in *HIP1* knock-out mice showed that loss of the SHH inhibitor HIP1 results in up-regulation of SHH signaling and almost complete repression of *FGF10* expression with a resultant loss of secondary branching morphology (Chuang et al., 2003). It should be noted that not all FGFs are down regulated by SHH - the same culture paradigm that resulted in inhibition of *FGF10* expression produced up-regulation of *FGF7* (Lebeche et al., 1999), demonstrating that the interaction between SHH and FGFs is FGF specific. Up-regulation of FGF by HH signaling has been observed in several systems including the eye and brain. In the *Xenopus* eye, expression of *Banded*

*Hedgehog* increases expression of *FGF8* (Lupo et al., 2005). In the zebrafish forebrain, inhibition of Hh signaling decreases expression of *FGF3*, *FGF8* and *FGF19* (Miyake et al., 2005). In this case, FGF19 appears to act downstream of HH signaling since over-expression of *FGF19* can at least partially rescue the effects of HH inhibition. Hedgehog also regulates *FGF* expression in the *zebrafish* mid/hindbrain (Blaess et al., 2006). When SHH signaling is inhibited by conditional knockout of the pathway component Smoothened, *FGF8* expression is severely reduced and expression of the Hh target and transcription repressor *GLI3* increases. This is in agreement with the observation that the *FGF8* expression domain increases in size in *GLI3* mutant mice (Aoto et al., 2002), and suggests that *FGF8* expression is maintained by inhibition of GLI3 activity due to SHH signaling.

Conversely, *HH* expression may require FGF signaling. For example, in the zebrafish forebrain, inhibition of both *FGF3* and *FGF8* expression resulted in a down-regulation of *SHH* (Walshe and Mason, 2003). Alternatively, the HH and FGF pathways can integrate at the level of intracellular components. FGF has been shown to induce expression of *GLI2*, a transcription factor and HH signaling effector in ventroposterior development in zebrafish (Brewster et al., 2000). In chick, ectopic application of SHH results in retinal regeneration, and addition of an FGFR antagonist blocks SHH-mediated regeneration (Spence et al., 2004). Similarly, addition of an FGFR antagonist to cultured mouse neocortical precursors inhibits SHH-mediated generation of oligodendrocyte precursors (Kessaris et al., 2004). Furthermore, inhibition of the MAPK pathway also blocked SHH-mediated events. Addition of SHH does not detectably activate MAPK,

suggesting that low endogenous levels of MAPK activation are sufficient for SHH signaling. The requirement for MAPK activation in SHH signaling has also been observed in NIH 3T3 cells (Riobo et al., 2006). Of course the classic example of FGF and SHH interplay is the development of the chick limb bud (Martin, 1998). In this system, several FGFs set up a signaling center at the tip of the bud that turns on expression of *SHH* in the posterior limb mesenchyme. In turn, SHH signaling is required for maintenance of *FGF4*, *FGF9* and *FGF17* expression in the bud tip. This function of SHH occurs through the expression of *Gremlin*, an inhibitor of Bone Morphogenetic Protein signaling (Zuniga et al., 1999). Gremlin inhibition of Bone Morphogenetic Protein signaling prevents down-regulation of the FGFs. Thus a positive feedback loop exists between SHH and FGFs, mediated by Gremlin. FGF and HH signaling are also critical to initiate the proliferation of neural stem cells, or neuroblasts, in the *Drosophila* larval brain (Park et al., 2003b). In this system, Branchless (Bnl, a *Drosophila* FGF homolog) and Hh signaling are modulated by the proteoglycan Trol (the *Drosophila* Perlecan homolog). Decreased signaling by either Bnl or Hh results in fewer neuroblasts beginning cell division at late 1$^{st}$ instar. However, whether this is due to independent parallel pathways that target different subsets of neuroblasts or interaction between the two pathways to control neuroblast division is not yet known. In this study we have found evidence of a positive feedback loop between Hh and Bnl signaling in the larval brain. We demonstrate that *hh* expression and signaling depend on Bnl activity, and vice versa. Both *hh* and *bnl* expression are present in the larval brain lobes upon hatching, as are expression of the Hh and Bnl response genes *patched*

(*ptc)* and *pointed* (*pnt)*, respectively. Use of the temperature-sensitive *hh* allele $hh^{ts2}$ demonstrated that the Hh Bnl feedback loop is initiated during embryogenesis. Finally, epistatic and double mutant studies also support a positive feedback loop model with Bnl signaling as the output of the pathway that activates the division of all mitotically arrested neuroblasts in the brain lobe.

## MATERIALS AND METHODS

### *Genetic strains and transgenes*

Flies were grown in standard medium at 25°C, unless otherwise stated. Markers and balancer chromosomes are described in flybase. Due to the variability of genetic background and their effects on neuroblast division and gene expression, crosses were designed such that sibling controls could be used in all studies.

### *BrdU incorporation and neuroblast counting*

5-bromodeoxyuridine (BrdU) incorporation was preformed by placing 1$^{st}$ instar larvae on Kankel/White medium containing 0.1mg/ml BrdU from 16-20 hours post hatching (hph). The larvae were then dissected, fixed, and labeled. BrdU visualization was observed with a primary mouse anti-BrdU antibody 1:100 dilution (BD-Biosciences) and a goat anti-mouse horseradish peroxidase secondary 1:200 dilution (Jackson ImmunoResearch). Signaling was developed using diaminobenzidine (DAB) and mounted in PBST for visualizing on a Zeiss axiophot compound microscope. Neuroblast counting was preformed by visual examination. Proliferating neuroblasts

were identified by morphology of their nucleus when labeled with BrdU.

*Developmental staging*

Larvae were developmentally synchronized by collecting newly hatched 1st instar larvae in one-hour windows.

*RNA isolation and Real Time PCR*

For RNA isolation**,** total RNA was extracted using Trizol Reagent (Invitrogen) according to manufacturer's protocol. For qRT-PCR, total RNA was DNase (Invitrogen) treated and reverse transcribed with SuperScript First Strand RT-PCR kit (Invitrogen) using oligo(dT) primers. SYBR Green (Applied Biosystems) was used to run the reactions on a BioRad iCycler. Each sample was run in triplicate at three different concentrations. All primer set sequences are available upon request.

*Statistical analysis*

Standard deviation for each sample group was calculated. Student's *t*-test was used to determine the confidence limits between experimental and control groups.

**RESULTS AND DISCUSSION**

*Hh pathway activity is necessary and sufficient to regulate bnl expression and signaling*

To determine if Hh and Bnl act as independent pathways to activate neuroblast division in the larval brain, we evaluated *bnl* expression and pathway activity in brains

with decreased Hh signaling. Our genetic studies had already demonstrated that the weak *trol*$^{b22}$ mutation results in decreased neuroblast proliferation when combined with a single copy of the null *hh* allele *hh*$^{AC}$ (Park et al., 2003b). Therefore we expected to observe reduced Hh signaling in *trol*$^{b22}$*; hh*$^{AC}$/+ brains. We used quantitative Real-Time PCR (qRT-PCR) to assay for expression of *bnl* and its target gene *pointed* (*pnt*) and to confirm decreased expression of *hh* and Hh signaling by monitoring the Hh target gene *patched (ptc)*. Siblings with normal neuroblast proliferation levels were used as a control population. In animals hemizygous for *trol*$^{b22}$ and carrying the one copy of the null allele *hh*$^{AC}$ (*trol*$^{b22}$*; hh*$^{AC}$/+), *hh* expression and signaling were significantly reduced, with a reduction in expression of both *bnl* and its response gene *pnt* (Figure 2.1A, B). To eliminate the possibility that the alteration in *bnl* expression and signaling levels were due to the mutation in *trol*, we then asked if decreasing *hh* signaling using the temperature sensitive *hh* allele *hh*$^{ts2}$ also decreased *bnl* expression and signaling. Homozygous *hh*$^{ts2}$ animals were raised at the permissive temperature (18ºC) through embryogenesis and then transferred to the restrictive temperature (25ºC) upon larval hatching. Heterozygous *hh*$^{ts2}$/+ animals treated to the same temperature regimen were used as controls. *hh*$^{ts2}$ homozygotes had a 75% drop in *hh* signaling and decreased *bnl* and *pnt* expression compared to controls (Figure 2.1C). BrdU analysis showed that the *hh*$^{ts2}$ homozygotes also had decreased neuroblast proliferation (Figure 2.1D). These results indicate that the activity of the Hh pathway is necessary for normal levels of Bnl signaling. We then asked whether increasing Hh signaling is sufficient to produce increased *bnl* expression and signaling activity. The inducible *hs-hh* allele was used to

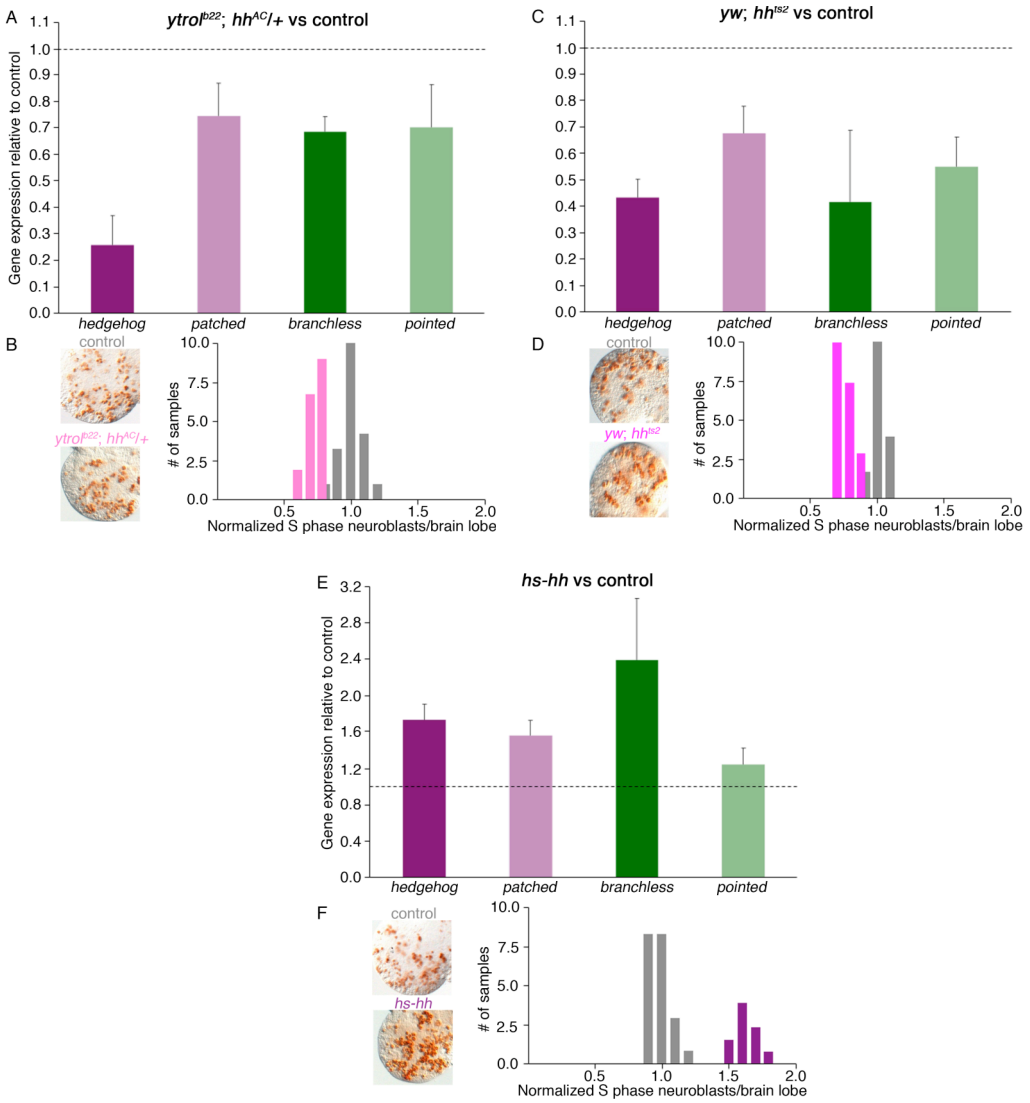


**Figure 2.1. *bnl* expression and signaling respond to Hh pathway activity.** (A, C, E) Expression of *hh*, *ptc*, *bnl*, and *pnt* were quantified by qRT-PCR in 1st instar larval brains at 19-20 hours post hatching (hph). Error bars indicate standard deviation. All samples were run in triplicate at three different concentrations. (A) in $trol^{b22}$; $hh^{AC}$/ + animals relative to $trol^{b22}$ control (C) in $hh^{ts2}$ homozygous animals relative to $hh^{ts2}$/ + heterozygotes both raised at 18°C during embryogenesis and moved to 25°C upon larval hatching (E) in *hs-hh* animals relative to *hs-hh*/ + heterozygotes both raised at 18°C during embryogenesis and moved to 25°C upon larval hatching. (B, D, F) S-phase neuroblasts/brain lobe were quantified and normalized to the average sibling control value.

increase *hh* expression; heterozygous *hs-hh* animals were used as sibling controls. Brains from homozygous *hs-hh* animals had a significant increase in *hh* expression and increased Hh signaling even over siblings with one copy of the inducible transgene (Figure 2.1E). The increase in Hh signaling correlated with increase expression of *bnl* and *pnt*, as well as increased neuroblast proliferation (Figure 2.1F). These studies demonstrate that *bnl* expression and activity in the larval brain is dependent on the level of Hh signaling.

*Bnl pathway activity determines the level of hh expression and signaling*

To ascertain if Hh signaling was similarly dependent on Bnl activity, we examined *hh* and *ptc* expression in animals with reduced Bnl signaling. We first studied animals hemizygous for $trol^{b22}$ and heterozygous for the putative null allele, $bnl^{P1}$. As expected, expression of both *bnl* and *pnt* dropped in the brains of these animals compared to controls, as did the number of BrdU labeled neuroblasts, although there was still some expression of the Bnl response gene *pnt* (Figure 2.2A, B). Our qRT-PCR analysis showed that *hh* and *ptc* message levels also decline in the $trol^{b22}$; $bnl^{P1}$ / + brains (Figure 2.2A), suggesting that *hh* expression and signaling is dependent on Trol or Bnl activity. To establish whether the drop in *hh* expression and signaling were due to the mutation in *trol* or decreased Bnl signaling, we examined *hh* and *ptc* expression in the brains of animals homozygous for $bnl^{P1}$ but raised at 18°C to enable generation of mutant larvae. The fact that we could obtain $bnl^{P1}$ mutant larvae at 18°C but not 25°C as well as the detection of *pnt* expression in the $bnl^{P1}$ mutants suggests that $bnl^{P1}$ is not a

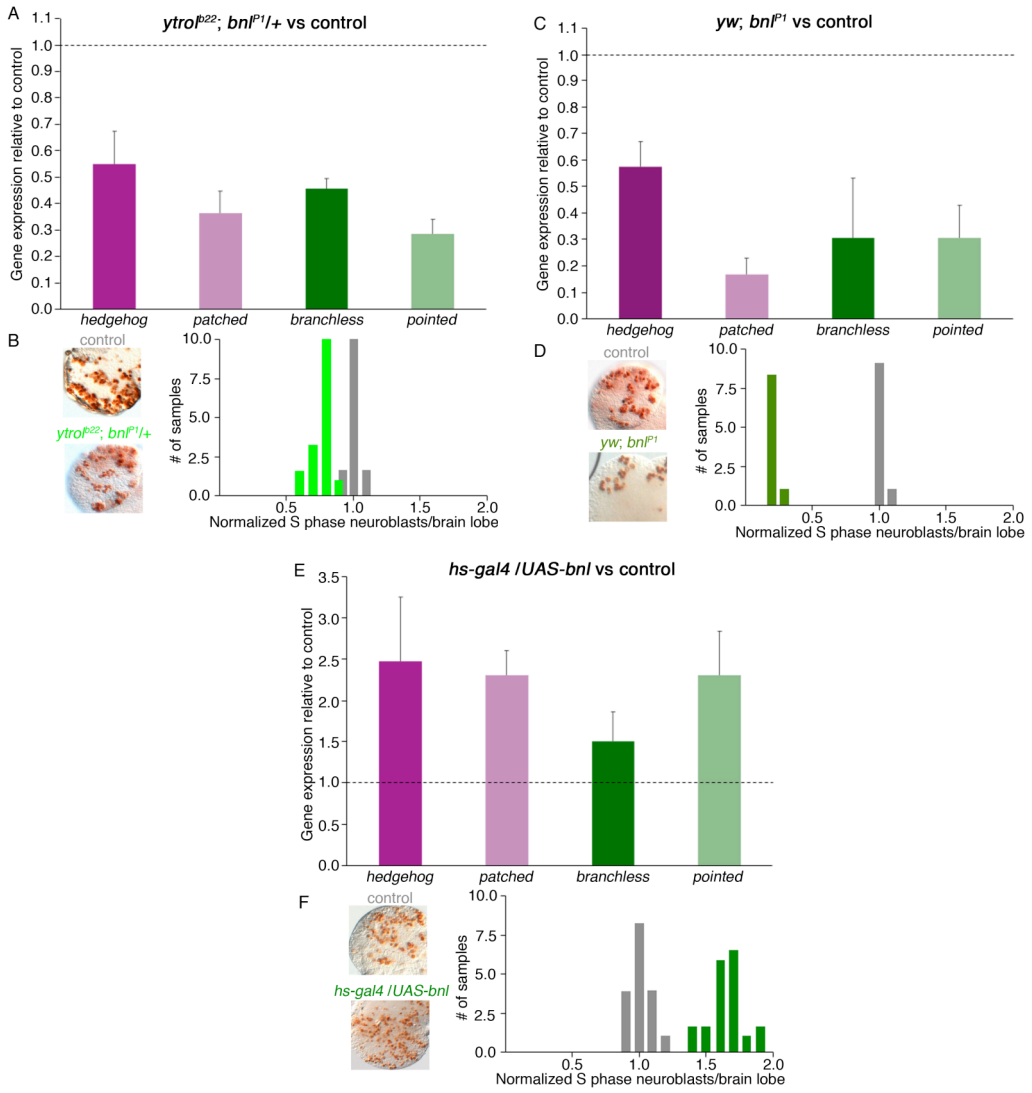


**Figure 2.2. *hh* expression and signaling respond to Bnl pathway activity**. (A, C, E) Expression of *hh*, *ptc*, *bnl*, and *pnt* were quantified by qRT-PCR in 1st instar larval brains at 19-20 hph. Error bars indicate standard deviation. All samples were run in triplicate at three different concentrations. (A) in $trol^{b22}$; $bnl^{P1}$/ + animals relative to $trol^{b22}$ control (C) in $bnl^{P1}$ homozygous animals raised at 18°C during embryogenesis and moved to 25°C upon larval hatching relative to wild-type controls (E) in *UAS-bnl* + / + *hs-gal4* animals relative to *UAS-bnl* animals both raised at 18°C during embryogenesis and moved to 25°C upon larval hatching. (B, D, F) S-phase neuroblasts/brain lobe were quantified and normalized to the average sibling control value.

true null. For this study we used $bnl^{P1}$ / + sibling animals subjected to the same temperature regimen. qRT-PCR studies confirmed a 70% drop in *bnl* and *pnt* message levels in $bnl^{P1}$ homozygotes versus control, as well as a dramatic decrease in *hh* and *ptc* expression (Figure 2.2C). The number of BrdU labeled neuroblasts (4.4±0.1) significantly decreased compared to controls (Figure 2.2D). The observation that only 4-5 neuroblasts were BrdU labeled in $bnl^{P1}$ homozygotes at 20 hours post hatching suggests that all the mitotically regulated neuroblasts require Bnl signaling to begin cell division, although from this data a requirement for some minimum level of Hh signaling cannot be eliminated. This hypothesis will be addressed further in a following section. The neuroblasts labeled had cellular morphology and spatial positioning consistent with identification as mushroom body or ventral lateral neuroblasts. The four mushroom body neuroblasts and the single ventral lateral neuroblast in each brain lobe are the only neuroblasts in the larval brain that are dividing upon larval hatching and divide continuously through larval life (Datta, 1995; Ito and Hotta, 1991). They are also the only neuroblasts in the brain lobe not affected by mutations in *trol* that decrease signaling by Bnl (Datta, 1995; Park et al., 2003b). The results of the *bnl* mutant studies also indicate that normal levels of activity of the Bnl pathway are necessary for normal levels of Hh signaling. We then investigated whether increased Bnl signaling is sufficient to increase *hh* expression and signaling. Up-regulation of Bnl signaling was accomplished by using a *hs-GAL4* construct to drive expression of a *UAS-bnl* transgene. Animals were maintained at 18ºC to minimize expression from the *hs* promoter and activity of the GAL4 transcription factor during embryogenesis. Upon larval hatching,

animals were transferred to 25ºC to induce *bnl* expression. Increased expression and activity of *bnl* were confirmed by qRT-PCR and correlated with increased expression of both *hh* and *ptc* as well as increased numbers of BrdU labeled neuroblasts (Figure 2.2E, F). Taken together, these results indicate that *hh* expression and activity is dependent on the level of Bnl signaling in the larval brain.

*Decreasing both Bnl and Hh signaling causes a further decrease in neuroblast proliferation*

The question then arose as to whether the relative ratio of Hh and Bnl signaling was critical for activation of neuroblast division (i.e. *hh null / hh+: bnl null / bnl+* would work as well as *hh+ / hh+: bnl+ / bnl+*), or if the absolute level of signaling (compared to wild-type controls) is important. To address this issue, we evaluated the amount of neuroblast division in $trol^{b22}$ mutant animals heterozygous for both $hh^{AC}$ and $bnl^{P1}$ and compared it to that in $trol^{b22}$, $trol^{b22}$; $hh^{AC}$/+ and $trol^{b22}$; $bnl^{P1}$ / + animals (Figure 2.3A). Statistical analysis showed that the decrease in numbers of BrdU labeled neuroblasts in the $trol^{b22}$; $bnl^{P1}$ + / + $hh^{AC}$ brains was significantly greater than in either single heterozygote ($p< 9 \times 10^{-11}$). qRT-PCR showed roughly equivalent decreases in expression of both the ligands and their target genes (Figure 2.3B). The increased severity of the neuroblast proliferation phenotype in the double *hh bnl* heterozygote indicates that maintenance of the overall magnitude of Bnl and Hh signaling is essential for normal neuroblast proliferation.

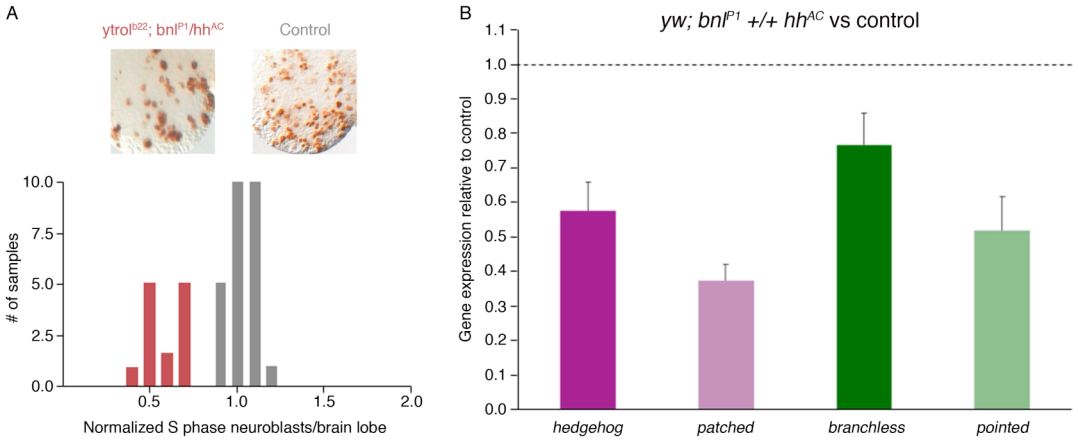


**Figure 2.3. Maintenance of both Hh and Bnl signaling is required for normal neuroblast proliferation**. (A) S-phase neuroblasts/brain lobe were quantified and normalized to the average sibling control value. Expression of *hh*, *ptc*, *bnl*, and *pnt* were quantified by qRT-PCR in 1st instar larval brains at 19-20 hph (B) in $trol^{b22}$; $bnl^{P1}$ +/ + $hh^{AC}$ animals relative to $trol^{b22}$ control. Error bars indicate standard deviation. All samples were run in triplicate at three different concentrations.

*The initiation of the Hh-Bnl feedback loop observed in the larval brain occurs during embryogenesis*

Thus far, our studies are consistent with a positive feedback loop between Hh and Bnl that regulates the level of growth factor expression. The output of this loop then regulates the activation of neuroblast proliferation. Since Hh- and Bnl-dependent neuroblast proliferation does not begin until 8-10 hours post hatching, we asked when Hh and Bnl are first expressed in the larval brain. Larvae were collected in one-hour increments and the amount of *hh* and *bnl* message in the larval brain evaluated. Both *hh* and *bnl* are expressed upon larval hatching, and the level of expression does not significantly change during the first four hours of larval life (Figure 2.4A). We then asked if the level of Hh or Bnl signaling activity also remained constant during the first few hours of larval life. *ptc* and *pnt* show much more dynamic temporal pattern of expression than the level of pathway ligand (Figure 2.4B). Since both Hh and Bnl are stimulating expression of their response genes within an hour of larval hatching, the feedback loop could be initiated during embryogenesis, prior to larval hatching. If the Hh-Bnl feedback loop is initiated during embryogenesis, then decreasing Hh signaling only during embryogenesis should result in lowered *bnl* expression and Bnl signaling in the larval brain immediately upon hatching. To test this hypothesis, we used the temperature-sensitive *hh* allele, $hh^{ts2}$, and raised mutant animals at the restrictive (25°C) or permissive (18°C) temperature throughout embryogenesis. Both experimental and control plates were then placed at the permissive temperature (18°C) and newly hatched larvae collected in a two hour window. This

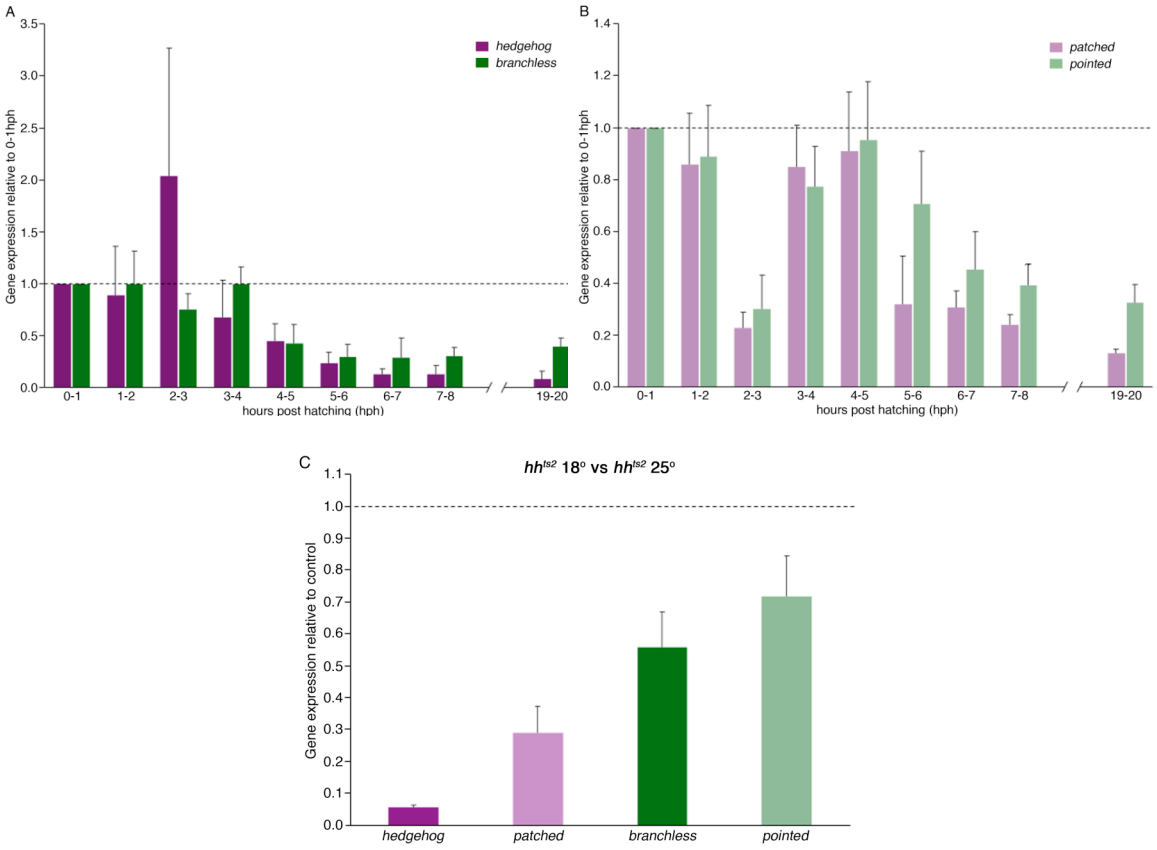


**Figure 2.4. Initiation of the Hh-Bnl feedback loop occurs during embryogenesis**. Canton-S larval brains were collected in one hour increments from 0-20 hph at 25°C and qRT-PCR used to quantify (A) *hh* and *bnl* expression (B) *ptc* and *pnt* expression. Expression of *hh*, *ptc*, *bnl*, and *pnt* were quantified by qRT-PCR in (C) $hh^{ts2}$ homozygous larval brains from 0-1 hph raised at 25°C throughout embryogenesis compared to larval brains from 0-1 hph raised at 18°C throughout embryogenesis. Error bars indicate standard deviation. All samples were run in triplicate at three different concentrations.

experimental design resulted in decreased Hh signaling only during embryogenesis in the experimental samples. Larval brains were dissected and assayed for levels of *hh*, *ptc*, *bnl* and *pnt* expression. Our qRT-PCR results show that the levels of both *bnl* and its response gene *pnt* decreased in the larval brains of $hh^{ts2}$ animals raised at the restrictive temperature compared to animals raised at the permissive temperature. The expected decrease in expression of *hh* and the Hh response gene *ptc* in experimental samples compared to controls was verified by qRT-PCR (Figure 2.4C). This result demonstrates that lowering Hh signaling during embryogenesis results in decreased Bnl production and signaling and is consistent with the hypothesis that the Hh-Bnl feedback loop in the brain is already operational by larval hatching.

*Bnl is epistatic to Hh for the proliferation of regulated neuroblasts in the larval brain lobe*

So far, our results show that Bnl and Hh signal in a positive feedback loop that is initiated prior to larval hatching. We next asked if the activity of both signaling pathways was necessary for neuroblast proliferation or if over-expression of one signal could rescue a deficit in the other signal. The inducible *hs-hh* allele was used to increase *hh* expression in a $bnl^{P1}$ homozygous mutant. Animals were maintained at the 18°C to minimize expression from the *hs* promoter and activity of the GAL4 transcription factor during embryogenesis. Upon larval hatching, animals were transferred to 25°C to induce *hh* expression. Increased expression and activity of *hh* were confirmed by qRT-PCR, and *bnl* expression and activity mirrored that of $bnl^{P1}$ homozygotes, indicating that

misexpression of *hh* does not bypass or suppress the *bnl* mutant phenotype (Figure 2.5A). More strikingly, over-expression of *hh* does not rescue neuroblast proliferation in the $bnl^{P1}$ mutant (Figure 2.5B). As noted previously when analyzing $bnl^{P1}$ homozygotes, we observed only 4.4 ± 0.1 neuroblasts labeled with BrdU in *hs-hh;* $bnl^{P1}$ samples (indicative of the mushroom body and ventral lateral neuroblasts, which are not affected by Hh or Bnl signaling), compared to approximately 20 observed in normal controls and the 30-35 observed in *hs-hh* animals alone. The failure of *hh* over-expression to overcome the effects of a *bnl* null mutation confirms the hypothesis that all the mitotically regulated neuroblasts require Bnl signaling to initiate cell division. This data also suggests that Bnl activity is the signaling output of the positive feedback loop. To confirm this conclusion, up-regulation of Bnl using the same *hs-GAL4*/*UAS-bnl* expression system described previously was examined in an $hh^{ts2}$ homozygous animal. Animals were again maintained at the 18°C to minimize expression from the *hs* promoter and activity of the GAL4 transcription factor during embryogenesis. Upon larval hatching, animals were transferred to 25°C to induce *bnl* expression. Increased expression and activity of *bnl* were confirmed by qRT-PCR (Figure 2.5C). BrdU incorporation studies demonstrated that over-expression of *bnl* in a $hh^{ts2}$ homozygote resulted in significant increase ($p < 0.016$) in the number of S phase neuroblasts over that normally observed in $hh^{ts2}$ homozygotes at the restrictive temperature (Figure 2.5D, $hh^{ts2}/hh^{ts2}$ show 14.7 BrdU labeled neuroblasts/brain lobe ± 0.3). In fact, over-expression of bnl in a $hh^{ts2}$ homozygote produced an over-proliferation phenotype (23.2 BrdU labeled neuroblasts/brain lobe ± 1.6) compared to the normal 20 neuroblasts/brain

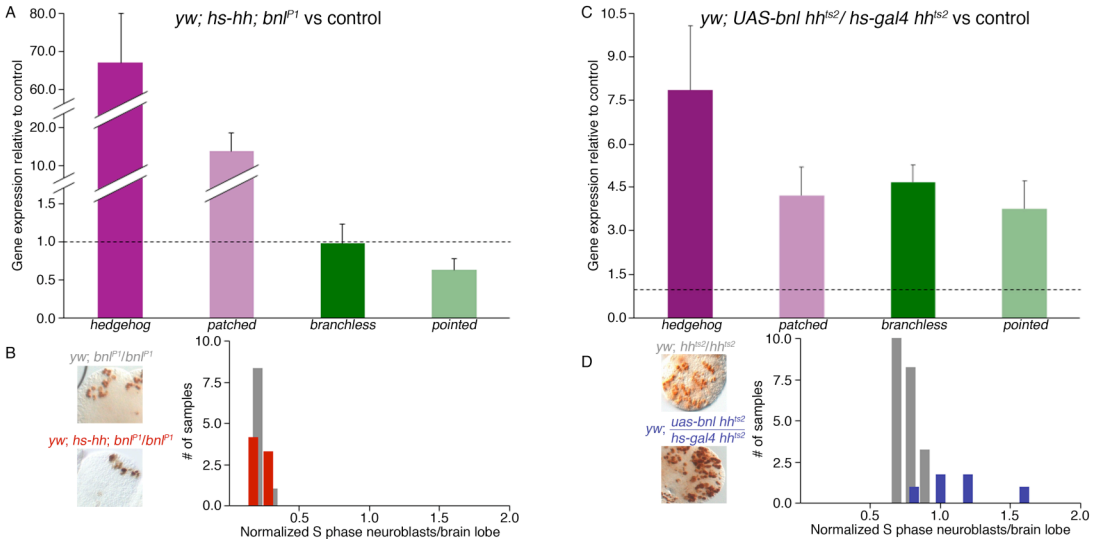


**Figure 2.5. Bnl is epistatic to Hh for activation of proliferation in the regulated neuroblasts of the larval brain lobe.** (A, C) Expression of *hh*, *ptc*, *bnl*, and *pnt* were quantified by qRT-PCR in 1st instar larval brains at 19-20 hph. Error bars indicate standard deviation. All samples were run in triplicate at three different concentrations. (A) in *hs-hh; bnl$^{P1}$* animals relative to *bnl$^{P1}$* control both raised at 18°C during embryogenesis and moved to 25°C upon larval hatching (C) in *UAS-bnl hh$^{ts2}$/ hs-gal4 hh$^{ts2}$* animals relative to *hh$^{ts2}$* control both raised at 18°C during embryogenesis and moved to 25°C upon larval hatching. (B, D) S-phase neuroblasts/brain lobe were quantified and normalized to the average sibling control value.

lobe observed in wild-type controls. Altogether, these studies establish that Bnl signaling activity is the essential output of the Hh-Bnl feedback loop that regulates the activation of neuroblast proliferation.

*Integration of FGF and Hh signaling*

Our studies have demonstrated that Hh and Bnl act in a positive feedback loop in the larval brain to control the onset of neuroblast proliferation (Figure 2.6). The feedback loop acts at the transcriptional level, such that Hh signaling activity is essential to control the level of *bnl* expression and vice versa. Our double mutant analyses showed that an absolute level of signaling by both Bnl and Hh are required to maintain normal neuroblast activation, rather than other possible models that would suggest a certain balance of signaling activity (for example more Bnl than Hh) is sufficient regardless of the exact magnitude of signaling activity. The discovery that Bnl signaling is the critical output of the feedback loop suggests that Hh signaling acts to maintain the proper level of Bnl production and signaling. Furthermore, the observation that only the mushroom body and ventral lateral neuroblasts continue to divide in *bnl* null mutants regardless of the level of Hh signaling indicates that all the regulated neuroblasts, both optic lobe and central brain sets, require the input of the Bnl pathway to enter S phase. Thus the Hh Bnl feedback loop appears to control cell cycle progression in all the mitotically arrested neuroblasts that begin cell division in 1$^{st}$ instar. The model of the Hh-Bnl feedback loop proposed here is most similar to the classic SHH-FGF feedback loop described in the vertebrate limb bud. We do not yet know whether the regulation of

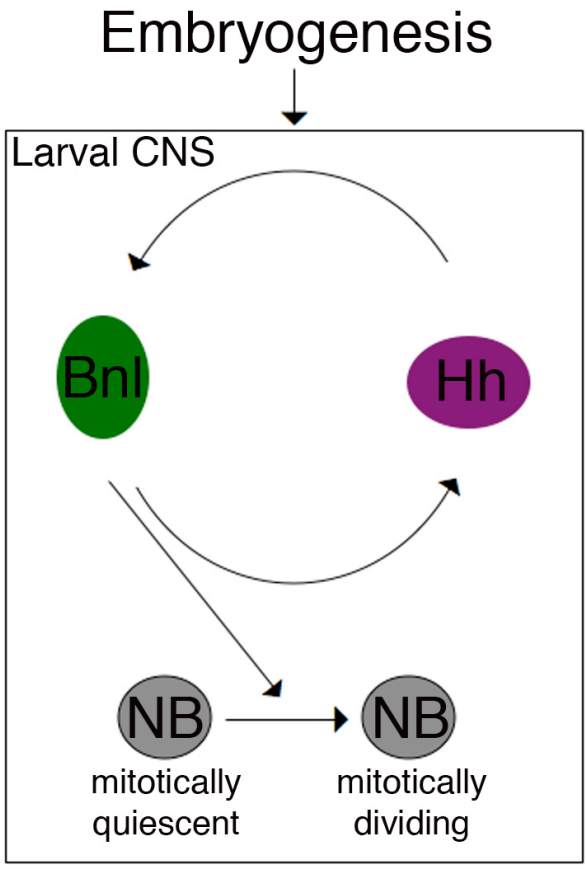


**Figure 2.6. Model of Bnl-Hh positive feedback loop.**

*bnl* expression by Hh signaling is direct or if it is mediated by another signaling pathway such as the Gremlin/Bone Morphogenetic Protein connection that operates in the limb bud (Nissim et al., 2006; Zuniga et al., 1999). However, we have already shown that like the distinct domains of FGF and SHH in the limb bud (Martin, 1998), *bnl* and *hh* expression also occur in distinct regions of the brain lobe (Park et al., 2003b). The fact that the Hh-Bnl feedback loop is activated during embryogenesis, but that the first regulated neuroblasts do not enter S phase until 8-10 hours after larval hatching (Datta, 1995; Ebens et al., 1993; Truman and Bate, 1988; White and Kankel, 1978) also suggests that additional events must take place downstream of Bnl signaling to permit mitotically arrested stem cells to transit through G1 to S phase (Caldwell and Datta, 1998; Park et al., 2003a). One such possibility is exposure to the steroid hormone ecdysone, which is necessary during 1$^{st}$ larval instar for the initiation of neuroblast division a few hours later (Datta, 1999). Both SHH and FGF2 have been shown to be necessary for the division of different subsets of neural stem cells in many different vertebrate and mammalian models and in multiple contexts (Bertrand and Dahmane, 2006; Maric et al., 2007). The next challenge will be to determine whether different molecular mechanisms tying these two signaling pathways are used for different developmental decisions such as progeny cell fate, initiation of cell division and maintenance of stem cell identity.

# CHAPTER III

# DETERMINATION OF THE INSTABILITY OF *gal4* EXPRESSION FROM A P-ELEMENT INSERTION IN *DROSOPHILA*

## INTRODUCTION

Several processes have been identified that induce genomic instability (i.e. irradiation, chemical alteration, and mobile elements). The transposon or mobile genetic element, is a movable DNA segment that can occasionally "jump" around chromosomes and promote genetic rearrangement. These mobile genetic elements were first described in the early 1950's by Barbara McClintock, who pioneered genetic research in maize and is most noted for her work in genetic recombination (McClintock, 1953). Her report that specific segments of chromosomes could "transpose" to other positions as a controlled phenomenon was not initially accepted by the scientific community. It would take several decades for her work to become recognized.

Transposons are defined as segments of DNA that can change positions in the genome through a process called transpositional recombination, a form of genetic recombination. They show modest sequence specificity of insertion site and will insert into a gene, causing gene disruption. It is hypothesized that this is the most common source of new mutations generated in organisms. With >50% of the maize and human genome being composed of transposon-like sequences, it is not hard to see that transposons could play an important role in genome stability and genetic variation. Transposons can be classified into 3 major families of transposable elements; DNA

transposons, viral-like retrotransposons, and Poly-A retrotransposons. DNA transposons move through a cut-and-paste mechanism and remain in DNA form throughout the transposition process. In contrast, both retrotransposons go through a RNA intermediate before being reinserted into the genome (Albornoz and Dominguez, 1999; Watson et al., 2004).

Over 50 years ago a member of the DNA transposon family, the P-element, was identified as entering the *Drosophila melanogaster* population and has since spread to most wild and laboratory populations (Engels, 1997). P-elements contain a *transposase* gene and long terminal repeats (LTR) that are the site of action of the Transposase. Transposition is restricted to the germ line where splicing of the *transposase* gene produces a functional product, unlike splicing in somatic cells where alternative splicing results in a repressive form of Transposase that inhibits mobility of the transposon. The P-element also exists as a nonautonomous variant that contains only long terminal repeats and therefore can only be mobilized when Transposase is added in trans (Pinsker et al., 2001; Ryder and Russell, 2003). Using these unique features, researchers have been able to manipulate P-elements to their advantage and they have become one of the most widely used genetic tools for studying gene functions in *Drosophila*.

Once such P-element tool is the *gal4/UAS* system. The *gal4/UAS* system is a bipartite misexpression system that is used to express a particular target gene in a tissue-specific manner (Brand and Perrimon, 1993). The system utilizes two P-element inserted transgenes for this process, the *enhancer-gal4* transgene and the *UAS-reporter* transgene. The *enhancer-gal4* transgene is a construct that comprises a specific

promoter/enhancer sequence upstream of the yeast *gal4* gene. This sequence drives temporal and/or spatial expression of the yeast Gal4 transcription factor. The *UAS-reporter* transgene is a construct that comprises multiple Gal4 binding sites called upstream activating sequences (UAS) followed by a gene of interest, such as a reporter gene like *gfp* or *lacZ*. When the *enhancer-gal4* and *UAS-reporter* transgenes are present in the same fly, Gal4 will drive expression of the reporter gene in a tissue specific manner allowing the researcher to follow cells expressing the reporter through developmental and/or functional processes. Neither *gal4* nor *UAS* are present endogenously in *Drosophila*, which allows for temporal and spatial expression specific to transgene components. These characteristics make the *Gal4/UAS* system a very powerful genetic tool for the analysis of development and function in the fly.

In this study, we examine a P-element generated *gal4* transgene, which lacks the *transposase* gene, yet shows loss of *gal4* by an unknown mechanism. We show that the *gal4* gene is lost stochastically from generation to generation by excision of a segment of the gene while retaining the rest of the P-element gene structure. We also show gradual silencing of Gal4 activity in offspring from the same parental cross over a short period of time. More interesting is that both mechanisms of loss can be rescued by tetracycline treatment of the *Drosophila* line suggesting a bacterial influence. Here we explore the possible bacteria and mechanisms they utilize to induce gene loss/silencing of P-element transgenes.

## MATERIALS AND METHODS

*Drosophila strains*

Flies were grown under standard laboratory conditions at 25°C on cornmeal/molasses media supplemented with yeast, unless otherwise stated. Dr. Scott Selleck at University of Minnesota provided the *c529* line. The *UAS-lacZ* construct was obtained from the Bloomington Stock Center and Dr. Ginger Carney at Texas A&M University provided the *UAS-GFP:lacZ.nls* construct. Dr. Vlad Panin at Texas A&M University graciously provided *Wolbachia* positive fly strains.

*PCR assay*

DNA extractions of single *c529* adults or larvae were done. PCR temperature conditions of 95°C for 60 sec, 60°C for 30 sec, and 72°C for 45 sec was used for 40 cycles with the following primers:
gal4 F2 (5′-CAGTTCTTTGTGCTGCATCGCT-3′) and
gal4 R2 (5′-AAGTGCGACATCATCATCGGAA-3′).

DNA extractions and PCR conditions for the detection of *Wolbachia* were done as described in (O'Neill et al., 1992) and the following primers specific for the *Wolbachia* 16S rRNA gene were used for detection in genomic DNA:
99F (5′-TTGTAGCCTGCTATGGTATAACT-3′) and
994R (5′-GAATAGGTATGATTTTCATGT-3′) described in (O'Neill et al., 1992).

The following primers were used in separate PCRs as a control for the quality of DNA extractions (band at ~550bp):

F1 (5′-CCACCACGCAGTACCAGTG-3′) and

R1 (5′- CTCCTGCCCGCCGATG -3′).

*Histological analysis*

Dissection of the larval central nervous system (CNS) and salivary glands (SG) was performed at specific developmental stages and β-galactosidase visualization was achieved by fixing tissue with ET fix (1 X buffer B: formaldehyde) for 10 min at RT, washing three times with 1X PBST, and incubating tissue in X-gal stain for ~3 hours at 37°C.

*Developmental staging*

Larval developmental stages were identified by morphological characteristics or by hours post-hatching (hph).

*Tetracycline treatment*

Flies were raised at 25°C on cornmeal/molasses media with or without 0.03 mg $ml^{-1}$ tetracycline (Sigma Aldrich, cat# T3383-25G) for one generation and the allowed to pass through two generations before beginning experimental analysis (Erickson, 2004; Starr and Cline, 2002).

## RESULTS AND DISCUSSION

*c529 is gal4 driver that labels brain neuroblasts*

*c529* is a Gal4 enhancer trap line generated during a screen for expression patterns in the embryo, larval brain, imaginal discs, and ovary of *Drosophila.* It is described as showing an expression pattern that labeled cells in the outer proliferative center (OPC), inner proliferative center (IPC), ventral ganglion (VG), in the pouch of the wing, and haltere discs (Manseau et al., 1997). Through further analysis, we determined that the *c529* enhancer trap line labeled 4-5 optic lobe (OL) and/or central brain (CB) neuroblasts (unpublished data) (Figure 3.1).

*Loss of reporter gene expression over time*

Upon characterization of the larval expression pattern in progeny generated by crossing a homozygous *c529* male to a homozygous *UAS-lacZ* female, high and distinct expression levels were seen. However, over time many progeny started exhibiting low or no expression in the larval brain. This variation in reporter gene expression was somewhat puzzling since every offspring examined should be transheterozygous for *c529* and *UAS-lacZ*, and therefore should exhibit the same level of expression. There are several possibilities for loss of reporter gene expression, which include: loss of the *gal4* gene in the genome either by heterozygosity in one or both parental strains, excision of the P-element, silencing of *gal4* expression, or an accumulation of mutations in the *gal4* gene.

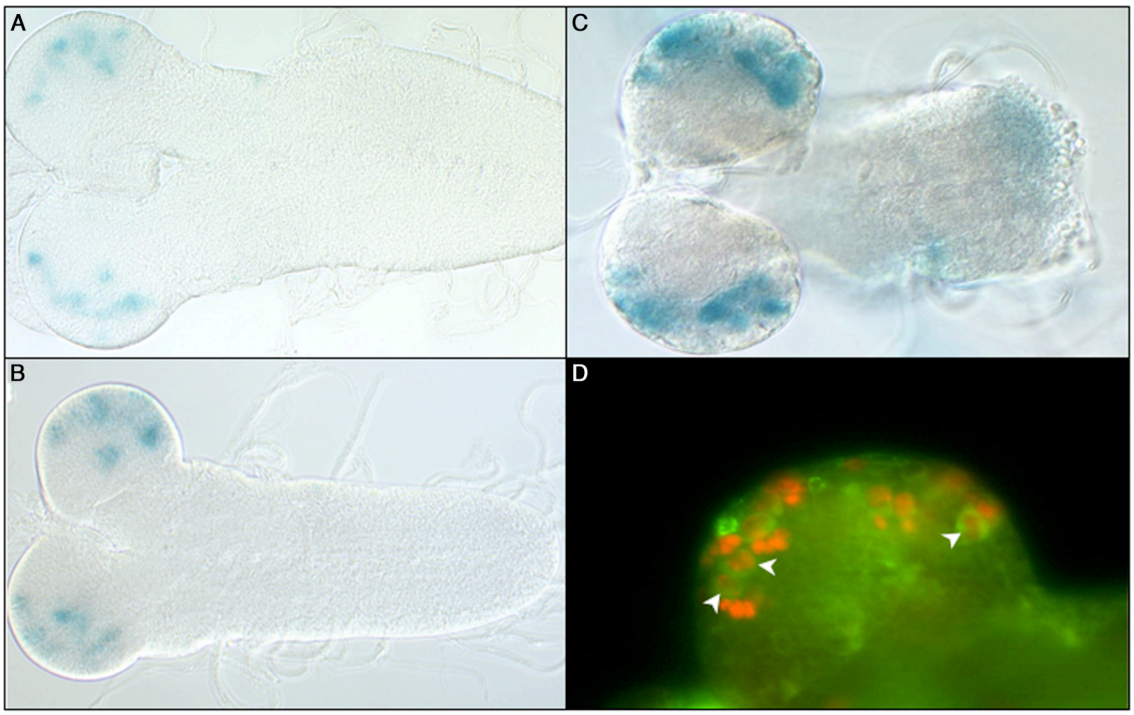


**Figure 3.1. *c529* expression profile throughout larval development.** Homozygous *c529* female's were crossed to homozygous *UAS-lacZ* male's and the expression profile in the central nervous system (CNS) resolved by staining for β-galactosidase activity in (A) late 1st instar, (B) mid 2nd instar and (C) early 3rd instar. (D) Fluorescent staining of c529 expression (green) and S-phase nuclei (red) in the CNS of a 1st instar larvae at 19-20 hours post-hatching (hph). Larvae were fed media containing BrdU from 16-20 hph. White arrowheads indicate several *c529* labeled neuroblasts.

To address the first possibility, we looked for the presence of the P-element insertion that includes the *gal4* gene in the *c529* stock. Due to the nature of the procedure for introduction of P-elements into *Drosophila*, each P-element also includes a phenotypic marker, in this case $w^+$, that allows for rapid identification of flies carrying P-element insertions. Therefore, any fly that did not have a P-element insertion should have white eyes, while flies that contained the P-element should have red eyes. Upon examination of the stock, it was determined that every fly exhibited red eyes (data not shown). However, it could still be possible for the *c529* stock to be heterozygous for the P-element insertion. To test for homozygosity, we again utilized the presence of the $w^+$ marker in the P-element. If a *c529* male is homozygous and is crossed to a *w* female, all progeny will exhibit red eyes. However, if a *c529* male is heterozygous and is crossed to a *w* female, 50% of the progeny will exhibit red eyes and the other 50% will exhibit white eyes. The results of this experiment showed that 100% of the progeny had red eyes, indicating that the *c529* stock is homozygous for the P-element insertion and loss of reporter gene expression is not due to loss of the P-element (data not shown).

The second possibility is that the *gal4* gene is being silenced by some unknown mechanism. First, we wanted to determine if the loss of reporter gene expression was stochastic or gradual. To address this issue, we crossed a homozygous *c529* male to a homozygous *UAS-lacZ* female and dissected the CNS and salivary glands from developmentally staged 1$^{st}$ instar larvae (19-20 hours post-hatching) at 4, 5, and 6 days after mating. We then compared the expression levels of the *lacZ* reporter gene in each sample. Remarkably, a dramatic decrease in the *lacZ* reporter gene expression is seen in

just two days time, going from high expression in ~5 neuroblasts and the salivary gland to no expression in the neuroblasts and very little expression in the salivary glands (Figure 3.2). To ensure that the results are not an artifact of using the *UAS-lacZ* transgene, a second reporter line, *UAS-GFP:lacZ.nls*, was used and reporter gene expression decreased in the same manner (data not shown). These data suggest that a gradual loss or silencing of *gal4* gene expression/activity is occurring in progeny born later to the same parental flies. This then poses the question of whether silencing or loss of *gal4* expression/activity might be occurring in the germ line cells and if reversing the parental genotypes would alter the results. Therefore, we crossed a homozygous *c529* female to a homozygous *UAS-lacZ* male and followed reporter gene expression in the same fashion as previously described. Again, a gradual loss of reporter gene expression is observed (data not shown). Therefore, silencing or loss of the *gal4* gene expression/activity is occurring independently of sex and reporter construct. However, the question still remains as to whether the *gal4* gene is being silenced due to detrimental effects of Gal4 activity, or if the *gal4* gene is acquiring mutations that affect expression or activity.

To address this question, we utilized the temperature sensitivity of Gal4 activity to determine if lowering the activity threshold would allow for continuous reporter gene expression, albeit at a lower level. Two crosses were set up of homozygous *c529* male's and homozygous *UAS-lacZ* female's, which were allowed to mate at 18°C and 22°C, respectively. At 18°C, *lacZ* expression in developmentally staged 1$^{st}$

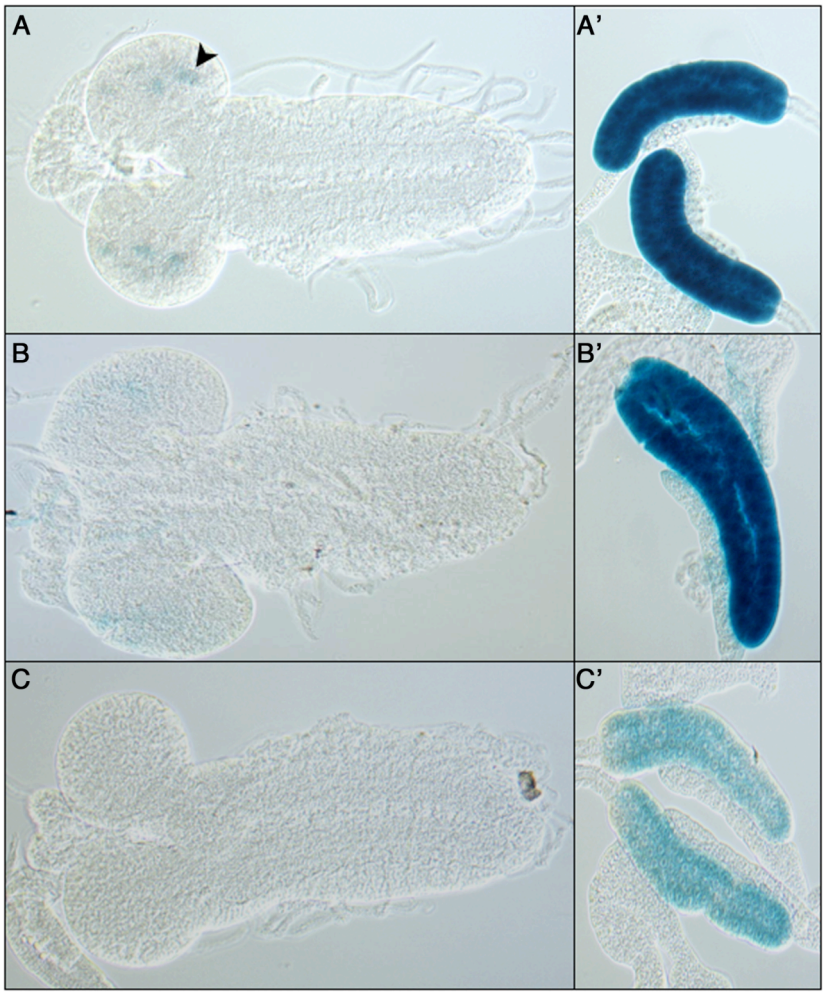


**Figure 3.2. Loss of *UAS-lacZ* expression in $F_1$ progeny from same parental cross.** A homozygous *c529* male was crossed to a homozygous *UAS-lacZ* female and expression levels examined in the (A, B, C) central nervous system and (A′, B′, C′) salivary glands of developmentally staged 1st instar larvae (19-20 hours post-hatching) generated on the (A, A′) 4th, (B, B′) 5th, and (C, C′) 6th day after mating. All samples were processed for the same time period with the same staining protocol. Parental cross and $F_1$ larvae were raised at 25°C.

instar larvae (38-40 hours post-hatching) was followed at 8, 10, and 12 days after mating. At 22°C, *lacZ* expression in developmentally staged 1st instar larvae (28.5-30 hours post-hatching) was followed at 6, 8, and 10 days after mating. Both crosses, at 18°C and 22°C, showed a decrease in *lacZ* expression over time, similar to that seen at 25°C (Figure 3.3). These data suggest that the loss of reporter gene expression in progeny from the same parental cross over time is not due to a detrimental effect of Gal4 activity since the same phenotypic anomaly is also seen at temperatures that permit limited Gal4 activity.

Next, we looked for possible mutations/deletions of the *gal4* gene by PCR amplification of a specific region of *gal4* in single flies of the *c529* stock. We extracted genomic DNA from 50 individual flies, 25 male and 25 female, and performed PCR analyses on each fly. Fourty two out of 50 Genomic DNA extractions were determined to be of good quality by PCR analysis with the control primers F1 and R1 that amplify a segment of the endogenous *trol* gene. Then, PCR reactions with primers specific for the C-terminal region of *gal4* were carried out on the 42 high-quality samples. Analysis of the PCR products demonstrated that only 4 out of 42 (9.5%) flies contained this region of the *gal4* gene (Figure 3.4). This is a surprising result since we previously reported that all of the C529 stock contained flies with red eyes, therefore indicating presence of the P-element insertion. These data suggest that there is not only gradual loss of Gal4 activity but also loss of *gal4* coding sequences.

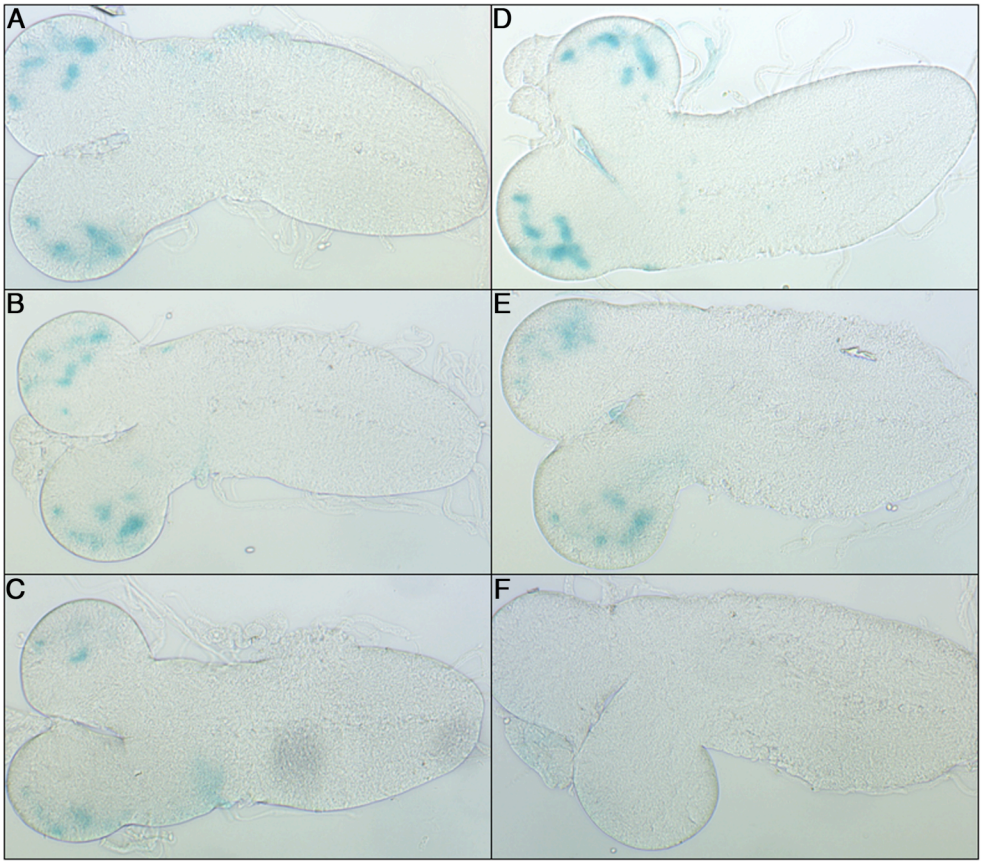


**Figure 3.3. Loss of *UAS-lacZ* expression in $F_1$ progeny is not due to detrimental effect of Gal4 activity.** Two crosses were set up of a homozygous *c529* male and a homozygous *UAS-lacZ* female, which were allowed to mate at 22°C or 18°C, respectively. (A, B, C) The central nervous system (CNS) of developmentally staged 1$^{st}$ instar larvae (28.5-30 hours post-hatching) raised at 22°C were dissected from progeny produced on the (A) 6$^{th}$, (B) 8$^{th}$, and (C) 10$^{th}$ day after mating and activation of *lacZ* expression produced by Gal4 transcriptional activity examined by staining for β-galactosidase activity. (D, E, F) The central nervous system of developmentally staged 1$^{st}$ instar larvae (38-40 hours post-hatching) raised at 18°C were dissected from progeny produced on the (D) 8$^{th}$, (E) 10$^{th}$, and (F) 12$^{th}$ day after mating and activation of *lacZ* expression produced by Gal4 transcriptional activity examined by staining for β-galactosidase activity.

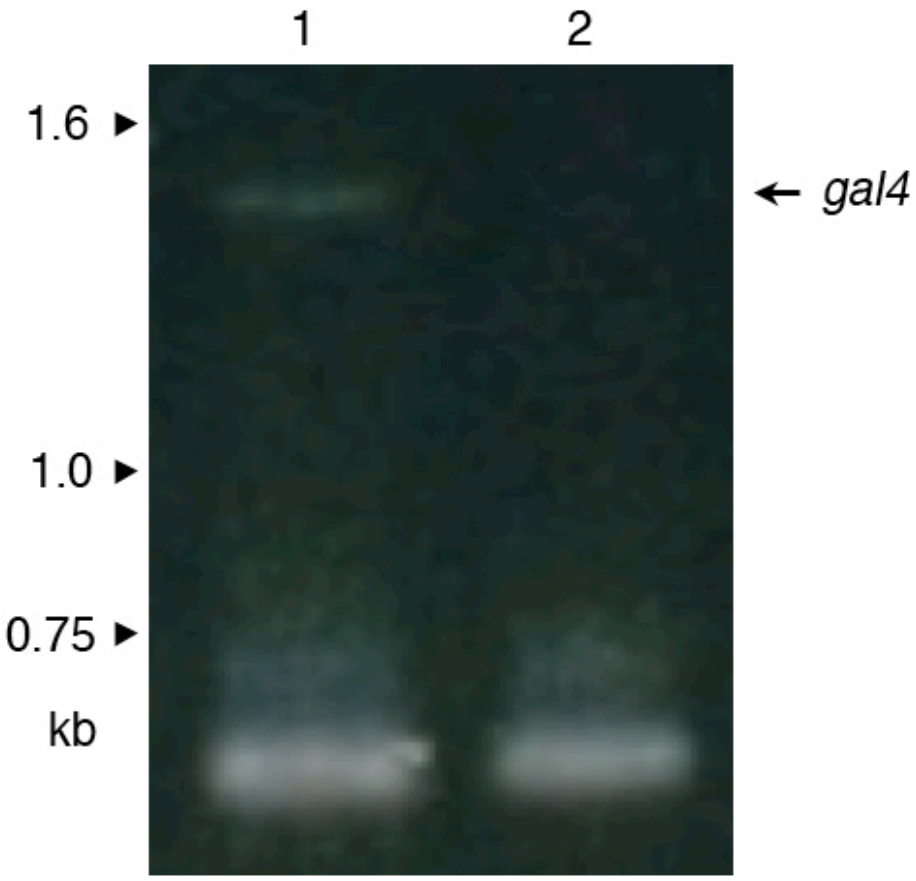


**Figure 3.4. Loss of a portion of the *gal4* gene from the genome of the *c529* stock.** PCR reactions of genomic DNA extracted from individual flies from the *c529* stock using primers that amplify a segment in the C-terminal region of *gal4* and control primers that amplify a segment of the endogenous *trol* gene are shown. Individual reactions were preformed with each primer set, then combined together during resolution, respectively. Lane 1 shows a PCR product at ~1.5 kb which represents the C-terminal region of *gal4*. Lane 2 does not show a *gal4* amplification product.

*Rescue of gal4 instability and reporter gene expression*

It has been shown that infection of *Drosophila* with the bacterial endosymbiont, *Wolbachia pipientis,* rescues the defective fertility phenotype in *Sex-lethal* (*Sxl)* mutants (Starr and Cline, 2002) indicating that Wolbachia infection can affect gene expression or function. Furthermore, a recent report documented Wolbachia infection of a large portion of Drosophila stocks present in a major community stock center (Clark et al., 2005). Due to the unique nature of the phenotype discussed above it postulated that a parasitic infection might be the cause. Therefore, I took a subpopulation of the *c529* stock and raised it at 25°C on cornmeal/molasses media with the addition of the antibiotic tetracycline (0.03 mg $ml^{-1}$) for one generation, then allowing for a two-generation recovery time. By treating the flies with an antibiotic, it would be possible to "cure" the stock of any bacterial infection that could be causing the novel *gal4* phenotype. After antibiotic treatment, genetic and phenotypic analyses of *c529* segregation and activity were followed for two generations compared to the original "untreated" *c529* stock. The experimental design is explained in greater detail in Figure 3.5. Assuming that the P-element in *c529* follows Mendelian segregation and that the parental stocks are homozygous and their *gal4* expression/activity is at 100%, the $F_1$ progeny would be expected to show presence of the *gal4* gene and β-galactosidase activity at 100%. The $F_2$ progeny would be expected to show presence of the *gal4* gene and β-galactosidase activity at 50%. However, when the "untreated" *c529* stock was analyzed $F_1$ progeny show presence of the *gal4* gene and β-galactosidase activity at 58% and 10%, respectively and $F_2$ progeny showed presence of the *gal4* gene and β-

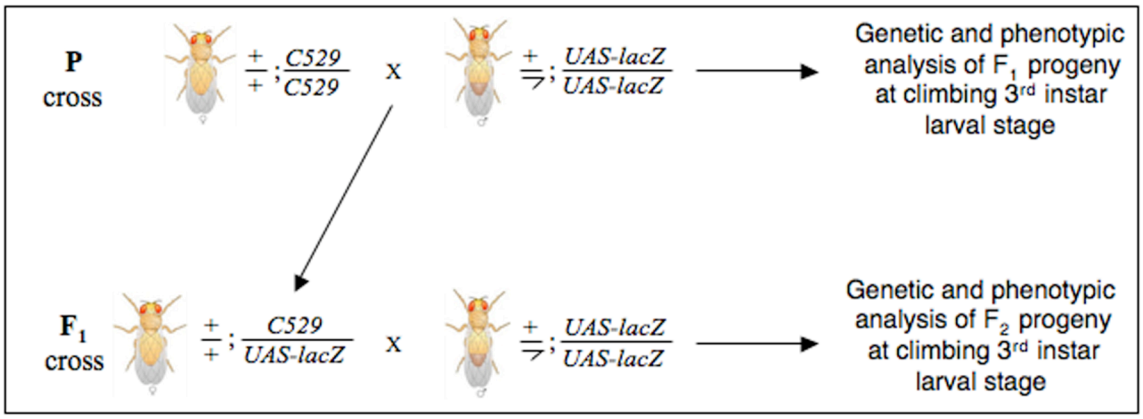


**Figure 3.5. Experimental design for examining Mendelian segregation and activity of the *c529* line.** A homozygous *c529* female, tetracycline treated or untreated control, was crossed to a homozygous *UAS-lacZ* male. From the progeny ($F_1$) generated, CNS and salivary glands were dissected from 10 climbing 3$^{rd}$ instar larvae and stained for β-galactosidase activity. Individual genomic DNA extractions and PCR analyses for the presence of *gal4* in the remaining larval bodies were also done. Then 10 adult female $F_1$ progeny, with one genetic copy of *c529* and *UAS-lacZ* each, were backcrossed to a homozygous *UAS-lacZ* male. From the progeny ($F_2$) generated in each cross, CNS and salivary glands were dissected from 10 climbing 3$^{rd}$ instar larvae and stained for β-galactosidase activity. Individual genomic DNA extractions and PCR analyses for the presence of *gal4* in the remaining larval bodies were also done.

galactosidase activity at 73% and 2%, respectively. When *c529* is treated with tetracycline, $F_1$ progeny show both presence of the *gal4* gene and β-galactosidase activity at 100% and $F_2$ progeny showed presence of the *gal4* gene and β-galactosidase activity at 73% and 43%, respectively (Figure 3.6). Therefore, tetracycline treatment rescues loss of a portion of the *gal4* gene and the resulting β-galactosidase activity.

However, an unexpected result was observed in the percentage of $F_2$ offspring that were PCR-positive for the *gal4* gene. Approximately 73% of both of the untreated controls and tetracycline treated lines contained the *gal4* gene instead of the expected Mendelian ratio of 50%. The observed percentage of gal4 containing $F_2$ progeny is consistent with the hypothesis that the *c529* line contains two copies of the P-element in its genome instead of only one copy, and that these two copies segregate independently in a Mendelian fashion. The presence of two insertions is not at all unusual since P-elements may insert into the genome multiple times during generation of transgenic lines. Furthermore, the possibility that there are two *gal4* carrying P-element insertions in *c529* also suggests that the *gal4* gene causing the larval expression pattern I am monitoring is being lost at an even higher frequency than the data would initially indicate. The loss of the larval brain-expressed *gal4* would be hidden in some animals by the presence of the *gal4* gene in the second P-element insertion. If this is true, we would expect to observe the presence of *gal4* at a higher frequency that β-galactosidase activity in the larval brain, which is indeed observed. Taken together, these data suggest that the original *c529* stock is infected with a bacterium that is the causative agent in genomic/phenotypic loss of the *gal4* gene.

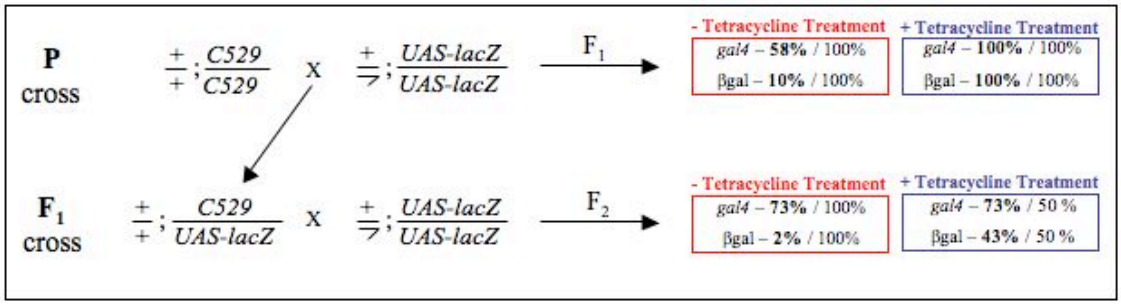


**Figure 3.6. Tetracycline treatment rescues the instability of the *gal4* gene and loss of β-galactosidase activity.** The $F_1$ progeny generated from the parental cross were analyzed for β-galactosidase activity in the CNS and salivary glands and presence of the *gal4* gene from the remaining larval body of 10 climbing 3rd instar. From Ten $F_1$ backcrosses, 10 climbing 3rd instar larvae from each cross were analyzed for β-galactosidase activity in the CNS and salivary glands and presence of the *gal4* gene from the remaining larval body. Values shown in bold are the percentage of larvae analyzed that tested positive for *gal4* and stained for β-galactosidase activity, which is compared to the expected percentages, not in bold, assuming proper Mendelian segregation, gene expression, and enzymatic activity. Both the *c529* stock treated with tetracycline and untreated controls were analyzed.

*Identification of bacterial infection*

Since treatment with tetracycline rescues presence of the *gal4* gene and expression of the lacZ reporter gene, a bacterial parasite is most likely the cause. To date, *Wolbachia pipientis* is the only bacterium that has been shown to alter the phenotype of a *Drosophila* mutant. Therefore, we wanted to determine if the bacterial infection in *c529* was in fact a *Wolbachia* infection. Primers specific for *Wolbachia* detection in genomic DNA extractions of the host were used (O'Neill et al., 1992). A known *Drosophila* strain infected with *Wolbachia* was used as a positive control. Upon PCR analysis, it was determined that neither *c529* with or without treatment with tetracycline showed infection by *Wolbachia* (Figure 3.7). This presents as an interesting result because our data suggest that an unknown bacterium is the cause of a mechanism of genomic instability novel to the *Drosophila* community.

In August 2005, a manuscript describing the "widespread prevalence of *Wolbachia* in laboratory stocks and the implications for *Drosophila* research" was published from Timothy Karr's laboratory (Clark et al., 2005; Clark and Karr, 2002). Like Karr's findings, the results presented here serve to inform the *Drosophila* community of another, yet unknown, bacterium that has the potential to alter not only the phenotype but also the genotype of a host P-element transgene when infected. Further analysis to determine the type of bacterial infection and mechanism/mechanisms utilized by that bacterium to alter host functions is currently under way.

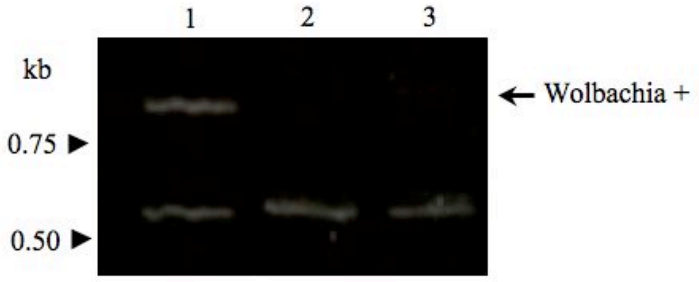


**Figure 3.7. Bacterial infection is not *Wolbachia pipientis*.** PCR reactions of genomic DNA extracted from a *Wolbachia* infected *Drosophila* strain and the *c529* stock before and after tetracycline treatment using primers that amplify a segment specific to the *Wolbachia* 16S rRNA gene and control primers that amplify a segment of the endogenous *trol* gene are shown. Individual reactions were preformed with each primer set, then combined together during resolution, respectively. Lane 1 shows a PCR product at ~ 0.9 kb which represents *Wolbachia* specific 16S rRNA gene. Lane 2 and 3 shows no PCR product for the *Wolbachia* specific 16S rRNA gene.

# CHAPTER IV

# CONCLUSIONS AND FUTURE DIRECTIONS

I am interested in understanding the mechanisms employed in the activation of post-embryonic neural stem cell (neuroblast) proliferation. I have used *Drosophila melanogaster* as a model system to address questions on how specific signaling molecules instruct neuroblasts to exit a quiescent state and begin proliferation. More specifically, I have focused my research on the involvement of the Branchless and Hedgehog signaling pathways in the activation of neuroblast proliferation during a second wave of neurogenesis that occurs in larval development. By utilizing the unique features of larval neurogenesis, I hoped to elucidate the activation mechanism of neuroblast proliferation by Hedgehog and Branchless signaling. With this knowledge, I not only would gain a greater understanding of basic signaling mechanisms but also contribute significantly to the field of stem cell biology.

## HEDGEHOG AND BRANCHLESS SIGNAL THROUGH A POSITIVE FEEDBACK LOOP TO ACTIVATE NEUROBLAST PROLIFERATION

The adult *Drosophila* central nervous system (CNS) is generated through two phases of neurogenesis. The first phase of neurogenesis involves initial identification of the neurogenic region in the embryo followed by neural stem cell (neuroblast) specification and rapid generation of the basic brain and ventral nerve cord structural morphology. The second phase of neurogenesis occurs during larval life and

encompasses reactivation of proliferation in neuroblasts that entered into a quiescent state in late embryogenesis. Through exploitation of larval neurogenesis (second phase), I was able to examine activation of post-embryonic neural stem cell division. My analysis uncovered a positive feedback loop between two signaling molecules, Fibroblast Growth Factor (FGF) and Hedgehog (Hh), which is required for proper activation of post-embryonic neuroblast proliferation (Chapter II).

Both FGF and Hh signaling have been extensively studied and their involvement implicated in numerous processes including cell growth, proliferation, wound healing, and tumorigenesis. More specifically, their roles in development and homeostasis of the central nervous has been widely scrutinized (Ahn and Joyner, 2005; Dono, 2003; Ruiz i Altaba et al., 2002). Previous work in our lab showed that *hh* and the *Drosophila* FGF, *branchless (bnl)*, mutants, in a *trol* mutant background, negatively affected post-embryonic neuroblast proliferation (Park et al., 2003b). This initial look at growth factor signaling and neuroblast proliferation brought to light many questions. Do the Hh and Bnl pathways signal in a dependent or independent manner? Do all of the brain neuroblasts require both Hh and Bnl signaling to exit quiescence or can signals from only one pathway suffice?

To address these questions, I utilized a histological assay to assess neuroblast proliferation and qRT-PCR to monitor the interaction between the *bnl* and *hh* signaling pathways. I found that when Bnl signaling was decreased, causing a defect in neuroblast proliferation, that *hh* expression and activity, determined by expression of the Hh target gene *patched*, were also negatively affected. The same was true when Hh signaling was

decreased, showing the same neuroblast proliferation phenotype. *bnl* expression and activity, determined by expression of its target gene *pointed*, were negatively affected. The converse over-expression experiments again demonstrated dependence, this time in a positive manner, between the *hh* and *bnl* signaling pathways. These studies suggest that *hh* and *bnl* expression and signaling are inter-dependent in the larval CNS. The feed back loop I observed is partially consistent with interactions seen between Shh and specific FGFs in several areas of the vertebrate brain. Embryos injected with both FGF3- and FGF8-morpholinos show a decrease in *shh* expression in the hypothalamus of the developing Zebrafish brain. Expression analysis examined in the ventral thalamus, adjacent to the hypothalamus, showed that only *tiggywinkle hedgehog (twhh)* is regulated by FGF3 and FGF8 activity. This suggests that FGF3 and FGF8 regulate *shh* and *twhh* expression in a region specific manner (Bertrand and Dahmane, 2006; Walshe and Mason, 2003).

True FGF-Hh positive feedback loops have been shown in development of the vertebrate limb bud and chick retinal regeneration (Niswander et al., 1994; Spence et al., 2007). This is the first time that a true Hh-FGF feedback loop has been demonstrated in the invertebrate or vertebrate CNS. However, the question still remains as to whether all of the quiescent brain neuroblasts receive the same signal or if there are neuroblasts that only respond to one signaling molecule? A recent study from the Joyner lab showed that two neurogenic regions of the post-embryonic vertebrate brain, the dentate gyrus and subventricular zone (SVZ), show activation of quiescent neural stem cells, called astrocytes, in response to Shh signaling (Ahn and Joyner, 2005). From these data, you

could therefore postulate that it would seem reasonable for all neuroblasts in the same region to require the same signal. If both FGF and Hh signaling directly activated neuroblast proliferation, then defects in neuroblast proliferation by loss of one signaling pathway should be partially or fully rescued by over expression of the other signaling pathway. However, if only one signaling pathway directly activates neuroblast proliferation, then a defect in that same pathway would not be rescued by over expression of the other pathway. In fact, that is exactly what we see for activation of CB and OL neuroblasts in the *Drosophila* 1$^{st}$ larval instar brain. In null *bnl* homozygous mutants, proliferation is seen in only the MB and VL neuroblasts. Amazingly, when *hh* is over expressed in the same null *bnl* mutants, none of the CB or OL neuroblasts are induced to proliferate, leaving the MB and VL neuroblasts as the only cells proliferating. As expected, the opposite finding is seen when *bnl* is over expressed in $hh^{ts2}$ mutants, not only is neuroblast proliferation fully rescued, but expression of *hh* and *hh* target genes is upregulated, further evidence of Bnl and Hh inter-dependent signaling.

Elucidation of this FGF-Hh feedback loop with respect to regulation of *Drosophila* neuroblast proliferation is significant because it could help shed light on the mechanisms used to induce proliferation of adult neural stem cells in the higher systems like the mammalian or vertebrate brain, which is sorely lacking. Currently, there have been two main areas of neurogenesis identified in the vertebrate adult brain. The subventricular zone (SVZ) of the lateral ventricle and the dentate gyrus subgranular zone (SGZ) within the hippocampus (Cayuso and Marti, 2005; Temple and Alvarez-Buylla,

1999). *In vitro* and *in vivo*, studies have been done on neural stems cells of these areas to define the factors that guide proliferation, differentiation, and survival.

Many factors important in development of the adult brain persist after embryogenesis and function in the adult brain, which make these factors an attractive focus for possible involvement in regulation of neural stem cell proliferation. In the SVZ, *in vitro* or *in vivo* stimulation of neural stem cell proliferation by FGF-2, EGF, VEGF, TGFα or Shh have been shown. Most of the same molecules, except TGFα and Eph/ephrin, have also been shown to increase neural stem cell proliferation in the dentate gyrus using *in vitro* or *in vivo* methods (Alvarez-Buylla and Lim, 2004; Alvarez-Buylla et al., 2002; Craig et al., 1996; Gage, 2000; Gritti et al., 1999; Wagner et al., 1999). However, the mechanism/s of growth factor interactions/signaling in the initiation of neural stem cell proliferation has not been widely studied.

The first evidence showing induction of neural stem cell proliferation and neurogenesis by a growth factor was done *in vitro* with the isolation of proliferating cells from the striatum of the adult mouse brain (Reynolds and Weiss, 1992).When cells were cultured in serum free media plus Epidermal Growth Factor (EGF), most cells died in culture. However a small percentage of the cells instead underwent proliferation. Unfortunately, addition of basic Fibroblast Growth Factor (bFGF), Platelet-derived Growth Factor (PDGF), or Nerve Growth Factor (NGF failed to induced the same response. After ~8 days *in vitro* (DIV) all of the EGF responsive proliferating cells detached from the culture plate and associated together in a sphere, called a neurosphere. The proliferating cells initially stained positive for the neural stem cell marker Nestin, an

intermediate filament found in neuroepithelial cells. It was then postulated that the cells that formed the neurosphere were ependymal stem cells located in the striatum. After ~25 DIV, cells were seen starting to migrate out of the neurosphere and marker analysis determined that cells with the morphological and antigenic property of both neurons and astrocytes were being generated. Adult neurogenesis does not occur in the striatum after approximately 1 day post-natal, however these data suggested that embryonic populations of neural stem cells survive in the adult striatum in a quiescent state and are shown to be responsive to EGF signaling *in vitro*. Similar experiments done in other areas of the adult brain identified multipotent stem cells present in the subventricular zone of the lateral ventricle, the 3$^{rd}$ and 4$^{th}$ ventricles, and all regions of the spinal cord (Morshead et al., 1994; Weiss et al., 1996). All were responsive to either EGF or an EGF/bFGF combination.

Another very elegant set of *in vivo* experiments showed that injection of EGF or bFGF in the subventricular layer (SVZ) of the lateral ventricle increased the number of proliferating cells, although at differing levels, ~16- and 2.4-fold, respectively. This increase in cell proliferation was shown to be an increase in proliferation of neural stem cell that were previously quiescent, shown by the large increase in the number of neurospheres formed *in vitro* with prior *in vivo* injection of either EGF or bFGF, 370% and 49% increase, respectively. These findings go in line with the effects I see in growth factor stimulation of *Drosophila* post-embryonic neuroblasts although only at the level of stimulation of proliferation through growth factor signaling. My findings advance our knowledge of growth factor signaling and stem cell activation by looking at not only

stimulation of neural stem cell proliferation but also the mechanisms underlying the initial activation of cell division. I am the first to show that FGF and Hh signal through an inter-dependent pathway by way of regulation of growth factor and pathway component expression. Many of the studies that have looked at growth factor regulation of neural stem cell proliferation have looked at either FGF or EGF signaling. Only limited studies have been done with regards to other growth factor involvement in neural stem cell proliferation. To date only a handful of studies have shown that Shh may play a role in stimulation of adult neural stem cells in the vertebrate brain (Lai et al., 2003; Palma et al., 2005). However, correlation between Shh signaling and other signaling pathways known to be involved in neural stem cell proliferation has yet to be examined. This leaves a huge gap in our knowledge of neural stem cell regulation. I believe that my work has provided a major stepping-stone for guidance of future research in elucidating the mechanisms involved in neural stem cell proliferation. I also believe that my model of FGF and Hh pathway interaction in stimulation of quiescent neural stem cells may be conserved in the vertebrate system, shown not only by the conservation of pathway components but the evidence of functional conservation seen in processes like embryonic patterning and organ development between flies and vertebrates.

To date, elucidation of the signaling mechanisms/interactions utilized by growth factors to stimulate quiescent neural stem proliferation has yet to be addressed. Although still in its infancy, understanding neural stem cell regulation poses as possibly one of the most exciting areas of stem cell biology at present. Many neurological diseases involve the death of specific types of neurons required for proper neurological

function. Therefore, understanding how to manipulate endogenous neural stem cells to generate new neurons for repaired neurological function is tantamount to the ultimate goal for neural stem cell researchers.

Since the introduction of stem cells to the scientific community, it has been shown that almost every organ in the body contains some form of stem cells (Mimeault et al., 2007). This begs the question as to whether stem cell regulation in one environment is similar to or completely different from regulation in a different environment. Extensive research has been done on a wide variety of stem cell types including germ-line, embryonic, and hematopoietic stem cells, for example. In the hematopoietic system, hematopoietic stem cells (HSC) are stem cells that give rise to all blood cell types in the body (Metcalf, 1998a). Most of the information known about HSCs involves the elucidation of their origin and lineage tracing. A substantial amount of research is also devoted to the factors that regulate differentiation and development of mature hematopoietic cells. Several growth factors/cytokines have been shown to regulate formation of progenitor cells from stem cells. IL-1, IL-3, IL-6, SCF, and G-CSF are just a few known regulators of HSC proliferation. Each factor has been shown to regulate HSC populations, however it has been shown that combinations of factors are required for proliferation of HSCs (Metcalf, 1993; Metcalf, 1998b). Only limited expansion of these findings with regards to pathway interactions has been looked at to date. Again, a major aspect of activation of stem cell proliferation remains to be elucidated. Therefore, a molecular dissection of the activation of stem cell proliferation

needs to be undertaken. The work that I have presented in this dissertation provides direction for future research throughout the stem cell community.

*Future directions*

I have clearly established the presence of a positive feedback loop between Hh and Bnl in the larval CNS. I have also shown that Bnl signaling activation is required by all of the quiescent neuroblasts to begin proliferation. These results provide a strong foundation for elucidating the complete mechanism of action taken when Bnl and Hh signal to quiescent neuroblasts, inducing them into a proliferative state. Several aspects of this signaling model need to be addressed. First and foremost, I believe that the identification of the Hh and Bnl producing/responding cells is a key piece of information missing from the puzzle that would greatly help in understanding the requirements needed for neural stem cell reactivation. It is possible, even though Bnl and Hh signaling have been shown to induce activation of neuroblast proliferation, that neither Bnl nor Hh directly signal to a neuroblast. Another player could be involved.

Secondly, a way to label individual or small groups of neuroblasts in the 1$^{st}$ instar brain is needed. Neuroblast molecular marker maps have been published for embryonic and post-embryonic (3$^{rd}$ instar) neuroblasts, however none of the molecular markers we have tried are visible in the 1$^{st}$ instar CNS (Doe, 1992; Urbach and Technau, 2003a; Urbach and Technau, 2003b). This would allow for finer dissection of the mechanism of growth factor signaling at a signal cell level.

Another facet of the Bnl-Hh feedback loop that needs to be addressed is the mechanism of pathway interaction. Does Bnl signal through the RAS/MAP Kinase cascade to regulate *hh* and/or *hh* target gene expression at the transcriptional level? Or do the Bnl and Hh pathways interact through an unknown intermediate? Further elucidating the interactions between Bnl and Hh will not only increase our understanding of signal transduction pathways and development in Drosophila, but also help advance the field of stem cell biology.

## HOST-PARASITE INFECTION CONTRIBUTES TO *gal4* INSTABILITY IN P-ELEMENT INSERTION

Almost every species on Earth in some way or another relies on a Host-parasite interaction. These interactions exist in many forms, which in some cases go completely unnoticed or in others are extremely detrimental to the host. Therefore, the study of the effects of parasite infection on host competence is a broad and critical field of research. I have examined the effects of bacterial infection on genomic stability in *Drosophila melanogaster*. My analysis discovered a unique host-parasite interaction that causes, by an unknown mechanism, P-element instability through partial excision/loss of segments of the P-element in the host genome (Chapter 3).

P-elements are transposable forms of DNA whose unique features have been harnessed in the development of the GAL4/UAS system (Brand and Perrimon, 1993). The system allows for spatial and temporal expression of a particular target gene within the *Drosophila* organism. A *Drosophila* P-element insertion line, called *c529*,

containing the yeast *gal4* gene, unexpectedly showed loss of reporter gene expression. This loss was more specifically observed to be a gradual loss in reporter expression in progeny from the same parental cross over just a few days time. I also observed genomic loss of a segment of the *gal4* gene in the *c529* stock. There are several possibilities for this phenomenon, which include loss of the *gal4* gene in the genome either by heterozygosity in either parental strain, excision of the P-element, silencing of *gal4* expression, or an accumulation of mutations in the *gal4* gene, to name a few.

Through genetic and phenotypic analysis, I showed that loss of a segment in the *gal4* gene and reporter gene expression was not due to parental heterozygosity, whole P-element excision, or detrimental affects of Gal4 activity. Since the loss of the *gal4* gene and reporter activity could not but attributed to some of these events, it was proposed that a secondary agent could be the effector. Interestingly, a published study from the Cline lab showed alteration of the *Sex lethal (Sxl)* mutant phenotype upon infection with the bacterial endosymbiont *Wolbachia pipientis* (Starr and Cline, 2002). This study suggested that *Wolbachia* could affect gene expression/function. More recently, another study published from the Karr lab showed that a large proportion of the stocks from a widely used *Drosophila* stock center (Bloomington Stock Center) were infected with *Wolbachia* (Clark et al., 2005). I then asked if a bacterial infection could be the causative agent in the establishment of this unique genomic instability and whether treatment with the antibiotic, tetracycline, could rescue this phenotype. After "curing" with tetracycline, I showed that loss of *gal4* and reporter activity was rescued. I believed

that *Wolbachia* was the most likely candidate for infection. However, PCR analysis showed that the bacterial infection was not *Wolbachia*.

The results presented here serve to inform the *Drosophila* community of another, yet unknown, bacterium that has the potential to alter not only the phenotype but also the genotype of a host P-element transgene when infected.

*Future directions*

I have established that a bacterial infection causes, by some unknown mechanism, the gradual loss of reporter gene activity and loss of a segment of the *gal4* gene in a P-element generated *Drosophila* line, called c529. First, the identification the infecting bacterium through a wide spread PCR analysis is crucial to discerning possible mechanisms employed in upon infection.

Secondly, to molecularly decipher loss of only a segment of the *gal4* gene the complete sequence of excised DNA must be determined. Lastly, P-element insertional analysis should be carried out on the c529 line to determine if more than one P-element is inserted and where they are present in genome.

## CONCLUSIONS

Using powerful genetic and molecular tools available in *Drosophila melanogaster*, I have participated in research that has significantly added to the field of stem cell biology. These studies have provided new insight into the activation of

proliferation in post-embryonic neural stem cells and laid the solid foundation for understanding the basic signaling pathway interactions.

# REFERENCES

Abate-Shen, C., and Shen, M. M. 2000. Molecular gentics of prostate cancer. Genes Dev 14**,** 2410.

Agren, M., Kogerman, P., Kleman, M. I., Wessling, M., and Toftgard, R. 2004. Expression of the PTCH1 tumor suppressor gene is regulated by alternative promoters and a single functional Gli-binding site. Gene 330**,** 101-14.

Ahn, S., and Joyner, A. L. 2005. *In vivo* analysis of quiescent adult neural stem cells responding to Sonic hedgehog. Nature 437**,** 894-7.

Albornoz, J., and Dominguez, A. 1999. Spontaneous changes in *Drosophila melanogaster* transposable elements and their effects on fitness. Heredity 83 ( Pt 6)**,** 663-70.

Alvarez-Buylla, A., and Lim, D. A. 2004. For the long run: maintaining germinal niches in the adult brain. Neuron 41**,** 683-6.

Alvarez-Buylla, A., Seri, B., and Doetsch, F. 2002. Identification of neural stem cells in the adult vertebrate brain. Brain Res Bull 57**,** 751-8.

Aoto, K., Nishimura, T., Eto, K., and Motoyama, J. 2002. Mouse GLI3 regulates Fgf8 expression and apoptosis in the developing neural tube, face, and limb bud. Dev Biol 251**,** 320-32.

Arendt, D., and Nubler-Jung, K. 1999. Comparison of early nerve cord development in insects and vertebrates. Development 126**,** 2309-25.

Bai, C. B., and Joyner, A. L. 2001. Gli1 can rescue the *in vivo* function of Gli2. Development 128**,** 5161-72.

Barnett, D. H., Huang, H. Y., Wu, X. R., Laciak, R., Shapiro, E., and Bushman, W. 2002. The human prostate expresses sonic hedgehog during fetal development. J Urol 168**,** 2206-10.

Bellaiche, Y., The, I., and Perrimon, N. 1998. Tout-velu is a *Drosophila* homologue of the putative tumour suppressor EXT-1 and is needed for Hh diffusion. Nature 394**,** 85-8.

Bellusci, S., Grindley, J., Emoto, H., Itoh, N., and Hogan, B. L. 1997. Fibroblast growth factor 10 (FGF10) and branching morphogenesis in the embryonic mouse lung. Development 124**,** 4867-78.

Bellusci, S., Henderson, R., Winnier, G., Oikawa, T., and Hogan, B. L. 1996. Evidence from normal expression and targeted misexpression that bone morphogenetic protein (Bmp-4) plays a role in mouse embryonic lung morphogenesis. Development 122**,** 1693-702.

Berman, D. M., Desai, N., Wang, X., Karhadkar, S. S., Reynon, M., Abate-Shen, C., Beachy, P. A., and Shen, M. M. 2004. Roles for Hedgehog signaling in androgen production and prostate ductal morphogenesis. Dev Biol 267**,** 387-98.

Berman, D. M., Karhadkar, S. S., Hallahan, A. R., Pritchard, J. I., Eberhart, C. G., Watkins, D. N., Chen, J. K., Cooper, M. K., Taipale, J., Olson, J. M., and Beachy, P. A. 2002. Medulloblastoma growth inhibition by hedgehog pathway blockade. Science 297**,** 1559-61.

Berman, D. M., Karhadkar, S. S., Maitra, A., Montes De Oca, R., Gerstenblith, M. R., Briggs, K., Parker, A. R., Shimada, Y., Eshleman, J. R., Watkins, D. N., and Beachy, P. A. 2003. Widespread requirement for Hedgehog ligand stimulation in growth of digestive tract tumours. Nature 425**,** 846-51.

Bertrand, N., and Dahmane, N. 2006. Sonic hedgehog signaling in forebrain development and its interactions with pathways that modify its effects. Trends Cell Biol 16**,** 597-605.

Blaess, S., Corrales, J. D., and Joyner, A. L. 2006. Sonic hedgehog regulates Gli activator and repressor functions with spatial and temporal precision in the mid/hindbrain region. Development 133**,** 1799-809.

Bongso, A., and Richards, M. 2004. History and perspective of stem cell research. Best Pract Res Clin Obstet Gynaecol 18**,** 827-42.

Bonkhoff, H. 1996. Role of the basal cells in premalignant changes of the human prostate: a stem cell concept for the development of prostate cancer. Eur Urol 30**,** 201-5.

Bornemann, D. J., Duncan, J. E., Staatz, W., Selleck, S., and Warrior, R. 2004. Abrogation of heparan sulfate synthesis in *Drosophila* disrupts the Wingless, Hedgehog and Decapentaplegic signaling pathways. Development 131**,** 1927-38.

Bostwick, D. G., Burke, H. B., Djakiew, D., Euling, S., Ho, S. M., Landolph, J., Morrison, H., Sonawane, B., Shifflett, T., Waters, D. J., and Timms, B. 2004. Human prostate cancer risk factors. Cancer 101**,** 2371-490.

Bottcher, R. T., and Niehrs, C. 2005. Fibroblast growth factor signaling during early vertebrate development. Endocr Rev 26**,** 63-77.

Brand, A. H., and Perrimon, N. 1993. Targeted gene expression as a means of altering cell fates and generating dominant phenotypes. Development 118**,** 401-15.

Brewster, R., Mullor, J. L., and Ruiz i Altaba, A. 2000. Gli2 functions in FGF signaling during antero-posterior patterning. Development 127**,** 4395-405.

Burke, R., Nellen, D., Bellotto, M., Hafen, E., Senti, K. A., Dickson, B. J., and Basler, K. 1999. Dispatched, a novel sterol-sensing domain protein dedicated to the release of cholesterol-modified hedgehog from signaling cells. Cell 99**,** 803-15.

Caldwell, M. C., and Datta, S. 1998. Expression of *cyclin E* or *DP/E2F* rescues the G1 arrest of *trol* mutant neuroblasts in the *Drosophila* larval central nervous system. Mech Dev 79**,** 121-30.

Campbell, G. 2002. Distalization of the *Drosophila* leg by graded EGF-receptor activity. Nature 418**,** 781-5.

Cayuso, J., and Marti, E. 2005. Morphogens in motion: growth control of the neural tube. J Neurobiol 64**,** 376-87.

Chandran, S., Kato, H., Gerreli, D., Compston, A., Svendsen, C. N., and Allen, N. D. 2003. FGF-dependent generation of oligodendrocytes by a hedgehog-independent pathway. Development 130**,** 6599-609.

Chen, J. K., Taipale, J., Cooper, M. K., and Beachy, P. A. 2002. Inhibition of Hedgehog signaling by direct binding of cyclopamine to Smoothened. Genes Dev 16**,** 2743-8.

Chuang, P. T., Kawcak, T., and McMahon, A. P. 2003. Feedback control of mammalian Hedgehog signaling by the Hedgehog-binding protein, Hip1, modulates Fgf signaling during branching morphogenesis of the lung. Genes Dev 17**,** 342-7.

Clark, M. E., Anderson, C. L., Cande, J., and Karr, T. L. 2005. Widespread prevalence of *Wolbachia* in laboratory stocks and the implications for *Drosophila* research. Genetics 170**,** 1667-75.

Clark, M. E., and Karr, T. L. 2002. Distribution of *Wolbachia* within *Drosophila* reproductive tissue: Implications for the expression of Cytoplasmic Incompatibility. Integ. and Comp. Biol. 42**,** 332-339.

Cohen, I. R., Murdoch, A. D., Naso, M. F., Marchetti, D., Berd, D., and Iozzo, R. V. 1994. Abnormal expression of perlecan proteoglycan in metastatic melanomas. Cancer Res 54**,** 5771-4.

Conlon, E. M., Goode, E. L., Gibbs, M., Stanford, J. L., Badzioch, M., Janer, M., Kolb, S., Hood, L., Ostrander, E. A., Jarvik, G. P., and Wijsman, E. M. 2003. Oligogenic segregation analysis of hereditary prostate cancer pedigrees: evidence for multiple loci affecting age at onset. Int J Cancer 105**,** 630-5.

Cornell, R. A., and Ohlen, T. V. 2000. Vnd/nkx, ind/gsh, and msh/msx: conserved regulators of dorsoventral neural patterning? Curr Opin Neurobiol 10**,** 63-71.

Craig, C. G., Tropepe, V., Morshead, C. M., Reynolds, B. A., Weiss, S., and van der Kooy, D. 1996. In vivo growth factor expansion of endogenous subependymal neural precursor cell populations in the adult mouse brain. J Neurosci 16**,** 2649-58.

Dahmane, N., Lee, J., Robins, P., Heller, P., and Ruiz i Altaba, A. 1997. Activation of the transcription factor Gli1 and the Sonic hedgehog signalling pathway in skin tumours. Nature 389**,** 876-81.

Dahmane, N., and Ruiz i Altaba, A. 1999. Sonic hedgehog regulates the growth and patterning of the cerebellum. Development 126**,** 3089-100.

Dahmane, N., Sanchez, P., Gitton, Y., Palma, V., Sun, T., Beyna, M., Weiner, H., and Ruiz i Altaba, A. 2001. The Sonic Hedgehog-Gli pathway regulates dorsal brain growth and tumorigenesis. Development 128**,** 5201-12.

Datta, M. W., Hernandez, A. M., Schlicht, M. J., Kahler, A. J., DeGueme, A. M., Dhir, R., Shah, R. B., Farach-Carson, C., Barrett, A., and Datta, S. 2006a. Perlecan, a candidate gene for the CAPB locus, regulates prostate cancer cell growth via the Sonic Hedgehog pathway. Mol Cancer 5**,** 9.

Datta, S. 1995. Control of proliferation activation in quiescent neuroblasts of the *Drosophila* central nervous system. Development 121**,** 1173-82.

Datta, S. 1999. Activation of neuroblast proliferation in explant culture of the *Drosophila* larval CNS. Brain Res 818**,** 77-83.

Datta, S., and Datta, M. W. 2006. Sonic Hedgehog signaling in advanced prostate cancer. Cell Mol Life Sci.

Datta, S., and Kankel, D. R. 1992. *l(1)trol* and *l(1)devl*, loci affecting the development of the adult central nervous system in *Drosophila melanogaster*. Genetics 130**,** 523-37.

Datta, S., Pierce, M., and Datta, M. W. 2006b. Perlecan signaling: helping hedgehog stimulate prostate cancer growth. Int J Biochem Cell Biol 38**,** 1855-61.

De Marzo, A. M., Nelson, W. G., Meeker, A. K., and Coffey, D. S. 1998. Stem cell features of benign and malignant prostate epithelial cells. J Urol 160**,** 2381-92.

DeMarzo, A. M., Nelson, W. G., Isaacs, W. B., and Epstein, J. I. 2003. Pathological and molecular aspects of prostate cancer. Lancet 361**,** 955-64.

Doe, C. Q. 1992. Molecular markers for identified neuroblasts and ganglion mother cells in the *Drosophila* central nervous system. Development 116**,** 855-63.

Doe, C. Q. 1996. Asymmetric cell division and neurogenesis. Curr Opin Genet Dev 6**,** 562-6.

Doetsch, F., Caille, I., Lim, D. A., Garcia-Verdugo, J. M., and Alvarez-Buylla, A. 1999. Subventricular zone astrocytes are neural stem cells in the adult mammalian brain. Cell 97**,** 703-16.

Dong, J., Gailani, M. R., Pomeroy, S. L., Reardon, D., and Bale, A. E. 2000. Identification of PATCHED mutations in medulloblastomas by direct sequencing. Hum Mutat 16**,** 89-90.

Dono, R. 2003. Fibroblast growth factors as regulators of central nervous system development and function. Am J Physiol Regul Integr Comp Physiol 284**,** R867-81.

Easton, D. F., Schaid, D. J., Whittemore, A. S., and Isaacs, W. J. 2003. Where are the prostate cancer genes?-A summary of eight genome wide searches. Prostate 57**,** 261-9.

Ebens, A. J., Garren, H., Cheyette, B. N., and Zipursky, S. L. 1993. The *Drosophila anachronism* locus: a glycoprotein secreted by glia inhibits neuroblast proliferation. Cell 74**,** 15-27.

Egger, B., Boone, J. Q., Stevens, N. R., Brand, A. H., and Doe, C. Q. 2007a. Regulation of spindle orientation and neural stem cell fate in the *Drosophila* optic lobe. Neural Develop 2**,** 1.

Egger, B., Chell, J. M., and Brand, A. H. 2007b. Insights into neural stem cell biology from flies. Philos Trans R Soc Lond B Biol Sci.

Engels, W. R. 1997. Invasions of P elements. Genetics 145**,** 11-5.

Erickson, J. (2004). pp. personal communication.

Ericson, J., Morton, S., Kawakami, A., Roelink, H., and Jessell, T. M. 1996. Two critical periods of Sonic Hedgehog signaling required for the specification of motor neuron identity. Cell 87**,** 661-73.

Fallon, J., Reid, S., Kinyamu, R., Opole, I., Opole, R., Baratta, J., Korc, M., Endo, T. L., Duong, A., Nguyen, G., Karkehabadhi, M., Twardzik, D., Patel, S., and Loughlin, S. 2000. *In vivo* induction of massive proliferation, directed migration, and differentiation of neural cells in the adult mammalian brain. Proc Natl Acad Sci U S A 97**,** 14686-91.

Fan, L., Pepicelli, C. V., Dibble, C. C., Catbagan, W., Zarycki, J. L., Laciak, R., Gipp, J., Shaw, A., Lamm, M. L., Munoz, A., Lipinski, R., Thrasher, J. B., and Bushman, W. 2004. Hedgehog signaling promotes prostate xenograft tumor growth. Endocrinology 145**,** 3961-70.

Ford-Perriss, M., Abud, H., and Murphy, M. 2001. Fibroblast growth factors in the developing central nervous system. Clin Exp Pharmacol Physiol 28**,** 493-503.

Freestone, S. H., Marker, P., Grace, O. C., Tomlinson, D. C., Cunha, G. R., Harnden, P., and Thomson, A. A. 2003. Sonic hedgehog regulates prostatic growth and epithelial differentiation. Dev Biol 264**,** 352-62.

Gage, F. H. 2000. Mammalian neural stem cells. Science 287**,** 1433-8.

Gage, F. H., Ray, J., and Fisher, L. J. 1995. Isolation, characterization, and use of stem cells from the CNS. Annu Rev Neurosci 18**,** 159-92.

Gallet, A., Rodriguez, R., Ruel, L., and Therond, P. P. 2003. Cholesterol modification of hedgehog is required for trafficking and movement, revealing an asymmetric cellular response to hedgehog. Dev Cell 4**,** 191-204.

Geldmacher-Voss, B., Reugels, A. M., Pauls, S., and Campos-Ortega, J. A. 2003. A 90-degree rotation of the mitotic spindle changes the orientation of mitoses of zebrafish neuroepithelial cells. Development 130**,** 3767-80.

Gibbs, M., Stanford, J. L., McIndoe, R. A., Jarvik, G. P., Kolb, S., Goode, E. L., Chakrabarti, L., Schuster, E. F., Buckley, V. A., Miller, E. L., Brandzel, S., Li, S., Hood, L., and Ostrander, E. A. 1999. Evidence for a rare prostate cancer-susceptibility locus at chromosome 1p36. Am J Hum Genet 64**,** 776-87.

Goodrich, L. V., Johnson, R. L., Milenkovic, L., McMahon, J. A., and Scott, M. P. 1996. Conservation of the hedgehog/patched signaling pathway from flies to mice: induction of a mouse patched gene by Hedgehog. Genes Dev 10**,** 301-12.

Grachtchouk, V., Grachtchouk, M., Lowe, L., Johnson, T., Wei, L., Wang, A., de Sauvage, F., and Dlugosz, A. A. 2003. The magnitude of hedgehog signaling activity defines skin tumor phenotype. Embo J 22**,** 2741-51.

Green, P., Hartenstein, A. Y., and Hartenstein, V. 1993. The embryonic development of the *Drosophila* visual system. Cell and Tissue Research 273**,** 583-598.

Greene, M. H. 1999. The genetics of hereditary melanoma and nevi. 1998 update. Cancer 86**,** 2464-77.

Gritti, A., Frolichsthal-Schoeller, P., Galli, R., Parati, E. A., Cova, L., Pagano, S. F., Bjornson, C. R., and Vescovi, A. L. 1999. Epidermal and fibroblast growth factors behave as mitogenic regulators for a single multipotent stem cell-like population from the subventricular region of the adult mouse forebrain. J Neurosci 19**,** 3287-97.

Groth, C., and Lardelli, M. 2002. The structure and function of vertebrate fibroblast growth factor receptor 1. Int J Dev Biol 46**,** 393-400.

Gryzik, T., and Muller, H. A. 2004. FGF8-like1 and FGF8-like2 encode putative ligands of the FGF receptor Htl and are required for mesoderm migration in the *Drosophila* gastrula. Curr Biol 14**,** 659-67.

Gutin, G., Fernandes, M., Palazzolo, L., Paek, H., Yu, K., Ornitz, D. M., McConnell, S. K., and Hebert, J. M. 2006. FGF signalling generates ventral telencephalic cells independently of SHH. Development 133**,** 2937-46.

Hahn, H., Wicking, C., Zaphiropoulous, P. G., Gailani, M. R., Shanley, S., Chidambaram, A., Vorechovsky, I., Holmberg, E., Unden, A. B., Gillies, S.,

Negus, K., Smyth, I., Pressman, C., Leffell, D. J., Gerrard, B., Goldstein, A. M., Dean, M., Toftgard, R., Chenevix-Trench, G., Wainwright, B., and Bale, A. E. 1996. Mutations of the human homolog of *Drosophila* patched in the nevoid basal cell carcinoma syndrome. Cell 85**,** 841-51.

Hartenstein, V. 1993. Atlas of *Drosophila* Development. Cold Spring Harbor Laboratory Press, Cold Spring Harbor, New York.

Hartenstein, V., Rudloff, E., and Campos-Ortega, J. A. 1987. The pattern of proliferation of the neuroblasts in the wild-type embryo of *Drosophila melanogaster*. Roux' Arch. Devl. Biol. 196**,** 473-485.

Hassell, J., Yamada, Y., and Arikawa-Hirasawa, E. 2002. Role of perlecan in skeletal development and diseases. Glycoconj J 19**,** 263-7.

Hecht, J. T., Hall, C. R., Snuggs, M., Hayes, E., Haynes, R., and Cole, W. G. 2002. Heparan sulfate abnormalities in exostosis growth plates. Bone 31**,** 199-204.

Ho, K. S., and Scott, M. P. 2002. Sonic hedgehog in the nervous system: functions, modifications and mechanisms. Curr Opin Neurobiol 12**,** 57-63.

Hofbauer, A., and Campos-Ortega, J. A. 1990. Proliferation pattern and early differentiation of the optic lobes in *Drosophila melanogaster*. Roux's Archives of Developmental Biology 198**,** 264-274.

Horoszewicz, J. S., Leong, S. S., Chu, T. M., Wajsman, Z. L., Friedman, M., Papsidero, L., Kim, U., Chai, L. S., Kakati, S., Arya, S. K., and Sandberg, A. A. 1980. The LNCaP cell line--a new model for studies on human prostatic carcinoma. Prog Clin Biol Res 37**,** 115-32.

Hynes, M., Stone, D. M., Dowd, M., Pitts-Meek, S., Goddard, A., Gurney, A., and Rosenthal, A. 1997. Control of cell pattern in the neural tube by the zinc finger transcription factor and oncogene Gli-1. Neuron 19**,** 15-26.

Ingham, P. W., and McMahon, A. P. 2001. Hedgehog signaling in animal development: paradigms and principles. Genes Dev 15**,** 3059-87.

Iozzo, R. V., Cohen, I. R., Grassel, S., and Murdoch, A. D. 1994. The biology of perlecan: the multifaceted heparan sulphate proteoglycan of basement membranes and pericellular matrices. Biochem J 302**,** 625-39.

Ito, K., and Hotta, Y. 1991. Proliferation pattern of postembryonic neuroblasts in the brain of *Drosophila melanogaster*. Developmental Biology 149**,** 134-148.

Janer, M., Friedrichsen, D. M., Stanford, J. L., Badzioch, M. D., Kolb, S., Deutsch, K., Peters, M. A., Goode, E. L., Welti, R., DeFrance, H. B., Iwasaki, L., Li, S., Hood, L., Ostrander, E. A., and Jarvik, G. P. 2003. Genomic scan of 254 hereditary prostate cancer families. Prostate 57**,** 309-19.

Jia, J., and Jiang, J. 2006. Decoding the Hedgehog signal in animal development. Cell Mol Life Sci 63**,** 1249-65.

Johnson, R. L., Rothman, A. L., Xie, J., Goodrich, L. V., Bare, J. W., Bonifas, J. M., Quinn, A. G., Myers, R. M., Cox, D. R., Epstein, E. H., Jr., and Scott, M. P. 1996. Human homolog of patched, a candidate gene for the basal cell nevus syndrome. Science 272**,** 1668-71.

Kaighn, M. E., Lechner, J. F., Narayan, K. S., and Jones, L. W. 1978. Prostate carcinoma: tissue culture cell lines. Natl Cancer Inst Monogr**,** 17-21.

Kan, M., Wang, F., Xu, J., Crabb, J. W., Hou, J., and McKeehan, W. L. 1993. An essential heparin-binding domain in the fibroblast growth factor receptor kinase. Science 259**,** 1918-21.

Kaplan-Lefko, P. J., Chen, T. M., Ittmann, M. M., Barrios, R. J., Ayala, G. E., Huss, W. J., Maddison, L. A., Foster, B. A., and Greenberg, N. M. 2003. Pathobiology of autochthonous prostate cancer in a pre-clinical transgenic mouse model. Prostate 55**,** 219-37.

Karhadkar, S. S., Bova, G. S., Abdallah, N., Dhara, S., Gardner, D., Maitra, A., Isaacs, J. T., Berman, D. M., and Beachy, P. A. 2004. Hedgehog signalling in prostate regeneration, neoplasia and metastasis. Nature 431**,** 707-12.

Katayam, M., Yoshida, K., Ishimori, H., Katayama, M., Kawase, T., Motoyama, J., and Kamiguchi, H. 2002. Patched and smoothened mRNA expression in human astrocytic tumors inversely correlates with histological malignancy. J Neurooncol 59**,** 107-15.

Kessaris, N., Jamen, F., Rubin, L. L., and Richardson, W. D. 2004. Cooperation between sonic hedgehog and fibroblast growth factor/MAPK signalling pathways in neocortical precursors. Development 131**,** 1289-98.

Kubo, M., Nakamura, M., Tasaki, A., Yamanaka, N., Nakashima, H., Nomura, M., Kuroki, S., and Katano, M. 2004. Hedgehog signaling pathway is a new therapeutic target for patients with breast cancer. Cancer Res 64**,** 6071-4.

Lai, K., Kaspar, B. K., Gage, F. H., and Schaffer, D. V. 2003. Sonic hedgehog regulates adult neural progenitor proliferation *in vitro* and *in vivo*. Nat Neurosci 6**,** 21-7.

Lamm, M. L., Catbagan, W. S., Laciak, R. J., Barnett, D. H., Hebner, C. M., Gaffield, W., Walterhouse, D., Iannaccone, P., and Bushman, W. 2002. Sonic hedgehog activates mesenchymal Gli1 expression during prostate ductal bud formation. Dev Biol 249**,** 349-66.

Lau, J., Kawahira, H., and Hebrok, M. 2006. Hedgehog signaling in pancreas development and disease. Cell Mol Life Sci 63**,** 642-52.

Laufer, E., Nelson, C. E., Johnson, R. L., Morgan, B. A., and Tabin, C. 1994. Sonic hedgehog and Fgf-4 act through a signaling cascade and feedback loop to integrate growth and patterning of the developing limb bud. Cell 79**,** 993-1003.

Lebeche, D., Malpel, S., and Cardoso, W. V. 1999. Fibroblast growth factor interactions in the developing lung. Mech Dev 86**,** 125-36.

Lee, J., Platt, K. A., Censullo, P., and Ruiz i Altaba, A. 1997. Gli1 is a target of Sonic hedgehog that induces ventral neural tube development. Development 124**,** 2537-52.

Lee, J. J., Ekker, S. C., von Kessler, D. P., Porter, J. A., Sun, B. I., and Beachy, P. A. 1994. Autoproteolysis in hedgehog protein biogenesis. Science 266**,** 1528-37.

Lim, D. A., Huang, Y. C., and Alvarez-Buylla, A. 2007. The adult neural stem cell niche: lessons for future neural cell replacement strategies. Neurosurg Clin N Am 18**,** 81-92, ix.

Lum, L., and Beachy, P. A. 2004. The Hedgehog response network: sensors, switches, and routers. Science 304**,** 1755-9.

Lum, L., Zhang, C., Oh, S., Mann, R. K., von Kessler, D. P., Taipale, J., Weis-Garcia, F., Gong, R., Wang, B., and Beachy, P. A. 2003. Hedgehog signal transduction via Smoothened association with a cytoplasmic complex scaffolded by the atypical kinesin, Costal-2. Mol Cell 12**,** 1261-74.

Lupo, G., Liu, Y., Qiu, R., Chandraratna, R. A., Barsacchi, G., He, R. Q., and Harris, W. A. 2005. Dorsoventral patterning of the *Xenopus* eye: a collaboration of Retinoid, Hedgehog and FGF receptor signaling. Development 132**,** 1737-48.

Machold, R., Hayashi, S., Rutlin, M., Muzumdar, M. D., Nery, S., Corbin, J. G., Gritli-Linde, A., Dellovade, T., Porter, J. A., Rubin, L. L., Dudek, H., McMahon, A. P., and Fishell, G. 2003. Sonic hedgehog is required for progenitor cell maintenance in telencephalic stem cell niches. Neuron 39**,** 937-50.

Manseau, L., Baradaran, A., Brower, D., Budhu, A., Elefant, F., Phan, H., Philp, A. V., Yang, M., Glover, D., Kaiser, K., Palter, K., and Selleck, S. 1997. GAL4 enhancer traps expressed in the embryo, larval brain, imaginal discs, and ovary of *Drosophila*. Dev Dyn 209**,** 310-22.

Maric, D., Fiorio Pla, A., Chang, Y. H., and Barker, J. L. 2007. Self-renewing and differentiating properties of cortical neural stem cells are selectively regulated by basic fibroblast growth factor (FGF) signaling via specific FGF receptors. J Neurosci 27**,** 1836-52.

Martel, C. L., Gumerlock, P. H., Meyers, F. J., and Lara, P. N. 2003. Current strategies in the management of hormone refractory prostate cancer. Cancer Treat Rev 29**,** 171-87.

Martin, G. R. 1998. The roles of FGFs in the early development of vertebrate limbs. Genes Dev 12**,** 1571-86.

Matysiak, B. E., Brodzeller, T., Buck, S., French, A., Counts, C., Boorsma, B., Datta, M. W., and Kajdacsy-Balla, A. A. 2003. Simple, inexpensive method for automating tissue microarray production provides enhanced microarray reproducibility. Appl Immunohistochem Mol Morphol 11**,** 269-73.

Maurange, C., and Gould, A. P. 2005. Brainy but not too brainy: starting and stopping neuroblast divisions in *Drosophila*. Trends Neurosci 28**,** 30-6.

McClintock, B. 1953. Induction of Instability at Selected Loci in Maize. Genetics 38**,** 579-99.

Metcalf, D. 1993. Hematopoietic regulators: redundancy or subtlety? Blood 82**,** 3515-23.

Metcalf, D. 1998a. Regulatory mechanisms controlling hematopoiesis: principles and problems. Stem Cells 16 Suppl 1**,** 3-11.

Metcalf, D. 1998b. The molecular control of hematopoiesis: progress and problems with gene manipulation. Stem Cells 16 Suppl 2**,** 1-9.

Micchelli, C. A., The, I., Selva, E., Mogila, V., and Perrimon, N. 2002. Rasp, a putative transmembrane acyltransferase, is required for Hedgehog signaling. Development 129**,** 843-51.

Mimeault, M., Hauke, R., and Batra, S. K. 2007. Stem cells: a revolution in therapeutics-recent advances in stem cell biology and their therapeutic applications in regenerative medicine and cancer therapies. Clin Pharmacol Ther 82**,** 252-64.

Miura, G. I., and Treisman, J. E. 2006. Lipid modification of secreted signaling proteins. Cell Cycle 5**,** 1184-8.

Miyake, A., Nakayama, Y., Konishi, M., and Itoh, N. 2005. Fgf19 regulated by Hh signaling is required for zebrafish forebrain development. Dev Biol 288**,** 259-75.

Morshead, C. M., Reynolds, B. A., Craig, C. G., McBurney, M. W., Staines, W. A., Morassutti, D., Weiss, S., and van der Kooy, D. 1994. Neural stem cells in the adult mammalian forebrain: a relatively quiescent subpopulation of subependymal cells. Neuron 13**,** 1071-82.

Nackaerts, K., Verbeken, E., Deneffe, G., Vanderschueren, B., Demedts, M., and David, G. 1997. Heparan sulfate proteoglycan expression in human lung-cancer cells. Int J Cancer 74**,** 335-45.

Nelson, W. G., De Marzo, A. M., and Isaacs, W. B. 2003. Prostate cancer. N Engl J Med 349**,** 366-81.

Nissim, S., Hasso, S. M., Fallon, J. F., and Tabin, C. J. 2006. Regulation of Gremlin expression in the posterior limb bud. Dev Biol 299**,** 12-21.

Niswander, L., Jeffrey, S., Martin, G. R., and Tickle, C. 1994. A positive feedback loop coordinates growth and patterning in the vertebrate limb. Nature 371**,** 609-12.

Nusslein-Volhard, C., and Wieschaus, E. 1980. Mutations affecting segment number and polarity in *Drosophila*. Nature 287**,** 795-801.

Nybakken, K., and Perrimon, N. 2002. Hedgehog signal transduction: recent findings. Curr Opin Genet Dev 12**,** 503.

O'Neill, S. L., Giordano, R., Colbert, A. M., Karr, T. L., and Robertson, H. M. 1992. 16S rRNA phylogenetic analysis of the bacterial endosymbionts associated with cytoplasmic incompatibility in insects. Proc Natl Acad Sci U S A 89**,** 2699-702.

Oliver, T. G., Read, T. A., Kessler, J. D., Mehmeti, A., Wells, J. F., Huynh, T. T., Lin, S. M., and Wechsler-Reya, R. J. 2005. Loss of patched and disruption of granule cell development in a pre-neoplastic stage of medulloblastoma. Development 132**,** 2425-39.

Ornitz, D. M. 2000. FGFs, heparan sulfate and FGFRs: complex interactions essential for development. Bioessays 22**,** 108-12.

Ornitz, D. M., and Itoh, N. 2001. Fibroblast growth factors. Genome Biol 2**,** REVIEWS3005.

Palma, V., Lim, D. A., Dahmane, N., Sanchez, P., Brionne, T. C., Herzberg, C. D., Gitton, Y., Carleton, A., Alvarez-Buylla, A., and Ruiz i Altaba, A. 2005. Sonic hedgehog controls stem cell behavior in the postnatal and adult brain. Development 132**,** 335-44.

Palma, V., and Ruiz i Altaba, A. 2004. Hedgehog-GLI signaling regulates the behavior of cells with stem cell properties in the developing neocortex. Development 131**,** 337-45.

Park, H. L., Bai, C., Platt, K. A., Matise, M. P., Beeghly, A., Hui, C. C., Nakashima, M., and Joyner, A. L. 2000. Mouse Gli1 mutants are viable but have defects in SHH signaling in combination with a Gli2 mutation. Development 127**,** 1593-605.

Park, Y., Ng, C., and Datta, S. 2003a. Induction of *string* rescues the neuroblast proliferation defect in *trol* mutant animals. Genesis 36**,** 187-95.

Park, Y., Rangel, C., Reynolds, M. M., Caldwell, M. C., Johns, M., Nayak, M., Welsh, C. J., McDermott, S., and Datta, S. 2003b. *Drosophila perlecan* modulates FGF and hedgehog signals to activate neural stem cell division. Dev Biol 253**,** 247-57.

Pasca di Magliano, M., and Hebrok, M. 2003. Hedgehog signalling in cancer formation and maintenance. Nat Rev Cancer 3**,** 903-11.

Pepicelli, C. V., Lewis, P. M., and McMahon, A. P. 1998. Sonic hedgehog regulates branching morphogenesis in the mammalian lung. Curr Biol 8**,** 1083-6.

Pepinsky, R. B., Zeng, C., Wen, D., Rayhorn, P., Baker, D. P., Williams, K. P., Bixler, S. A., Ambrose, C. M., Garber, E. A., Miatkowski, K., Taylor, F. R., Wang, E. A., and Galdes, A. 1998. Identification of a palmitic acid-modified form of human Sonic hedgehog. J Biol Chem 273**,** 14037-45.

Pietsch, T., Waha, A., Koch, A., Kraus, J., Albrecht, S., Tonn, J., Sorensen, N., Berthold, F., Henk, B., Schmandt, N., Wolf, H. K., von Deimling, A., Wainwright, B., Chenevix-Trench, G., Wiestler, O. D., and Wicking, C. 1997. Medulloblastomas of the desmoplastic variant carry mutations of the human homologue of *Drosophila* patched. Cancer Res 57**,** 2085-8.

Pinsker, W., Haring, E., Hagemann, S., and Miller, W. J. 2001. The evolutionary life history of P transposons: from horizontal invaders to domesticated neogenes. Chromosoma 110**,** 148-58.

Podlasek, C. A., Barnett, D. H., Clemens, J. Q., Bak, P. M., and Bushman, W. 1999. Prostate development requires Sonic hedgehog expressed by the urogenital sinus epithelium. Dev Biol 209**,** 28-39.

Pomeroy, S. L., Tamayo, P., Gaasenbeek, M., Sturla, L. M., Angelo, M., McLaughlin, M. E., Kim, J. Y., Goumnerova, L. C., Black, P. M., Lau, C., Allen, J. C., Zagzag, D., Olson, J. M., Curran, T., Wetmore, C., Biegel, J. A., Poggio, T., Mukherjee, S., Rifkin, R., Califano, A., Stolovitzky, G., Louis, D. N., Mesirov, J. P., Lander, E. S., and Golub, T. R. 2002. Prediction of central nervous system embryonal tumour outcome based on gene expression. Nature 415**,** 436-42.

Porter, J. A., von Kessler, D. P., Ekker, S. C., Young, K. E., Lee, J. J., Moses, K., and Beachy, P. A. 1995. The product of hedgehog autoproteolytic cleavage active in local and long-range signalling. Nature 374**,** 363-6.

Porter, J. A., Young, K. E., and Beachy, P. A. 1996. Cholesterol modification of hedgehog signaling proteins in animal development. Science 274**,** 255-9.

Powers, C. J., McLeskey, S. W., and Wellstein, A. 2000. Fibroblast growth factors, their receptors and signaling. Endocr Relat Cancer 7**,** 165-97.

Prokop, A., and Technau, G. M. 1991. The origin of postembryonic neuroblasts in the ventral nerve cord of *Drosophila melanogaster*. Development 111**,** 79-88.

Raffel, C., Jenkins, R. B., Frederick, L., Hebrink, D., Alderete, B., Fults, D. W., and James, C. D. 1997. Sporadic medulloblastomas contain PTCH mutations. Cancer Res 57**,** 842-5.

Regl, G., Neill, G. W., Eichberger, T., Kasper, M., Ikram, M. S., Koller, J., Hintner, H., Quinn, A. G., Frischauf, A. M., and Aberger, F. 2002. Human GLI2 and GLI1 are part of a positive feedback mechanism in Basal Cell Carcinoma. Oncogene 21**,** 5529-39.

Reifenberger, J., Wolter, M., Weber, R. G., Megahed, M., Ruzicka, T., Lichter, P., and Reifenberger, G. 1998. Missense mutations in SMOH in sporadic basal cell carcinomas of the skin and primitive neuroectodermal tumors of the central nervous system. Cancer Res 58**,** 1798-803.

Reya, T., Morrison, S. J., Clarke, M. F., and Weissman, I. L. 2001. Stem cells, cancer, and cancer stem cells. Nature 414**,** 105-11.

Reynolds, B. A., and Weiss, S. 1992. Generation of neurons and astrocytes from isolated cells of the adult mammalian central nervous system. Science 255**,** 1707-10.

Rhim, J. S. 2000. *In vitro* human cell culture models for the study of prostate cancer. Prostate Cancer Prostatic Dis 3**,** 229-235.

Riobo, N. A., Haines, G. M., and Emerson, C. P., Jr. 2006. Protein kinase C-delta and mitogen-activated protein/extracellular signal-regulated kinase-1 control GLI activation in hedgehog signaling. Cancer Res 66**,** 839-45.

Roessler, E., Du, Y. Z., Mullor, J. L., Casas, E., Allen, W. P., Gillessen-Kaesbach, G., Roeder, E. R., Ming, J. E., Ruiz i Altaba, A., and Muenke, M. 2003. Loss-of-function mutations in the human GLI2 gene are associated with pituitary anomalies and holoprosencephaly-like features. Proc Natl Acad Sci U S A 100**,** 13424-9.

Rubin, J. B., Choi, Y., and Segal, R. A. 2002. Cerebellar proteoglycans regulate sonic hedgehog responses during development. Development 129**,** 2223-32.

Ruiz i Altaba, A., Palma, V., and Dahmane, N. 2002. Hedgehog-Gli signalling and the growth of the brain. Nat Rev Neurosci 3**,** 24-33.

Ruiz i Altaba, A., Stecca, B., and Sanchez, P. 2004. Hedgehog--Gli signaling in brain tumors: stem cells and paradevelopmental programs in cancer. Cancer Lett 204**,** 145-57.

Ryder, E., and Russell, S. 2003. Transposable elements as tools for genomics and genetics in *Drosophila*. Brief Funct Genomic Proteomic 2**,** 57-71.

Sanchez, P., Hernandez, A. M., Stecca, B., Kahler, A. J., DeGueme, A. M., Barrett, A., Beyna, M., Datta, M. W., Datta, S., and Ruiz i Altaba, A. 2004. Inhibition of prostate cancer proliferation by interference with SONIC HEDGEHOG-GLI1 signaling. Proc Natl Acad Sci U S A 101**,** 12561-6.

Savore, C., Zhang, C., Muir, C., Liu, R., Wyrwa, J., Shu, J., Zhau, H. E., Chung, L. W., Carson, D. D., and Farach-Carson, M. C. 2005. Perlecan Knockdown in Metastatic Prostate Cancer Cells Reduces Heparin-binding Growth Factor Responses *in vitro* and Tumor Growth *in vivo*. Clin Exp Metastasis 22**,** 377-90.

Schlicht, M., Matysiak, B., Brodzeller, T., Wen, X., Liu, H., Zhou, G., Dhir, R., Hessner, M. J., Tonellato, P., Suckow, M., Pollard, M., and Datta, M. W. 2004. Cross-species global and subset gene expression profiling identifies genes involved in prostate cancer response to selenium. BMC Genomics 5**,** 58.

Serafini, M., and Verfaillie, C. M. 2006. Pluripotency in adult stem cells: state of the art. Semin Reprod Med 24**,** 379-88.

Serakinci, N., and Keith, W. N. 2006. Therapeutic potential of adult stem cells. Eur J Cancer 42**,** 1243-6.

Sharma, B., Handler, M., Eichstetter, I., Whitelock, J. M., Nugent, M. A., and Iozzo, R. V. 1998. Antisense targeting of perlecan blocks tumor growth and angiogenesis *in vivo*. J Clin Invest 102**,** 1599-608.

Shaw, A., and Bushman, W. 2007. Hedgehog signaling in the prostate. J Urol 177**,** 832-8.

Sheng, T., Li, C., Zhang, X., Chi, S., He, N., Chen, K., McCormick, F., Gatalica, Z., and Xie, J. 2004. Activation of the hedgehog pathway in advanced prostate cancer. Mol Cancer 3**,** 29.

Shi, Y., Sun, G., Zhao, C., and Stewart, R. 2007. Neural stem cell self-renewal. Crit Rev Oncol Hematol.

Spence, J. R., Aycinena, J. C., and Del Rio-Tsonis, K. 2007. Fibroblast growth factor-hedgehog interdependence during retina regeneration. Dev Dyn 236**,** 1161-74.

Spence, J. R., Madhavan, M., Ewing, J. D., Jones, D. K., Lehman, B. M., and Del Rio-Tsonis, K. 2004. The hedgehog pathway is a modulator of retina regeneration. Development 131**,** 4607-21.

Starr, D. J., and Cline, T. W. 2002. A host parasite interaction rescues *Drosophila* oogenesis defects. Nature 418**,** 76-9.

Stathopoulos, A., Tam, B., Ronshaugen, M., Frasch, M., and Levine, M. 2004. *pyramus* and *thisbe*: FGF genes that pattern the mesoderm of *Drosophila* embryos. Genes Dev 18**,** 687-99.

Stecca, B., and Ruiz i Altaba, A. 2005. Brain as a paradigm of organ growth: Hedgehog-Gli signaling in neural stem cells and brain tumors. J Neurobiol 64**,** 476-90.

Stein, U., Eder, C., Karsten, U., Haensch, W., Walther, W., and Schlag, P. M. 1999. GLI gene expression in bone and soft tissue sarcomas of adult patients correlates with tumor grade. Cancer Res 59**,** 1890-5.

Stojkovic, M., Lako, M., Stojkovic, P., Stewart, R., Przyborski, S., Armstrong, L., Evans, J., Herbert, M., Hyslop, L., Ahmad, S., Murdoch, A., and Strachan, T. 2004. Derivation of human embryonic stem cells from day-8 blastocysts recovered after three-step *in vitro* culture. Stem Cells 22**,** 790-7.

Stone, K. R., Mickey, D. D., Wunderli, H., Mickey, G. H., and Paulson, D. F. 1978. Isolation of a human prostate carcinoma cell line (DU 145). Int J Cancer 21**,** 274-81.

Sutherland, D., Samakovlis, C., and Krasnow, M. A. 1996. *branchless* encodes a *Drosophila* FGF homolog that controls tracheal cell migration and the pattern of branching. Cell 87**,** 1091-101.

Taipale, J., Cooper, M. K., Maiti, T., and Beachy, P. A. 2002. Patched acts catalytically to suppress the activity of Smoothened. Nature 418**,** 892-6.

Taylor, M. D., Liu, L., Raffel, C., Hui, C. C., Mainprize, T. G., Zhang, X., Agatep, R., Chiappa, S., Gao, L., Lowrance, A., Hao, A., Goldstein, A. M., Stavrou, T.,

Scherer, S. W., Dura, W. T., Wainwright, B., Squire, J. A., Rutka, J. T., and Hogg, D. 2002. Mutations in SUFU predispose to medulloblastoma. Nat Genet 31**,** 306-10.

Temple, S. 1999. CNS development: The obscure origins of adult stem cells. Curr Biol 9**,** R397-9.

Temple, S., and Alvarez-Buylla, A. 1999. Stem cells in the adult mammalian central nervous system. Curr Opin Neurobiol 9**,** 135-41.

Thalmann, G. N., Sikes, R. A., Wu, T. T., Degeorges, A., Chang, S. M., Ozen, M., Pathak, S., and Chung, L. W. 2000. LNCaP progression model of human prostate cancer: androgen-independence and osseous metastasis. Prostate 44**,** 91-103 Jul 1;44(2).

Thayer, S. P., di Magliano, M. P., Heiser, P. W., Nielsen, C. M., Roberts, D. J., Lauwers, G. Y., Qi, Y. P., Gysin, S., Fernandez-del Castillo, C., Yajnik, V., Antoniu, B., McMahon, M., Warshaw, A. L., and Hebrok, M. 2003. Hedgehog is an early and late mediator of pancreatic cancer tumorigenesis. Nature 425**,** 851-6.

Thisse, B., and Thisse, C. 2005. Functions and regulations of fibroblast growth factor signaling during embryonic development. Dev Biol 287**,** 390-402.

Truman, J. W., and Bate, M. 1988. Spatial and temporal patterns of neurogenesis in the central nervous system of *Drosophila melanogaster*. Developmental Biology 125**,** 145-157.

Tsang, M., and Dawid, I. B. 2004. Promotion and attenuation of FGF signaling through the Ras-MAPK pathway. Sci STKE 2004**,** pe17.

Urbach, R., Schnabel, R., and Technau, G. M. 2003. The pattern of neuroblast formation, mitotic domains and proneural gene expression during early brain development in *Drosophila*. Development 130**,** 3589-606.

Urbach, R., and Technau, G. M. 2003a. Molecular markers for identified neuroblasts in the developing brain of *Drosophila*. Development 130**,** 3621-37.

Urbach, R., and Technau, G. M. 2003b. Segment polarity and DV patterning gene expression reveals segmental organization of the *Drosophila* brain. Development 130**,** 3607-20.

van der Horst, G., Farih-Sips, H., Lowik, C. W., and Karperien, M. 2003. Hedgehog stimulates only osteoblastic differentiation of undifferentiated KS483 cells. Bone 33**,** 899-910.

Venkataraman, G., Raman, R., Sasisekharan, V., and Sasisekharan, R. 1999. Molecular characteristics of fibroblast growth factor-fibroblast growth factor receptor-heparin-like glycosaminoglycan complex. Proc Natl Acad Sci U S A 96**,** 3658-63.

Vescovi, A. L., Reynolds, B. A., Fraser, D. D., and Weiss, S. 1993. bFGF regulates the proliferative fate of unipotent (neuronal) and bipotent (neuronal/astroglial) EGF-generated CNS progenitor cells. Neuron 11**,** 951-66.

Voigt, A., Pflanz, R., Schafer, U., and Jackle, H. 2002. Perlecan participates in proliferation activation of quiescent *Drosophila* neuroblasts. Dev Dyn 224**,** 403-12.

von Bohlen Und Halbach, O. 2007. Immunohistological markers for staging neurogenesis in adult hippocampus. Cell Tissue Res 329**,** 409-20.

Wagner, J. P., Black, I. B., and Dicicco-Bloom, E. 1999. Stimulation of Neonatal and Adult Brain Neurogenesis by Subcutaneous Injection of Basic Fibroblast Growth Factor. The Journal of Neuroscience 19**,** 6006-6016.

Walshe, J., and Mason, I. 2003. Unique and combinatorial functions of Fgf3 and Fgf8 during zebrafish forebrain development. Development 130**,** 4337-49.

Wang, B. E., Shou, J., Ross, S., Koeppen, H., De Sauvage, F. J., and Gao, W. Q. 2003. Inhibition of epithelial ductal branching in the prostate by sonic hedgehog is indirectly mediated by stromal cells. J Biol Chem 278**,** 18506-13.

Watkins, D. N., Berman, D. M., Burkholder, S. G., Wang, B., Beachy, P. A., and Baylin, S. B. 2003. Hedgehog signalling within airway epithelial progenitors and in small-cell lung cancer. Nature 422**,** 313-7.

Watson, J. D., Baker, T. A., Bell, S. P., Gann, A., Levine, M., and Losick, R. (2004). Molecular Biology of the Gene. Cold Spring Harbor Press.

Weiner, H. L., Bakst, R., Hurlbert, M. S., Ruggiero, J., Ahn, E., Lee, W. S., Stephen, D., Zagzag, D., Joyner, A. L., and Turnbull, D. H. 2002. Induction of medulloblastomas in mice by sonic hedgehog, independent of Gli1. Cancer Res 62**,** 6385-9.

Weiss, S., Dunne, C., Hewson, J., Wohl, C., Wheatley, M., Peterson, A. C., and Reynolds, B. A. 1996. Multipotent CNS stem cells are present in the adult mammalian spinal cord and ventricular neuroaxis. J Neurosci 16**,** 7599-609.

White, K., and Kankel, D. R. 1978. Patterns of cell division and cell movement in the formation of the imaginal nervous system in *Drosophila melanogaster*. Developmental Biology 65**,** 296-321.

Wolter, M., Reifenberger, J., Sommer, C., Ruzicka, T., and Reifenberger, G. 1997. Mutations in the human homologue of the *Drosophila* segment polarity gene patched (PTCH) in sporadic basal cell carcinomas of the skin and primitive neuroectodermal tumors of the central nervous system. Cancer Res 57**,** 2581-5.

Wu, H. C., Hsieh, J. T., Gleave, M. E., Brown, N. M., Pathak, S., and Chung, L. W. 1994. Derivation of androgen-independent human LNCaP prostatic cancer cell sublines: role of bone stromal cells. Int J Cancer 57**,** 406-12.

Xu, J., Gillanders, E. M., Isaacs, S. D., Chang, B. L., Wiley, K. E., Zheng, S. L., Jones, M., Gildea, D., Riedesel, E., Albertus, J., Freas-Lutz, D., Markey, C., Meyers, D. A., Walsh, P. C., Trent, J. M., and Isaacs, W. B. 2003. Genome-wide scan for prostate cancer susceptibility genes in the Johns Hopkins hereditary prostate cancer families. Prostate 57**,** 320-5.

Zeng, X., Goetz, J. A., Suber, L. M., Scott, W. J., Jr., Schreiner, C. M., and Robbins, D. J. 2001. A freely diffusible form of Sonic hedgehog mediates long-range signalling. Nature 411**,** 716-20.

Zhang, Y., and Kalderon, D. 2001. Hedgehog acts as a somatic stem cell factor in the *Drosophila* ovary. Nature 410**,** 599-604.

Zuniga, A., Haramis, A. P., McMahon, A. P., and Zeller, R. 1999. Signal relay by BMP antagonism controls the SHH/FGF4 feedback loop in vertebrate limb buds. Nature 401**,** 598-602.

Zurawel, R. H., Allen, C., Chiappa, S., Cato, W., Biegel, J., Cogen, P., de Sauvage, F., and Raffel, C. 2000. Analysis of PTCH/SMO/SHH pathway genes in medulloblastoma. Genes Chromosomes Cancer 27**,** 44-51.

# APPENDIX A

# INHIBITION OF PROSTATE CANCER PROLIFERATION BY INTERFERENCE WITH SONIC HEDGEHOG GLI1 SIGNALING*

## PERLECAN MODULATES SONIC HEDGEHOG SIGNALING IN ADVANCED PROSTATE CANCER

Advanced Prostate cancer is one of the most clinically significant neoplasias in American men, killing about 27,000 a year. It is imperative to find therapies that target transition to metastasis and increase survival rate. A hallmark of tumorigenesis is the misregulation of signaling pathways that are utilized during development, and are normally downregulated in adults. SONIC HEDGEHOG (SHH) signaling has an important role in prostate development (Ingham and McMahon, 2001) and has been shown to be upregulated in other types of cancer, such as lung cancer (Watkins et al., 2003). Our studies in the *Drosophila* brain show that the *Drosophila* homolog of SHH signaling is modulated by the Extracellular matrix proteoglycan PERLECAN. The single human *PERLECAN* gene maps to the CABP locus, which has been identified by human genetics studies as having an increased risk for prostate cancer and brain cancer (Janer et al., 2003).

---

Furthermore, there has been evidence of *PERLECAN* upregulation in prostate cancer cell lines (Iozzo et al., 1994). We hypothesize that PERLECAN modulates SHH signaling and regulates SHH-dependent cell proliferation in advanced prostate cancer.

**CONTRIBUTIONS**

My contribution to the work in (Sanchez et al., 2004) involved analysis of the Shh signaling pathway components in prostate tumors and matched normal tissue samples taken from six patients. I assisted Ana Maria Hernandez, a graduate student in Dr. Datta's lab, by performing several qRT-PCR experiments of both sample types to determine the expression levels of Shh, PTCH1, and GLI1/2/3 (Table A-2). From these data, it is suggested that overall expression levels of all pathway components increased (between 1.5- and ≈300-fold) in tumors sample compared to matched normal prostate tissue. However, there is some noted variability between tumor samples, which could be attributed to the known heterogeneity of prostate cancer.

**ABSTRACT**

Prostate cancer is the most common solid tumor in men, and it shares with all cancers the hallmark of elevated, nonhomeostatic cell proliferation. Here we have tested the hypothesis that the SONIC HEDGEHOG (SHH)-GLI signaling pathway is implicated in prostate cancer. We report expression of SHH-GLI pathway components in adult human prostate cancer, often with enhanced levels in tumors versus normal prostatic epithelia. Blocking the pathway with cyclopamine or anti SHH antibodies inhibits the proliferation of $GLI1^{+}/PSA^{+}$ primary prostate tumor cultures. Inversely, SHH

can potentiate tumor cell proliferation, suggesting that autocrine signaling may often sustain tumor growth. In addition, pathway blockade in three metastatic prostate cancer cell lines with cyclopamine or through *GLI1* RNA interference leads to inhibition of cell proliferation, suggesting cell autonomous pathway activation at different levels and showing an essential role for GLI1 in human cells. Our data demonstrate the dependence of prostate cancer on SHH-GLI function and suggest a novel therapeutic approach.

## INTRODUCTION

**S**ONIC HEDGEHOG (SHH) signaling has been implicated in different aspects of animal development, acting through several components, including the transmembrane proteins PATCHED1 (PTCH1) and SMOOTHENED (SMOH), to activate the GLI zinc-finger transcription factors (Ingham and McMahon, 2001; Ruiz i Altaba et al., 2002). In addition, we and others have shown that SHH signaling is implicated in a number of tumors (Pasca di Magliano and Hebrok, 2003; Ruiz i Altaba et al., 2002), such as basal cell carcinomas (Dahmane et al., 1997; Hahn et al., 1996; Johnson et al., 1996), medulloblastomas (Berman et al., 2002; Dahmane et al., 2001), gliomas (Dahmane et al., 2001), sarcomas (Hahn et al., 1996; Stein et al., 1999), tumors of the digestive tract (Berman et al., 2003), small cell lung cancers (Watkins et al., 2003), and pancreatic carcinomas (Thayer et al., 2003). To date there is no direct evidence linking SHH signaling to prostate cancer, the most common solid cancer in men (Nelson et al., 2003), although we have found that sporadic prostate tumors express *GLI1* (Dahmane et al., 2001), a reliable marker of SHH signaling (Hynes et al., 1997;

Lee et al., 1997). This observation allowed us to propose the hypothesis that the SHH-GLI pathway participates in prostate cancer (Dahmane et al., 2001). Consistently, Shh signaling has been found to be essential for prostate patterning and development (Barnett et al., 2002; Berman et al., 2004; Freestone et al., 2003; Lamm et al., 2002; Podlasek et al., 1999; Wang et al., 2003), and genetic mapping data has revealed that at least two key components of the SHH-GLI pathway [*SMOH* and *SUPPRESSOR OF FUSED* (*SUFUH*)] are located in chromosomal regions implicated in familial human prostate cancer (Easton et al., 2003; Xu et al., 2003). Here we have tested the involvement of SHH-GLI signaling in prostate cancer.

## METHODS

### *Cell Lines and Primary Cultures*

The PC3, LNCaP, and DU145 cell lines (Horoszewicz et al., 1980; Kaighn et al., 1978; Stone et al., 1978) were purchased from American Type Culture Collection and grown as specified. All primary prostate tumors were obtained following approved protocols. Tumors in PBS were chopped with a razor blade and incubated with Papain for 1 h at 37°C, they were then dissociated by passing them through a fire-polished pipette and washed several times in serum containing media. All dissociated primary tumors were plated in polyornithinand laminin-treated p16 plates in DMEM-F12 with 10% FBS at ~30,000 cells per p16 well. Primary cultures were used 2-4 days after plating, when the cells reached 60-70% confluence.

*In Situ Hybridization and Immunocytochemistry*

Immunocytochemistry was performed with anti-BrdUrd (Beckton Dickinson), anti- SHH (Santa Cruz Biotechnology), and anti-Ki-67 (DAKO), using FITC- or horseradish peroxidase (HRP)-conjugated secondary antibodies (Boehringer Mannheim) as described (Dahmane et al., 2001). For tissue arrays, slides were baked and deparaffinized before blocking of endogenous peroxides. They were then developed with HRPconjugated secondary antibodies and diaminobenzidine (DAB). *In situ* hybridizations on frozen sections with digoxygenin-labeled antisense RNA probes for *GLI1*, *PTCH1*, and *SHH* and a sense control *GLI1* were as described (Dahmane et al., 2001).

*Prostate Tissue Microarrays and Microdissection*

After institutional review board approval, tissue microarrays (Matysiak et al., 2003) were prepared from archived paraffin blocks from 288 radical prostatectomy cases from the Medical College of Wisconsin. For each case, 0.6-mm cores of tumor were isolated and placed in the array blocks, and 5-μm slides were prepared for immunohistochemistry. Slides were reviewed by a trained urologic pathologist (M.W.D.) and scored for the presence of benign prostate glands, high-grade prostatic intraepithelial neoplasia, or invasive tumor. The presence of tumor or high-grade prostatic intraepithelial neoplasia was confirmed by Immunohistochemical staining for high molecular mass cytokeratin (CK903 Ab, DAKO). Individual cores were examined as duplicates, and staining was correlated to a set of anonymous deidentified pathologic

and outcomes data with $\chi^2$ and Fisher's exact or two-tailed ANOVA analyses.

Normal and tumor tissue from the same patients for real-time PCR analyses were microdissected from sections with a laser capture microscope after pathological assessment.

*SHH, Anti-SHH Antibody, Cyclopamine, and Tomatidine Treatments*

Commercial N-SHH (R & D Systems) was used at 100 nM because we have found that this commercial protein is ~20 times less active than the octyl-modified SHH-N we had previously used from Curis in the C3H10T1/2 induction assay (data not shown). 5E1 anti-SHH blocking antibody (Ericson et al., 1996) was purchased from the Hybridoma Bank at the University of Iowa and was used at 8 μg/ml. Cyclopamine (Toronto Research Chemicals) and Tomatidine (Sigma) were used at 10 μM unless otherwise noted; for cells in culture, they were dissolved in ethanol, and ethanol alone was used as control. Treated cells were in 2.5% serum for 48 h instead of the usual 10% routinely used for standard growth.

*Proliferation Assays*

BrdUrd (Sigma) was given at 4 μg/ml before fixation. The time of the BrdUrd pulse depended on the growth rate of the cells tested. Cell lines were given a 2-h pulse, whereas primary tumor cultures, which grow less rapidly, were given 16-h pulses. Proliferation in tissue arrays was measured by the level of Ki-67 antigen expression.

*PCRs*

For RT-PCRs, the following primers were used (all 5′ to 3′). GLI1s, GGGATGATCCCACATCCTCAGTC, and GLI1a, CTGGAGCAGCCCCCCCAGT at 60°C; PSAs, CTTGTAGCCTCTCGTGGCAG, and PSAa, GACCTTCATAGCATCCGTGAG at 56°C. Primers for *PTCH1* and *GAPDH* were as described (Dahmane et al., 2001; Palma and Ruiz i Altaba, 2004).

For real-time PCR, total RNA was DNase treated (Invitrogen) and reverse transcribed with TaqMan (Applied Biosystems) using oligo(dT) primers as described by the manufacturer. Reactions were run by using SYBR Green (Applied Biosystems) on an ABI Prism 7700 machine. Each sample was run minimally at three concentrations in triplicate. All primer sets amplified 75- to 300-bp fragments. Sequences are available upon request. The raw data are available upon request from S.D.

*RNA Interference*

Double-stranded small interference RNAs (siRNAs, 21 nt long) were purchased from Dahrmacon, purified, and desalted. The sequences for the GLI1 siRNAs used was: AACUCCACAGGCAUACAGGAU; control siRNA was: AACGUACGCGGAAUACAACGA. This siRNA was also used FITCtagged. siRNA transfections (0.2 μM) were with Oligofectamine (Invitrogen) as described by the manufacturer. Cells were treated for 60 h before fixation.

**RESULTS**

To begin to analyze the role of SHH-GLI signaling in prostate cancer, we first tested for the expression of SHH-GLI pathway components in prostate cancer resections and normal tissue from the same patients. *In situ* hybridization showed that *GLI1*, *PTCH1*, and *SHH* are normally coexpressed in epithelial cells and not in the surrounding stroma (Figure A-1 *A*, *C*, *E*, *G*, *I*, *L*, and *O*). Prostate tumors were uniformly $SHH^{+}/GLI1^{+}/PTCH1^{+}$ (Figure A-1 *B*, *D*, *F*, *H*, *J*, *K*, *M*, *N*, *P*, and *Q*), although variable levels of expression were detected visually in the tumors. Coexpression of these markers in tumor cells is consistent with their derivation from the normal prostatic epithelium.

More sensitive real-time PCR analyses of six of the same microdissected matched pairs showed up-regulation of the expression of *SHH*, *PTCH1*, *GLI1*, *GLI2*, and *GLI3* (between 1.5- and ~300- fold) in many tumor cases compared to normal tissue after normalization to the ubiquitous similar expression of *β-actin* (Table A-1). Levels of expression within tumors were variable. Such differences could be related to the known heterogeneity of prostate cancer, because this is a general diagnosis that encompasses a broad range of histological phenotypes (Bostwick et al., 2004; DeMarzo et al., 2003; Kaplan-Lefko et al., 2003). Whereas varying levels have also been observed in other tumors (Ingham and McMahon, 2001; Ruiz i Altaba et al., 2002), the meaning of such differences is not known, although they have been proposed to correlate in a direct or inverse manner with tumor type or grade (Grachtchouk et al., 2003; Katayam et al., 2002; Pomeroy et al., 2002). What is important is that the loyal markers of an active

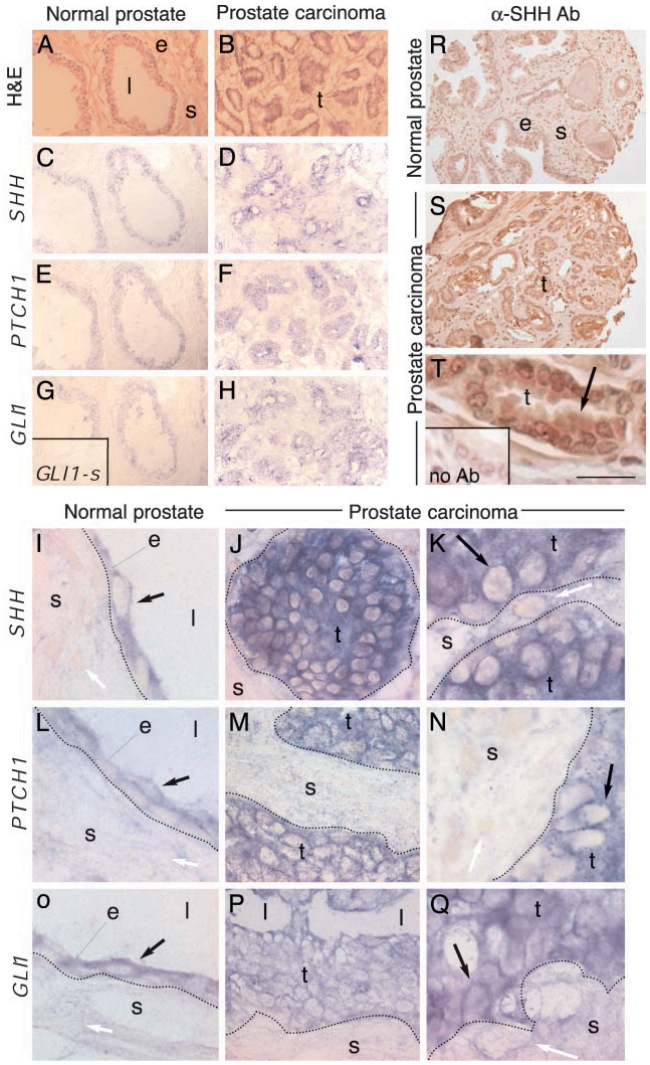


**Figure A-1. Expression of SHH–GLI pathway components in normal prostate tissue and prostate tumors.** Sections of normal prostate tissue (*A*, *C*, *E*, *G*, *I*, *L*, and *O*) and prostate tumors (*B*, *D*, *F*, *H*, *J*, *K*, *M*, *N*, *P*, and *Q*) show hematoxylin and eosin (H & E) staining (*A* and *B*) or the expression of *SHH* (*C*, *D*, and *I-K*), *PTCH1* (*E*, *F*, and *L-N*), and *GLI1* (*G*,*H*, and *O-Q*). (*GInset*) Sense *GLI1* probe control showing no background. Prostate tumors havemanysmall epithelial glandular structures. Black arrows point to expressing cells. White arrows point to nonexpressing cells. (*R-T*) Sections from the tissue microarrays of normal prostate tissue (*R*) and prostate tumors (*S* and *T*) showing expression of SHH protein with an anti-SHH antibody (αSHH Ab) (*R-T*) and a no primary antibody control (*T Inset*). All sections were counterstained with hematoxylin to visualize nuclei and tissue structure. Arrow in *T* points to localization of SHH protein in the cytoplasm of epithelial cells. e, epithelium; l, lumen; s, stroma; t, tumor. (Scale bar in *T* is 150 μm in *A-H*, *R*, and *S*, 20 μm in *J*, *M*, *P*, and *T*, and 10 μm in *I-L*, *N*, *O*, and *Q*.)

**Table A-1. SHH, GLI1, GLI2, GLI3, and PTCH1 expression in human prostate cancer.**

| | *SHH* | | *PTCH1* | | *GLI1* | | *GLI2* | | *GLI3* | |
|---|---|---|---|---|---|---|---|---|---|---|
| Patient | Fold Increase | Range | Fold Increase | Range | Fold Increase | Range | Fold Increase | Range | Fold Increase | Range |
| 829 | 0 | 0–0.01 | 1.5 | 1.1–2.1 | **26.1** | 20.8–32.7 | 0.02 | 0.02–0.02 | **72** | 53–99 |
| 887 | 0.2 | 0.05–0.9 | 8.5 | 7.6–9.5 | 0.09 | 0.07–0.13 | 0.43 | 0.37–0.51 | 1.1 | 0.8–1.6 |
| 921 | 2.9 | 1.3–6.3 | 50 | 30–84 | 2 | 1.1–3.4 | 3.8 | 2.4–6.1 | **12.5** | 7.7–20.4 |
| 945 | 9.8 | 6.2–15.7 | 7.8 | 5.7–10.7 | **22.7** | 21.6–23.9 | 0.7 | 0.5–1.0 | **2.2** | 2.1–2.4 |
| 1854 | 4.7 | 1.8–11.7 | **213** | 164–278 | **5.1** | 3.8–6.9 | 19.5 | 10.9–35.1 | **5.7** | 4.4–7.5 |
| 1866 | 4.6 | 4.1–5.2 | 3.4 | 3.1–3.7 | **299** | 260–342 | 0.03 | 0.02–0.03 | 0.18 | 0.15–0.2 |

Fold increase in gene expression in tumors versus matched normal tissue determined by real-time RT-PCR analyses as calculated by the ΔCT method. Range indicates ± 1 SD. Gene expression levels were normalized to β-actin. Increases of 2-fold or more are shown in bold.

SHH-GLI pathway, *GLI1* and *(Goodrich et al., 1996; Lee et al., 1997; Podlasek et al., 1999)*, are consistently transcribed in the examined tumor cells, showing the presence of an active pathway.

To extend these findings, we performed immunohistochemistry for SHH, as a secreted and potentially useful systemic marker for prostate cancer, on tissue microarrays representing 239 prostate carcinomas, 15 precancerous lesion high-grade prostatic intraepithelial neoplasia (HGPIN), and 135 benign prostate tissues from 297 patients. SHH expression was increased in tumors and was present as a secreted protein in the glandular lumens made by tumor cells (Figure A-1 *R-T*), likely reflecting the origin of tumors from the $SHH^+$ prostatic epithelia. Higher SHH levels, determined visually, were found in 33% of tumors compared to <1% of cases of normal adjacent tissue, indicating a significant correlation between high SHH levels and tumor presence. High SHH levels were also correlated with higher Ki-$67^+$ cell proliferation (Table A-2). The level of SHH expression was not correlated with Gleason score or other clinical parameters (Table A-2). This finding may indicate that inappropriately maintained or elevated SHH expression is an early and general event in prostate cancer, reflecting the origin of tumors from the $SHH^+$ prostatic epithelia.

The difficulty of growing human prostate cancer cells *in vitro* translates into a dearth of available cancer cells to test. Here we have chosen the three most widely used prostate cancer cell lines, LNCaP, an androgen sensitive cell line derived from a prostate cancer lymph node metastasis; and PC3 and DU145, androgen insensitive cell lines derived from prostate cancer bone metastases, to assay for the expression of SHH-GLI

**Table A-2. Correlation of elevated SHH expression with tumorigenesis and clinical features of prostate cancer.**

| | | SHH | | |
|---|---|---|---|---|
| | | Expression low | Expression high | $\chi^2$ or Fisher's exact test |
| Histology | Tumor | 141 | 70 | |
| | Normal | 126 | 1 | $P < 0.00005$ |
| | HGPIN | 13 | 1 | |
| | Normal | 126 | 1 | $P = 0.0563$ |
| Clinical stage | cT2 | 16 | 6 | |
| | cT3/4 | 2 | 1 | NS |
| Tumor grade | Gleason 6 | 30 | 1 | |
| | Gleason 7,8,9 | 57 | 7 | NS |
| Pathologic stage | pT1–pT2 | 50 | 4 | |
| | pT3 | 37 | 4 | NS |
| Nodal status | pN0 | 27 | 12 | |
| | pN1 | 1 | 0 | NS |
| Outcomes | PSA Recurrence | 8 | 1 | |
| | No PSA recurrence | 22 | 12 | NS |
| Vital status | Alive | 42 | 18 | |
| | Dead | 4 | 3 | NS |
| KI-67 expression | Sample no. | 275 | 69 | |
| | Mean % KI-67$^+$ nuclei | 5.1 | 7.6 | $P = 0.0141$* |

Significance was only found between SHH expression and tumorigenesis and SHH expression and higher proliferative levels as measured by Ki-67 staining. Tumor grade is presented as Gleason score. Pathologic staging uses the American Joint Comission on Cancer 2002 tumor staging criteria. HGPIN, high-grade prostatic intraepithelial neoplasia.

*Two-tailed ANOVA.

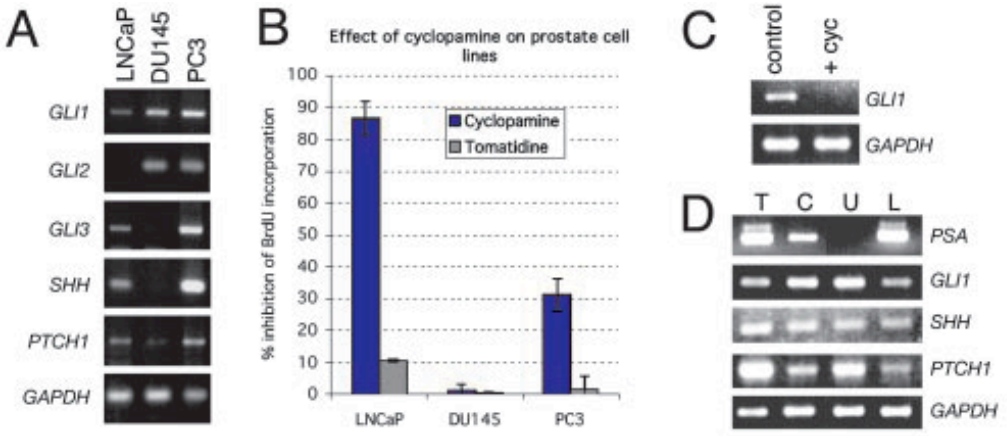


**Figure A-2. Response of prostate tumor cell lines to alterations in the SHH-GLI pathway.** (*A*) PCR analyses for the expression of SHH-GLI pathway components in three cell lines as indicated. In this and all other PCR assays, the expression of the ubiquitous gene *GAPDH* is measured as quantitative control. (*B*) Inhibition of prostate cell line proliferation as measured by BrdUrd incorporation in the three prostate cell lines used with cyclopamine. Tomatidine is used as control. (*C* and *D*) PCR analyses of the suppression of *GLI1* expression in LNCaP cells by cyclopamine treatment at 36 h (*C*) or of the expression of prostate specific antigen (PSA), *GLI1*, *SHH*, and *PTCH1* expression in whole prostate tumor tissue (T), primary culture (C), the glioblastoma cell line U87 (U), and LNCaP (L) cells (*D*). *PSA* is expressed in prostate but not in brain cells. All samples express *GLI1* and *SHH*. The whole tissue and primary culture correspond to PT6. (*E*) Histogram of the inhibition of BrdUrd incorporation in primary cultures of prostate tumor (PT3-PT8) by cyclopamine treatment. (*F-I*) Immunocytochemistry for BrdUrd incorporation with secondary FITC antibodies showing $BrdUrd^{+}$ nuclei (green) in a field of primary prostate cells (PT6) in control cells (treated with ethanol as the carrier for cyclopamine, *F*), cyclopamine (*G*), SHH protein (*H*), or anti-SHH antibody (αSHH Ab, *I*). All nuclei are stained with 4′, 6-diamidino-2-phenylindole (blue). (*J* and *K*) Histograms of the increase in (*J*) or inhibition of (*K*) BrdUrd incorporation of primary prostate tumors after treatment with SHH (*J*) or anti-SHH antibody (αSHH Ab, *K*) for 48 h. Histogram error bars represent SEM in all panels.

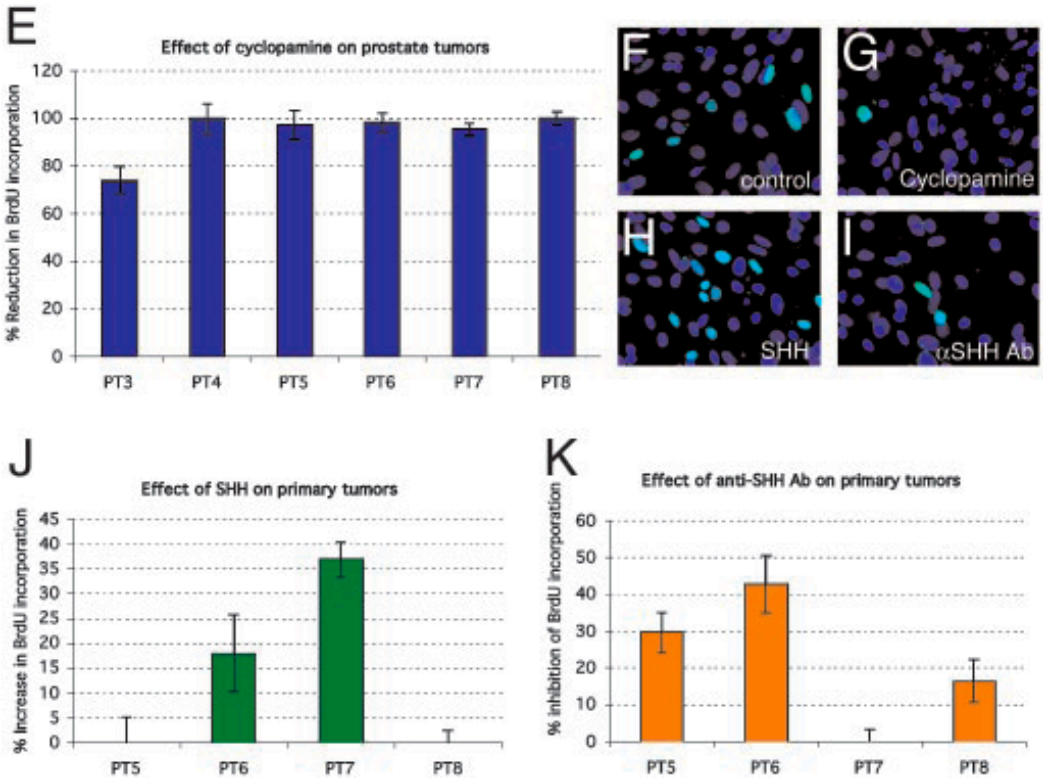


**Figure A-2 continued.**

pathway components. All of the cells expressed *GLI1* and *PTCH1* (Figure A-2*A*), consistent with our expression studies and indicating that they harbor an active pathway. Of these cell lines, only DU145 and PC3 cells expressed *GLI2*, and only LNCaP and PC3 cells expressed *GLI3* and *SHH* at detectable levels (Figure A-2*A*). *GLI1* is thus the only *GLI* gene consistently expressed at detectable levels in all of these cells, and thus, we have focused on *GLI1*.

To interfere with SHH-GLI signaling, we first used cyclopamine, a selective inhibitor of SMOH (Chen et al., 2002). Effects of cyclopamine treatment after 48 h were tested by BrdUrd incorporation as a sensitive measure of cell proliferation. Such treatment led to a large (>80%) decrease in BrdUrd incorporation in LNCaP cells, and a significant decrease (≈30%) in PC3 cells but had no effect in DU145 cells (Figure A-2*B*). Treatment with tomatidine (Chen et al., 2002)served as control and had little or no effect on BrdUrd incorporation (Figure A-2*B*). The lack of effects of cyclopamine on DU145 cells shows that this drug is not nonspecific. Because we used short-term assays to focus on early, direct effects on cell proliferation, the changes in total cell number were consequently relatively conservative. For instance, cyclopamine reduced total 4′, 6-diamidino-2-phenylindole-positive LNCaP cell number by 22.1±1.1% ($P$=0.0001) after 48 h. No cytotoxic effects or significant cell death were observed during these experiments. Cyclopamine treatment also led to a decrease in *GLI1* expression, consistent with the expected down-regulation of the SHH-GLI pathway (Figure A-2*C*).

Analyses of primary prostate tumors is complicated by the difficulty of growing primary human prostate cancer cultures (Rhim, 2000). Nevertheless, we were able to

dissociate and plate six of eight primary prostate tumors, although stable cultures were not obtained. Primary cells that remained attached after 2 days had a uniformcuboidal morphology, formed small clusters and expressed prostate-specific antigen (PSA), as well as *SHH*, *PTCH1*, and *GLI1* (Figure A-2*D*), proving their prostatic epithelial origin. Cyclopamine treatment led to a major (>70%) decrease in BrdUrd incorporation in all primary cultures as compared with carrier-treated samples (Figure A-2*E*-*G*), mimicking the results obtained in LNCaP cells. Here again, the insensitivity of DU145 to cyclopamine provides a control for the action of the drug. Indeed, although we have not tested the response of normal human prostate cells to cyclopamine, we expect that it would also inhibit the proliferation of normal $SHH^+$/ $PTCH1^+$/$GLI1^+$ prostate epithelial cells (Figure A-1). As with the cell lines, the total number of 4′, 6-diamidino-2-phenylindole-positive primary tumor cells was similarly reduced by cyclopamine treatment [e.g., 26.7 ± 1.1% decrease in primary tumor 6 (PT6), $P = 0.001$] after 48 h. Although stromal cells are likely to be present in our primary cultures, their numbers appear to be small because >90% of the cells examined microscopically had a similar cuboidal morphology. Moreover, the high inhibition levels by cyclopamine would be inconsistent with effects only in contaminating stromal cells, which do not appreciably express *PTCH1* or *GLI1* (Figure A-1).

We then tested for the ability of exogenous SHH to stimulate prostate cancer cell proliferation and for the possible existence of autocrine signaling. Addition of recombinant SHH protein led to an increase in BrdUrd incorporation in two of four primary cultures after 48 h (Figure A-2*F*, *H*, and *J*). In contrast, addition of the standard

blocking antibody against SHH (5E1; (Ericson et al., 1996)) resulted in an inhibition of BrdUrd incorporation by 15-40% for three of four tumors (Figure A-2*F*, *I*, and *K*), suggesting that several tumors display autocrine signaling. Interestingly, the only primary culture that was insensitive to Shh Ab blockade, PT7, being sensitive to cyclopamine [which targets SMOH (Chen et al., 2002), Figure 2*E*], was also the more sensitive to the addition of exogenous Shh. This might indicate that although the pathway is activated downstream of the site of ligand action in PT7, possibly affecting PTCH1 or SMOH, exogenous Shh can still increase the levels of signaling. Taken together, the functional heterogeneity that we detect parallels that found for *GLI* and *SHH* expression described above and may reflect independent activating events as well as the well known heterogeneity of prostate cancers.

Treatment of LNCaP, PC3 or DU145 cells with either blocking antibody recombinant Shh protein did not result in significant changes in BrdUrd incorporation (data not shown). LNCaP and PC3 cells could thus display an activated pathway at the membrane level (being sensitive to cyclopamine inhibition) that has lost responsiveness to ligand. Cyclopamine-insensitive DU145 cells may have an activated pathway downstream of SMOH (or at the level of SMOH affecting its inhibition by cyclopamine), having lost also the ability to respond to SHH. It remains possible that the different behavior of primary cultures versus established cell lines also reflects unrelated transformation or immortalization events.

The GLI zinc-finger transcription factors have been suggested to be essential for the mediation of HH signals (Ingham and McMahon, 2001; Ruiz i Altaba et al., 2002;

Ruiz i Altaba et al., 2004). However, Gli1 is apparently redundant in mouse development and tumorigenesis (Park et al., 2000; Weiner et al., 2002), and there is to date no data on the requirement for *GLI1* in human cells. Here, we tested the function of GLI1, the only GLI gene consistently expressed in all primary tumors and cell lines, by RNA interference to knockdown its function with a specific 21-nt-long small RNA. (This siRNA inhibits the effect of SHH on multipotent C3H10T1/2 cells; P.S. and A.R.A., unpublished data). Lipofection of primary cultures resulted in a negligible number of transfected cells, making it impractical to use siRNAs in such cultures. In contrast, lipofection of FITC-siRNA proved efficient (≈50-80%) in the LNCaP, PC3, and DU145 cell lines (Figure A-3*A*-*C*). It is important to note that, because transfection efficiencies are <100%, the results of cell pool assays necessarily underestimate the effects of RNA interference. Transfection of a control siRNA at the same concentration served as control in all tests.

The specificity of the *GLI1* siRNA was further tested in LNCaP cells. Reduction of *GLI1* mRNA levels by the *GLI1* siRNA was detected as early as 3 h after transfection and at 8 and 24 h, but not at 48 h (Figure A-3 *D* and *F* and data not shown), suggesting upregulation of *GLI1* after its inhibition, possibly because of the action of a rapid positive feedback loop (Dahmane et al., 2001; Regl et al., 2002). *GLI1* siRNA also robustly repressed *PTCH1*, a result most clearly seen at 48 h, but not the housekeeping gene *GAPDH* (Figure A-3*D* and data not shown). Because *PTCH1* is a SHH target (Goodrich et al., 1996), and in particular of GLI1 (Agren et al., 2004), this result indicates that interference with GLI1 function by RNAi is selective and effective in

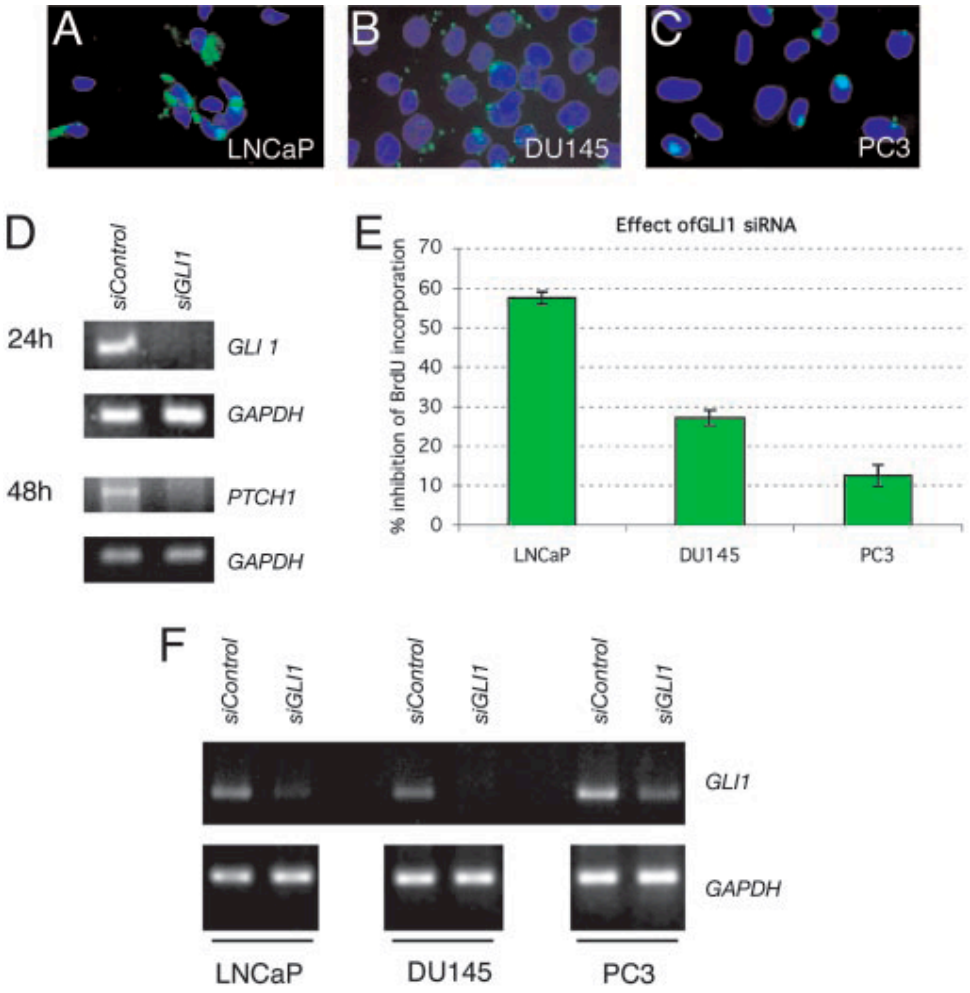


**Figure A-3. Response of prostate cell lines to *GLI1* RNA interference.** (*A-C*) Immunocytochemisty of the three prostate cell lines indicated showing the efficiency of lipofection of an FITC-tagged control siRNA (green). Note the lower efficiency in PC3 cells. (*D*) Effect of *GLI1* siRNA on gene expression. RNA interference reduces *GLI1* and *PTCH1* mRNA levels as seen at 24 and 48 h, respectively (*E*) Histogram of the inhibition of BrdUrd incorporation in prostate tumor cell lines by *GLI1* siRNA. (*F*) Specificity of the effects of *GLI1* siRNA on *GLI1* mRNA levels in the three prostate cell lines, compared with those of a control unrelated siRNA, 8 h after transfection. The levels of *GAPDH* are shown below as controls.

prostate cancer cells. *GLI1* siRNA also decreased *GLI1* mRNA levels in DU145 and PC3 cells after 8 h (Figure A-3*F*).

Inhibition of GLI1 by RNA interference led to a variable reduction in BrdUrd incorporation in all three cell lines, with strongest effects (≈60%) in LNCaP cells (Figure A-3*E*). These cells are thus very sensitive to inhibition by cyclopamine and *GLI1*interference, suggesting the presence of a fully active canonical pathway activated at the level of SMOH or upstream, but downstream of SHH, because treatment with the blocking anti-SHH Ab had no effect. DU145 cells are not sensitive to cyclopamine, but are sensitive to *GLI1* interference, suggesting activation downstream of SMOH and upstream or at the level of GLI1 function. In contrast, PC3 cells are sensitive to cyclopamine and less so to *GLI1* interference, perhaps suggesting compensation by the other GLI proteins because PC3 cells express *GLI2* [and this *GLI* gene mediates SHH signals (Roessler et al., 2003) and can behave like Gli1 in mice (Bai and Joyner, 2001)] or the presence of alternate pathways for tumor cell proliferation. We note, however, that lipofection efficiencies in PC3 cells (Figure A-3*C*) are the lowest (≈50%) of the three cells tested, indicating that the real effects of *GLI1* interference may be higher. Taken together, our results show the requirement of GLI1 in human prostate tumor cells.

**DISCUSSION**

Here we demonstrate the dependence of prostate cancer cell proliferation on SHH-GLI pathway activity. The data suggest activation of the pathway at different levels in primary prostate tumors and cell lines derived from metastatic lesions. These

findings, together with the involvement of this pathway in normal prostate development and growth (Barnett et al., 2002; Berman et al., 2004; Freestone et al., 2003; Lamm et al., 2002; Podlasek et al., 1999; Wang et al., 2003), indicate that the normal patterning role of SHH-GLI signaling is deregulated in cancer. This idea is consistent with the proposed events in other tissues, including brain, lung, stomach, muscle, pancreas, and skin, in which the SHH-GLI pathway regulates patterned growth and when deregulated can give rise to SHH-GLI dependent tumors (Barnett et al., 2002; Berman et al., 2004; Freestone et al., 2003; Lamm et al., 2002; Pasca di Magliano and Hebrok, 2003; Podlasek et al., 1999; Ruiz i Altaba et al., 2002; Wang et al., 2003). Thus, there is a surprising and unexpected parallel in the requirement of SHH-GLI signaling of prostate tumors with those in organs of very different origin, function, and location.

The deduction that prostate tumors display activation at different levels is consistent with findings in brain ((Dahmane et al., 2001)and P.S. and A.R.A., unpublished data) and pancreatic (Nelson et al., 2003) tumors, even though the entire set of activating events or mutations have not been described in any case. Indeed, our data suggest that the regulation of the SHH-GLI pathway in the normal prostatic epithelium is altered away from homeostasis in the tumors by epigenetic events or mutations in components such as PTCH1, SMOH, or SUFUH, similar to those already found in other tumors (e.g., (Dong et al., 2000; Pietsch et al., 1997; Raffel et al., 1997; Reifenberger et al., 1998; Taylor et al., 2002; Wolter et al., 1997; Zurawel et al., 2000)). However, the finding that the pathway is active as assessed by the expression of *GLI1* and *PTCH1* [as in the case of basal cell carcinomas (Dahmane et al., 1997), medulloblastomas

(Dahmane et al., 2001)and gliomas (Dahmane et al., 2001)] allows us to bypass the identification of the likely myriad of activating events to discern that tumor cells harbor an active pathway. Indeed, the finding that SHH expression levels are not correlated with Gleason score, but that all prostate tumor samples tested require continued pathway activity for proliferation, allows us to propose that this pathway is a critical and essential component of prostate cancer.

Specifically, we show the requirement for SHH, SMOH, and/or GLI1 for the proliferation of prostate cancer cells. The fact that all primary tumors tested are sensitive to cyclopamine indicates that SMOH, or upstream elements from it, are common targets leading to the activation of downstream mediators. Several primary cultures are also sensitive to inhibition by blocking anti-SHH Ab, suggesting that, like in stomach tumors (Berman et al., 2003), autocrine signaling is a frequent cause of pathway activation in prostate cancer. The consistent expression of *GLI1* in tumor cell lines and in primary tumors together with the effects of RNA interference indicate that this *GLI* gene plays a central and general role in prostate tumor cell proliferation, and demonstrate its requirement in human tumorigenesis. In contrast, *GLI2* and *GLI3* do not appear to be consistently expressed in prostate cancer cells. When expressed, they could have complementary or compensatory roles in some cases, although their roles remain to be determined.

Prostate cancer is thought to develop from a lesion in the epithelial layer to become an invasive tumor that spreads within the prostate and subsequently acquires the potential to metastasize to distant sites, most often the lymph nodes and bone (Abate-

Shen and Shen, 2000). Inhibition of testosterone-dependent tumor growth is the common treatment for advanced disease, but subsequent hormone-independent cell proliferation and metastasis often leads to patient death (Martel et al., 2003). Our data on the behavior of the three prostate cancer cell lines derived from metastatic lesions suggest that such tumors could harbor additional changes that may make them ligand-independent, albeit still being SHH-GLI pathway dependent, and explain their differential behavior in comparison with the primary cultures. Perhaps the gain of intracellular, cell-autonomous activation of the SHH-GLI pathway represents an advantage for metastatic cells, allowing efficient proliferation far from the prostatic epithelium, where SHH appears to be continually and abundantly produced.

The high inhibition of proliferation by SHH-GLI pathway blockade of the presumed androgen-sensitive primary tumors used in this study, which derive from patients that did not receive hormone treatments, and of the androgen sensitive LNCaP cell line might be related to the proposed requirement of Shh signaling for normal androgen function, because defects derived from loss of Shh signaling in mice can be rescued by exogenous androgens (Berman et al., 2004). Prostate cancer could therefore initiate through inappropriate maintenance or enhanced activity of SHH-GLI signaling, and more aggressive (androgen insensitive) states may require additional alterations. Nevertheless, the inhibition of the androgen-insensitive DU145 cell line by RNA interference suggests that even highly aggressive tumors may be sensitive, albeit to different degrees, to GLI1 inhibition.

Prostate stem cells may play a critical role in the epithelial development and

homeostasis (Bonkhoff, 1996; De Marzo et al., 1998). Because cancer may be a disease of stem cell lineages (discussed in (Pasca di Magliano and Hebrok, 2003; Reya et al., 2001; Ruiz i Altaba et al., 2002; Ruiz i Altaba et al., 2004)) and SHH-GLI signaling controls the behavior of precursors and of cells with stem cell properties in the mammalian brain (e.g., (Lai et al., 2003; Machold et al., 2003; Palma and Ruiz i Altaba, 2004)and V. Palma, D. Lim, N. Dahmane, N., P.S., Y. Gitton, A. Alvarez-Buylla, A., and A.R.A., unpublished data) and in other tissues and species (Park et al., 2003b; Zhang and Kalderon, 2001)), prostate cancer might derive from inappropriate expansion of prostatic epithelial stem cell lineages caused by abnormal SHH-GLI function.

Finally, our data suggest that SHH and GLI1 may not only be useful markers for prostate cancer but also good targets for anticancer therapies, with emphasis on GLI function as the last and essential step of the pathway, the inhibition of which will likely block signaling by upstream events at any level. SHH-GLI pathway blocking agents should thus provide attractive therapeutic strategies to combat prostate cancer of any grade.

# APPENDIX B

# *Perlecan*, A CANDIDATE GENE FOR THE CAPB LOCUS, REGULATES PROSTATE CANCER CELL GROWTH VIA THE SONIC HEDGEHOG PATHWAY*

## CONTRIBUTIONS

My contribution to the work in (Datta et al., 2006a) involved analysis of the effects PERLECAN has on SHH signaling in an established prostate cancer cell line series. I assisted Ana Maria Hernandez, a graduate student in Dr. Datta's lab, by performing several qRT-PCR experiments on *PERLECAN* RNAi treated LNCaP cells, which are the least invasive/most androgen sensitive cells in the prostate cancer cell line series. Results of this experiment showed a decrease in expression of *PTCH1* and *GLI1* (80% and 90% decrease, respectively), transcriptional targets of the SHH-GLI signaling pathway, compared to non-RNAi treated controls (Figure B-4A). This suggests that PERLECAN is a key modulator of SHH signaling in prostate cancer cells.

## ABSTRACT

Genetic studies associated the CAPB locus with familial risk of brain and prostate cancers. We have identified *HSPG2* (*Perlecan*) as a candidate gene for CAPB.

---

*Reprinted with permission from Datta, M.W., Hernandez, A.M., Schlicht, M.J., Kahler, A.J., DeGueme, A.M., Dhir, R., Shah, R.B., Farach-Carson, C., Barrett, A., and Datta, S. 2006. *Perlecan*, a candidate gene for the CAPB locus, regulates prostate cancer cell growth via the Sonic Hedgehog pathway. *Mol Cancer* **5**, 9. 

Previously we have linked Perlecan to Hedgehog signaling in *Drosophila*. More recently, we have demonstrated the importance of Hedgehog signaling in humans for advanced prostate cancer. Here we demonstrate *Perlecan* expression in prostate cancer, and its function in prostate cancer cell growth through interaction and modulation of Sonic Hedgehog (SHH) signaling. *Perlecan* expression in prostate cancer tissues correlates with a high Gleason score and rapid cell proliferation. *Perlecan* is highly expressed in prostate cancer cell lines, including androgen insensitive cell lines and cell lines selected for metastatic properties. Inhibition of *Perlecan* expression in these cell lines decreases cell growth. Simultaneous blockade of Perlecan expression and androgen signaling in the androgen-sensitive cell line LNCaP was additive, indicating the independence of these two pathways. *Perlecan* expression correlates with SHH in tumor tissue microarrays and increased tumor cell proliferation based on Ki-67 immunohistochemistry. Inhibition of *Perlecan* expression by siRNA in prostate cancer cell lines decreases SHH signaling while expression of the downstream SHH effector *GLI1* rescues the proliferation defect. Perlecan forms complexes with increasing amounts of SHH that correlate with increasing metastatic potential of the prostate cancer cell line. SHH signaling also increases in the more metastatic cell lines. Metastatic prostate cancer cell lines grown under serum-starved conditions (low androgen and growth factors) resulted in maintenance of *Perlecan* expression. Under low androgen, low growth factor conditions, *Perlecan* expression level correlates with the ability of the cells to maintain SHH signaling. We have demonstrated that Perlecan, a candidate gene for the CAPB locus, is a new component of the SHH pathway in prostate tumors and

works independently of androgen signaling. In metastatic tumor cells increased SHH signaling correlates with the maintenance of Perlecan expression and more Perlecan-SHH complexes. Perlecan is a proteoglycan that regulates extracellular and stromal accessibility to growth factors such as SHH, thus allowing for the maintenance of SHH signaling under growth factor limiting conditions. This proteoglycan represents an important central regulator of SHH activity and presents an ideal drug target for blocking SHH effects.

**BACKGROUND**

Genetic mapping studies for familial prostate cancer have identified numerous chromosomal regions linked to prostate cancer susceptibility. On chromosome one a genetic association has been demonstrated between clinically significant prostate cancer and the brain tumor glioblastoma multiforme at 1p36 (CArcinoma Prostate Brain, CAPB), suggesting the presence of a common oncogene for these tumors (Conlon et al., 2003; Gibbs et al., 1999; Janer et al., 2003; Park et al., 2003b; Zhang and Kalderon, 2001). Using bioinformatics based analysis of text mining and gene expression data we have identified candidate genes within the CAPB locus. One of these genes is HSPG2 (Perlecan). Perlecan is a heparan sulfate proteoglycan that is secreted into the extracellular matrix and can bind growth factors (Iozzo et al., 1994). Thus Perlecan can act as a reservoir or modulator of growth factor function. One growth factor associated with Perlecan is Hedgehog (Park et al., 2003b). Sonic Hedgehog signaling has recently been shown to be critical for cancer growth and metastasis in multiple tumor types

(Datta and Datta, 2006)In a large proportion of prostate cancers high levels of *Sonic Hedgehog* expression is observed along with expression of multiple members of the Hedgehog signaling pathway such as its receptor *Patched1*, downstream transcription factor *Gli1*, and intracellular modulator *Hedgehog Interacting Protein* (Sanchez et al., 2004; Sheng et al., 2004). Activation of the Hedgehog pathway has been detected in metastatic prostate tumors (Karhadkar et al., 2004; Sheng et al., 2004), and higher levels of pathway activity are associated with the metastatic phenotype (Karhadkar et al., 2004). Blocking the Sonic Hedgehog pathway with cyclopamine inhibits proliferation of prostate cancer cell lines (Karhadkar et al., 2004; Sanchez et al., 2004; Sheng et al., 2004) and primary prostate tumor cell cultures (Sanchez et al., 2004). Treatment of mice with cyclopamine results in the inhibition of tumor xenograft growth in multiple tumor types, including prostate tumors (Berman et al., 2003; Sanchez et al., 2004). Our bioinformatics analyses (Datta and Datta, 2006; Sanchez et al., 2004) suggested that genes encoding two components of the Sonic Hedgehog pathway, *Suppressor of Fused* (*Su(fu)*) and *Smoothened*, the target of cyclopamine, lie in chromosomal regions implicated in familial prostate cancer (Easton et al., 2003; Xu et al., 2003). Su(fu) is a negative regulator of pathway activity, thus loss of Su(fu) function would increase Sonic Hedgehog activity. Molecular analyses of prostate tumors revealed that Su(fu) protein is absent in most highly aggressive tumors and somatic truncation mutations in the *Su(fu)* gene have been identified (Sheng et al., 2004) consistent with the hypothesis that *Su(fu)* would act as a prostate tumor suppressor gene by inhibiting Sonic Hedgehog signaling. These studies demonstrate the critical nature of Sonic Hedgehog signaling in

tumorigenesis and metastasis. Thus identification of additional mechanisms for the regulation of Sonic Hedgehog signaling in cancer takes on added importance. Here we demonstrate that expression of the candidate CAPB gene *HSPG2* (*Perlecan*) is present in prostate cancers, up-regulated in aggressive prostate cancers and under poor cell growth conditions, and regulates prostate cancer cell proliferation. In addition, we demonstrate that Perlecan's effects on cell growth are independent of androgen signaling and occur through the binding of Sonic Hedgehog, resulting in modulation of the Sonic Hedgehog-Patched-Gli signaling pathway. This data, along with data linking Perlecan to metastatic tumor environments such a bone matrix (Savore et al., 2005), presents a general model in which *Perlecan* expression by tumor cells under poor growth conditions enhances their ability to utilize growth factors until their spread to suitable metastatic tumor microenvironments for accelerated growth.

## RESULTS

### *Perlecan is expressed in and associated with aggressive prostate cancers*

After identification of *Perlecan* as a candidate gene for the CAPB locus we sought to confirm the presence of Perlecan in primary prostate cancers. Immunohistochemical analysis for Perlecan in prostate cancer tissue microarrays with 600 patient samples demonstrated that Perlecan, a secreted proteoglycan, is present in the lumens of 54% of malignant prostate cancer glands, but not in normal glands (Figure B-1A–D, Table B-1). There was a significant increase in Perlecan levels in invasive tumors compared to either benign prostate tissue or the precancerous lesion high grade

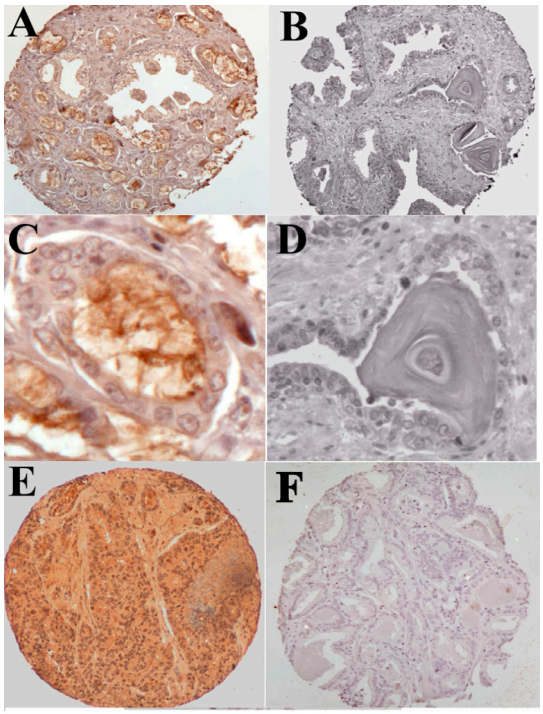


G

| Patient | Fold change in Perlecan mRNA expression | Range of Range of mRNA change | Gleason Grade |
|---|---|---|---|
| 945 | 4.2 | 4.0-4.4 | 6 |
| 1854 | 595 | 550-640 | 6 |
| 921 | 2.6 | 1.5-4.3 | 6 |
| 829 | 0.08 | 0.06-0.11 | 7 |
| 887 | 0.20 | 0.1-0.3 | 7 |
| 1863 | 2.3 | 1.5-3.5 | 8 |

H

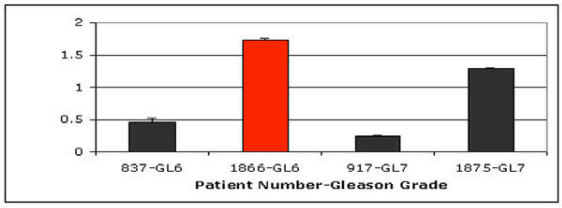


**Figure B-1. Perlecan protein levels in human prostate tumors.**
Immunohistochemistry of Perlecan protein in prostate cancer (A) and normal prostate (B). Perlecan is present as a secreted protein in the tumor gland lumens (C) but not in the lumens of benign glands or benign corpora amylacea secretions (D). Staining is also seen in metastatic prostate cancer specimens (E). Secondary antibody alone control fails to demonstrate staining (F). All images originally photographed at 400 X magnification. Quantitation of Perlecan mRNA expression by Real Time PCR (G) or protein by digitized dot blot (H) in normal prostate and tumor samples from individual patients presented as fold change in tumor versus normal. Gleason scores for the tumors are listed. Red numbers or columns indicate patients previously shown to have increased expression of *SHH*, *PTCH1* and *GLI1* (Dahmane et al., 2001).

**Table B-1. Immunohistochemical staining for Perlecan and co-localization with Ki-67.**

| | | Perlecan Negative | Perlecan Positive | |
|---|---|---|---|---|
| Histology | Tumor | 170 | 203 | |
| | Normal | 211 | 31 | p < 0.00005 |
| | Tumor | 170 | 203 | |
| | HGPIN | 46 | 7 | p < 0.00005 |
| Clinical Stage | cT2 | 11 | 12 | |
| | cT3/4 | 2 | 3 | N.S. |
| Tumor Grade | Gleason 6 | 26 | 5 | |
| | Gleason 7,8,9 | 38 | 23 | p = 0.0335 |
| Pathologic Stage | pT1-pT2 | 35 | 17 | |
| | pT3 | 29 | 11 | N.S. |
| Nodal Status | pN0 | 18 | 23 | |
| | pN1 | 0 | 1 | N.S. |
| Outcomes | PSA Recurrence | 4 | 5 | |
| | No PSA Recurrence | 13 | 22 | N.S. |
| Vital Status | Alive | 26 | 36 | |
| | Dead | 2 | 5 | N.S. |

**Perlecan Expression in Metastasis**

| Metastatic Site | Perlecan Negative | Perlecan Positive | P value vs. Prostate |
|---|---|---|---|
| Primary Tumor (Prostate) | 3 | 24 | |
| Lymph Node | 8 | 9 | p = 0.0073 |
| Soft Tissue | 15 | 18 | p = 0.0039 |
| Liver | 5 | 23 | p = 0.4781 |
| Lung | 3 | 24 | p = 1.000 |

**Association of Ki-67 (PCNA) Staining with Perlecan Staining**

| Sample Staining | Number of Samples | Mean % of Ki-67 positivity | Two-tailed ANOVA |
|---|---|---|---|
| Perlecan positive | 143 | 6.715278 | p = 0.0478 |
| Perlecan negative | 214 | 5.028571 | |

* Tumor grade is presented as Gleason score. Pathologic staging uses the American Joint Commission on Cancer (AJCC) 2002 tumor staging criteria. HGPIN = high grade prostatic intraepithelial neoplasia.

prostatic intraepithelial neoplasia (HGPIN). In particular *Perlecan* expression was associated with more aggressive tumors, as evidenced by their higher Gleason score (Gleason score 7,8,9 versus Gleason score 5 and 6 tumors). *Perlecan* expression was also significantly associated with increased prostate cancer cell proliferation, as demonstrated by Ki-67 (PCNA) Immunohistochemical staining (Table B-1). To extend the evaluation of Perlecan we examined *Perlecan* RNA (Figure B-1G) and/or protein (Figure B-1H) levels in matched benign and tumor samples from 10 individual patients. At the RNA level *Perlecan* was significantly increased in four out of six matched patient tumor and benign prostate samples. Perlecan protein was upregulated in two of four additional patient samples where protein was examined. An examination of the Gleason score for the primary tumor samples revealed that the only Gleason score 8 tumor upregulated Perlecan. These findings correlate with the results from the tissue microarrays (Table B-1). Perlecan Ki-67 staining was also evaluated in five of the patient samples, two with low Perlecan, and three with increased Perlecan expression. Immunoblotting demonstrated a direct correlation between increased Perlecan expression and increased Ki- 67 levels. These findings matched the Immunohistochemical staining results from the tissue microarrays (Table B-1). We also examined Perlecan protein expression on tissue microarray samples from patients with primary and metastatic prostate cancer identified at autopsy. In these samples Perlecan expression was upregulated in the primary prostate tumor and metastatic prostate cancer that had spread to the lungs and liver (Figure B-1E, Table B-1). Perlecan expression was lower in tumor present in lymph nodes or soft tissue metastasis, indicating site-specific

differences in Perlecan expression in metastatic prostate cancer.

*Basal Perlecan expression is highest in an androgen sensitive tumor cell line*

Baseline expression of *Perlecan* was examined in the metastatic prostate cancer cell lines LNCaP, DU-145, and PC3. Using analysis of spotted cDNA microarray expression data (Schlicht et al., 2004) quantitative Real Time PCR and immunoblotting, *Perlecan* expression was found in all three cell lines with the highest levels present in the androgen sensitive LNCaP cell line (Figure B-2A). We extended these findings by examining *Perlecan* expression with respect to tumor cell invasion and metastasis in an LNCaP tumor progression model. The LNCaP-derived cell line series (LNCaP, C4, C4-2, C4-2B) were derived from serial passage through nude mice (Thalmann et al., 2000; Wu et al., 1994). The androgen sensitive parental LNCaP line is incapable of forming tumors in nude mice without stromal cell support. The C4 subline will form tumors when injected into castrated males, indicating that it is androgen insensitive, but will not metastasize. C4-2 is an androgen insensitive line that will metastasize, and the C4-2B subline is an androgen insensitive line that rapidly forms bone metastases. When *Perlecan* expression was assayed in the LNCaP series (Figure B-2A) *Perlecan* RNA and protein was present in all the prostate cancer cell lines at levels lower than the androgen sensitive LNCaP cells. Thus all the androgen insensitive prostate cancer cell lines expressed lower levels of Perlecan RNA than he androgen sensitive cell line.

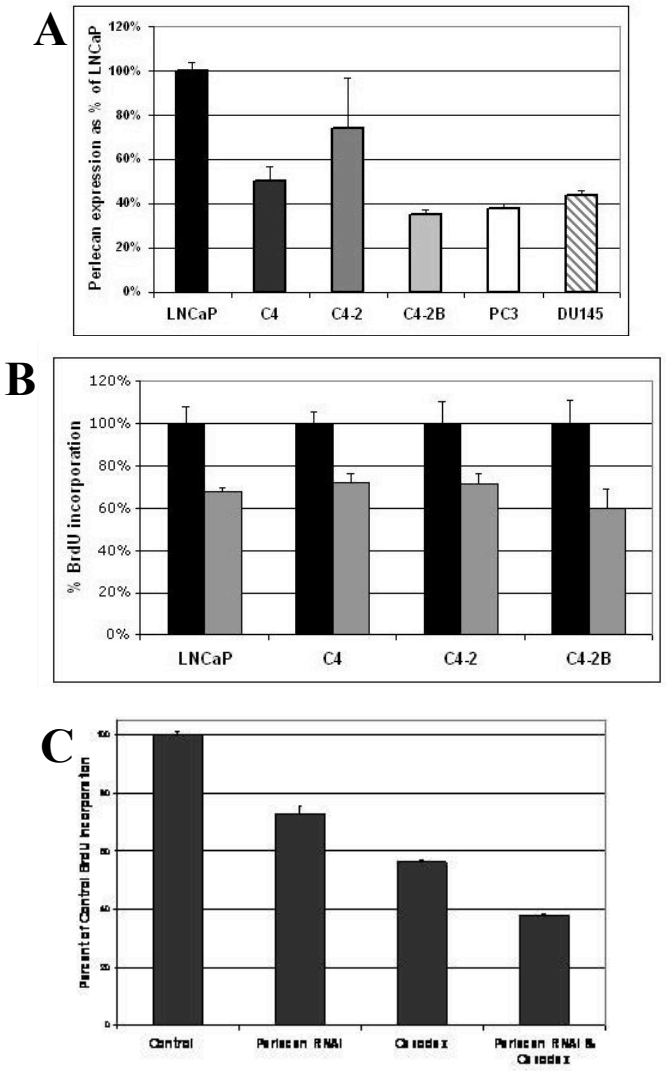


**Figure B-2. Perlecan expression and functional analysis in cell lines.** A. Relative Perlecan mRNA levels from Realtime PCR (LNCaP series) and spotted cDNA microarray data (LNCaP, DU145, PC3). All samples presented normalized to LNCaP at 100%. Androgen sensitive: LNCaP. Androgen insensitive: C4, C4-2, C4-2B, PC3, DU145. B. Inhibition by Perlecan siRNA decreases prostate cancer cell proliferation. BrdU incorporation in the LNCaP, C4, C4-2 and C4-2B cell lines. All samples were normalized to control (scrambled siRNA treated) cells at 100%. Black bars represent control samples transfected with scrambled siRNA. Grey bars represent samples transfected with Perlecan siRNA. Error bars represent n = 3 independent samples. C. Additive effect of Perlecan siRNA and androgen blockade on cell proliferation. BrdU incorporation in LNCaP cells after Perlecan siRNA and/or bicalutimide (Casodex) treatment. Control and Casodex alone samples were treated with a scrambled siRNA. $p < 0.0001$ for comparisons between groups. Error bars represent n = 6 for independent transfections.

*Inhibition of Perlecan decreases prostate cancer cell proliferation in androgen sensitive and androgen insensitive tumor cells*

To examine the direct effect of Perlecan on cancer cell growth we examined the ability of small interference RNA (siRNA) directed at *Perlecan* message to inhibit cell growth in the increasingly metastatic LNCaP cell line series LNCaP, C4, C4-2 and C4-2B. Proliferation assays demonstrated approximately equal decreases in BrdU incorporation for each cell line (Figure B-2B). To evaluate the relationship between Perlecan and androgens on cancer cell growth we performed BrdU incorporation studies on the androgen sensitive LNCaP cells utilizing androgen blockade with bicalutimide (Casodex) with *Perlecan* siRNA or a scrambled siRNA control (Figure B-2C). Independent application of *Perlecan* siRNA or androgen blockade resulted in 28% and 45% decreases in BrdU incorporation respectively. When combined, Perlecan siRNA and androgen blockade resulted in an additive effect with a 62% reduction.

*Perlecan correlates with Sonic Hedgehog expression*

Since androgen signaling and Perlecan effects on tumor cell proliferation are independent, we asked what other signaling pathway Perlecan might be modulating to support prostate cancer cell growth. Others and we have recently shown that Sonic Hedgehog regulates prostate cancer cell growth (Datta and Datta, 2006; Fan et al., 2004; Karhadkar et al., 2004; Sanchez et al., 2004; Sheng et al., 2004). Since Perlecan has been implicated in Hedgehog signaling in *Drosophila* (Park et al., 2003b), we examined the correlation and interaction of Perlecan with Sonic Hedgehog in prostate cancer samples.

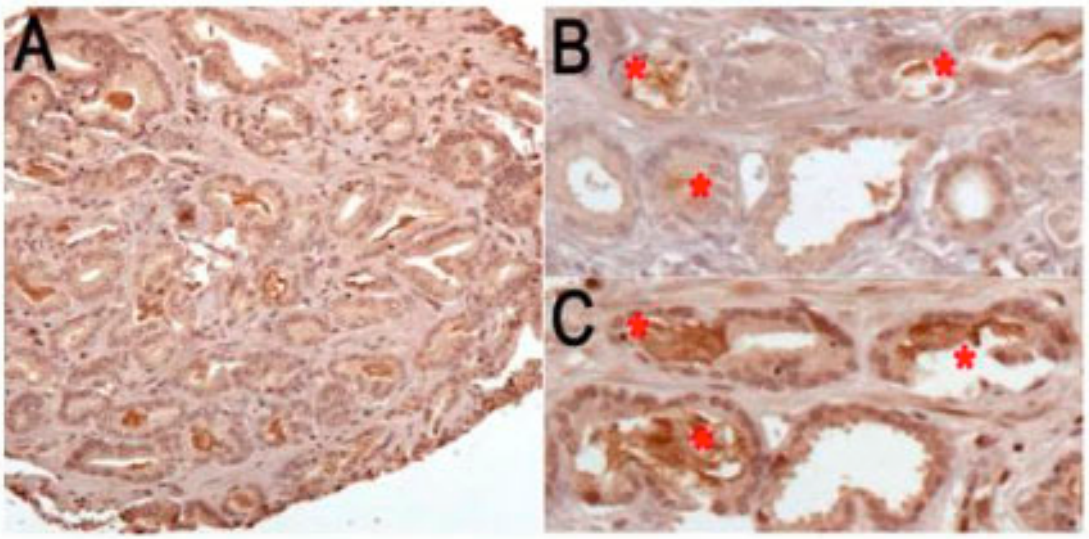


D

| Sample Co-localization | number of samples | mean % of Ki-67 positivity | Two-tailed ANOVA |
|---|---|---|---|
| PERLECAN and SHH positive | 58 | 7.620690 | p=0.0376 |
| PERLECAN and SHH negative | 270 | 5.283582 | |

**Figure B-3. Co-localization of Shh and Perlecan, and correlation with Ki-67 staining.** Immunohistochemistry for Sonic Hedgehog (A), demonstrating both weak cytoplasmic staining in prostate cancer epithelial cells and stronger intraluminal staining of secreted SHH. Co-localization of Perlecan (B) and Sonic Hedgehog (C) in consecutive sections of prostate carcinoma. Examples of co-localization of the secreted proteins in gland lumens are highlighted (red asterisks). All histologic images originally photographed at 400 X magnification. Significant co-localization of Perlecan and SHH staining was associated with higher cellular proliferation rates as indicated by Ki-67 nuclear staining by immunohistochemistry (D).

Using sequential slides from tissue microarrays we compared the staining patterns for Perlecan and Sonic Hedgehog (Figures B-3A–3C). Co-localization of Perlecan and Sonic Hedgehog staining was noted in a significant number of tumors, while luminal Sonic Hedgehog was not observed in normal prostate controls. In addition, co-localization of both Perlecan and Sonic Hedgehog correlated with increased tumor cell proliferation as shown by Ki-67 (PCNA) staining (Figure B-3D). Our previous studies (Sanchez et al., 2004) had examined expression of SHH pathway genes in six matched benign and tumor patient samples where we have also examined Perlecan mRNA or protein expression (Figure B-1G, B-1H). In four common samples where we observe up-regulation of Perlecan in tumor tissue, we previously detected up-regulation of *SHH*, *PTCH1* and *GLI1* (patients 945, 1854, 921 and 1866) suggesting a complete functional pathway in these tumors. In two common samples where we observe decreased *Perlecan* mRNA levels, we previously saw decreased *SHH* expression (patients 829 and 887). Thus in individual patients, tumor expression of *Perlecan* and *SHH* are correlated, in agreement with the co-localization of Perlecan and SHH in tissue microarrays.

*Inhibition of Perlecan blocks Sonic Hedgehog signaling in cancer cells*

To investigate whether Perlecan is directly involved in modulating SHH signaling we examined the effect of *Perlecan* siRNA on expression of *PTCH1* and *GLI1,* transcriptional targets of the SHH-GLI pathway (Lee et al., 1997) in LNCaP cells. Real-Time PCR analysis of *Perlecan* siRNA treated cells revealed the expected 80% decrease in Perlecan RNA, along with an 80% decrease in the level of *PTCH1* expression and a

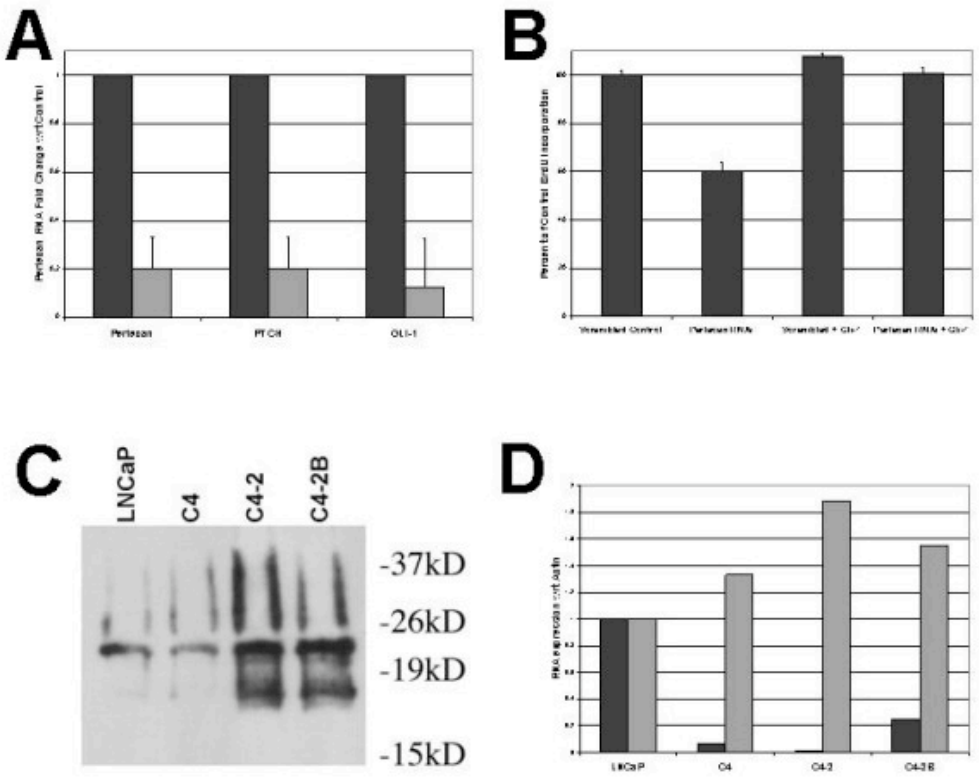


**Figure B-4. Perlecan and the SHH-GLI1 pathway.** A. Decreased Perlecan and SHH signaling in *Perlecan* RNAi treated LNCaP cells. Expression of *Perlecan*, and the SHH signaling molecules *PTCH1* and *GLI1* as determined by Real Time PCR. Black columns represent control samples, Grey columns represent Perlecan RNAi treated cells. All expression normalized to β-*actin* levels. Real Time PCR studies were run with an n = 9. Error bars indicate standard deviation. B. Gli-1 transfection restores BrdU Proliferation in Perlecan RNAi treated cells. Percent BrdU incorporation normalized to levels of BrdU incorporation in control (scrambled RNAi treated) cells. BrdU analysis was done with n = 6. Error bars indicate standard deviation. C. Immunoprecipitation with anti-Perlecan antibody pulls down SHH. Co-immunoprecipitation of SHH and Perlecan from equal amounts of medium conditioned by 80% confluent cells. Size marker is indicated. Due to modifications, mature SHH runs as an approximately 22 kD band. Note the increased amount of bound SHH in the C4-2 and C4-2B cell lines. D. Relative expression of the SHH pathway components in LNCaP series cells. Black columns represent SHH mRNA, grey columns represent PTCH mRNA, with expression presented as ratios with respect to expression in LNCaP cells. While *SHH* is lower, *PTCH* is higher in the androgen insensitive metastatic cell lines C4-2 and C4-2B compared to LNCaP. All mRNAs by QRT-PCR were normalized to Beta-actin.

90% decrease in *GLI1*expression compared to controls (Figure B-4A). A similar decrease in Perlecan protein levels in Perlecan siRNA treated LNCaP cells compared to control siRNA was noted (data not shown). These results demonstrate that Perlecan is required in androgen sensitive prostate cancer cells to achieve maximal SHH signaling activity. Given that Perlecan has been shown to modulate the signaling of multiple growth factors including FGF2, FGF10 and VEGF, we asked if the reduction of prostate cancer cell growth in Perlecan siRNA treated cells was a result of decreased SHH signaling. If the decreased BrdU incorporation was due to inhibition of SHH signaling, then expression of the SHH downstream effector *GLI1* should rescue the effects of Perlecan siRNA treatment. LNCaP cells were simultaneously transfected with Perlecan siRNA and an expression vector for *GLI1* and their proliferation compared to that of controls transfected only with Perlecan siRNA (Figure B-4B). As we observed earlier, transfection of Perlecan siRNA alone resulted in a drop in BrdU incorporation compared to controls. When Perlecan RNAi and the GLI1 expression vector were co-transfected, the percentage of BrdU labeling returned to control levels. Transfection of the *GLI1* expression vector alone did not appreciably change LNCaP cell proliferation. This demonstrates that the major role of Perlecan in LNCaP cells is to maintain levels of SHH signaling.

*Perlecan forms a complex with Sonic Hedgehog*

Finally, we asked how Perlecan might affect signaling by SHH. Previously, we had demonstrated that Perlecan from flies or mice forms a complex with Hedgehog

(Park et al., 2003b). To test for a tumor cell complex containing both Perlecan and SHH we performed co immunoprecipitation studies from the LNCaP series (Figure B-4C). Perlecan-SHH complexes were detected in the conditioned medium of all cell lines under normal growth conditions. The mature Sonic Hedgehog protein was identified by Western blotting in all protein extracts precipitated with anti-Perlecan antibodies but not from extracts precipitated with control antibodies. Increased amounts of SHH-Perlecan complexes were detected in C4-2 and C4-2B, the two metastatic cell lines. The level of Perlecan protein does not change appreciably in the LNCaP series (Figure B-5B), while the levels of *SHH* mRNA decrease across the series with increasing metastatic potential (Figure B-4D). The presence of higher levels of SHH bound to Perlecan in the C4-2 and C4-2B cells when the levels of Perlecan protein are similar across the cell lines suggests increased binding of SHH to the available Perlecan. The increased amount of bound SHH is apparently functional, as Real-Time PCR studies indicate a relative increase in *PTCH1* expression with respect to *SHH* in C4-2 and C4-2B when compared to LNCaP (Figure B-4D). Taken together, the results of our expression, inhibition, and biochemical studies link *Perlecan* expression and function to SHH-GLI pathway activity in advanced prostate cancer cells.

*Tumor cells maintain Perlecan under poor androgen/growth factor conditions*

The LNCaP series showed a large decrease in BrdU incorporation in response to Perlecan siRNA, indicating Perlecan based growth dependence under normal conditions regardless of their tumorigenic or metastatic potential. Our tissue microarray studies

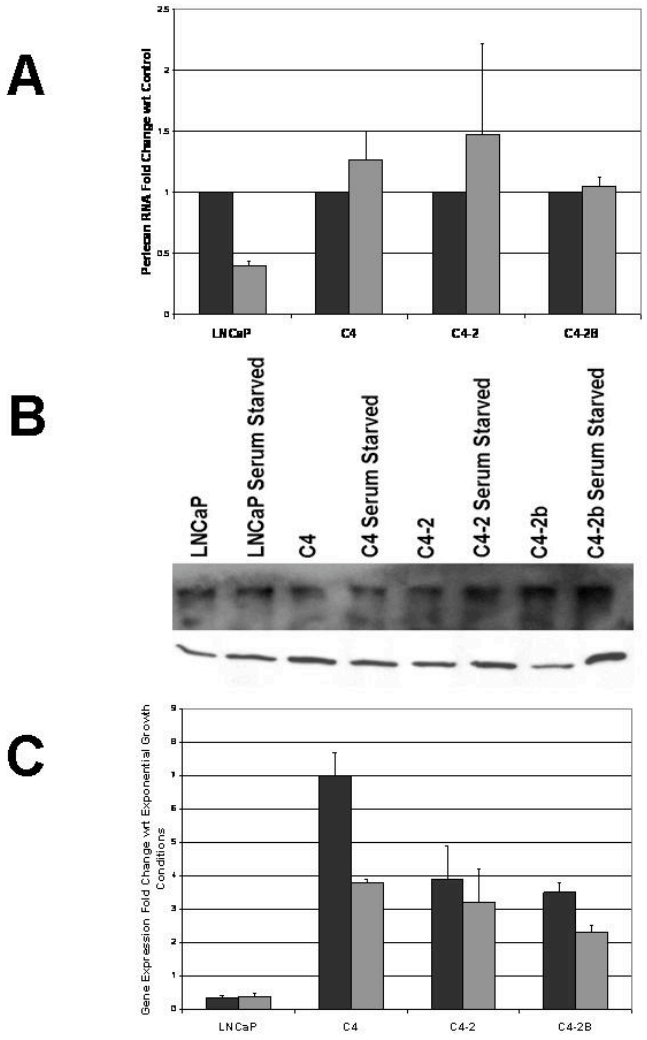


**Figure B-5. Perlecan function under androgen and growth factor limitation**. A. Minimal changes in Perlecan mRNA levels in LNCaP-derived cell lines upon serum starvation. RealTime PCR analysis of Perlecan mRNA levels presented as fold increase in Perlecan under normal (black bars) or starved (grey bars) growth conditions. While Perlecan mRNA is decreased in LNCaP, all other cell lines demonstrate no change in Perlecan mRNA levels. B. Top Panel: No change in Perlecan protein levels upon serum starvation. Agarose based western blots from protein extracts derived from exponentially growing or serum starved LNCaP, C4, C4-2, and C4-2B cells. No significant differences are noted in protein levels between the cell lines or under the differing conditions. Bottom Panel: Equivalent amounts of the same samples loaded on traditional SDS PAGE and probed for GAPDH as a loading control. C. Increases in expression of *SHH* and Gli-1 mRNA upon serum starvation. Real-Time PCR analysis of *SHH* (black bars) and *GLI1* (grey bars) as increased fold change compared to normal growth conditions. Gene expression determined by All Real Time PCR with an n = 9 and normalized to Beta-actin. Error bars indicate standard deviation.

showed a correlation between Perlecan/SHH co-localization and both higher Gleason grade and stronger Ki-67 staining, suggesting that more aggressive or metastatic cells are more likely to use Perlecan-mediated SHH signaling. Since rapidly growing tumors tend to create microenvironments depleted of growth factors we asked if growth factor/androgen depletion via serum starvation would trigger the upregulation of *Perlecan* in an effort to more effectively use limiting growth factors such as SHH. In the parental LNCaP cell line, Perlecan mRNA levels decreased upon serum starvation (Figure B-5A). However, the androgen insensitive C4, C4-2 and C4-2B lines maintained or increased their levels *Perlecan* expression upon serum starvation. Immunoblotting for Perlecan protein confirms these results for the cell lines under normal and serum starvation conditions (Figure B-5B). We then asked if the expression of *Perlecan* in more metastatic lines under poor growth conditions correlated with SHH signaling activity. Real-Time PCR analysis for mRNA expression of *SHH* and the SHH response gene *GLI1* upon starvation (Figure B-5C) demonstrated that while expression of both *SHH* and *GLI1* dropped in the LNCaP cell line, expression of both genes increased in the more tumorigenic and metastatic cell lines. Thus the level of *GLI1* expression correlates with changes in *Perlecan* expression upon serum starvation in the LNCaP series (Figure B-5A). This suggests that tumor cells such as C4, C4- 2 and C4-2B that are capable of forming tumors and/or metastasizing without stromal support maintain a high level of SHH signaling under adverse growth conditions by maintaining high levels of *Perlecan* and *SHH* expression.

## DISCUSSION

### *Perlecan, a candidate oncogene for the CAPB locus*

Using a bioinformatics based approach we identified Perlecan as a candidate oncogene involved in both prostate cancer and glioblastoma multiforme based on its genetic association with the CAPB locus at 1p36. Here we demonstrate Perlecan's expression and functional role in prostate cancer, and link it to the Sonic Hedgehog pathway known to be involved in glial tumorigenesis (Dahmane et al., 2001). Thus from genetic mapping, physiological, and expression data there is evidence to suggest that Perlecan is a strong candidate for the CAPB oncogene. The results of interference with Perlecan function demonstrate that this proteoglycan is required for the growth of prostate cancer cells, extending its previously described roles in melanoma, colon, and lung cancer (Cohen et al., 1994; Nackaerts et al., 1997; Sharma et al., 1998) and emphasizing Perlecan's role in multiple tumor types. Of note, genetic mapping studies have also identified a link between familial melanoma and 1p36, providing another link between Perlecan and tumorigenesis (Greene, 1999).

### *Perlecan's regulation of growth factors and the link to Sonic Hedgehog*

As Perlecan has been shown to bind a variety of growth factors in different tumors, the question as to which growth factor is being modulated in prostate cancer arose. Sonic Hedgehog has been associated with brain tumors and melanomas, two tumors with known genetic links to 1p36, where *Perlecan* is located (Greene, 1999; Janer et al., 2003). Sonic Hedgehog has recently been linked to prostate cancer through a

variety of studies (Datta and Datta, 2006). We have demonstrated an increased frequency of Sonic Hedgehog positivity in prostate cancer tissue microarrays, and that Sonic Hedgehog signaling regulates tumor cell growth in both primary prostate tumor samples and prostate cancer cell lines (Sanchez et al., 2004). High levels of Sonic Hedgehog activity, as monitored by *PTCH1*, *GLI1* or *HIP* expression, are present in all metastatic prostate cancer samples that have been tested (Karhadkar et al., 2004; Sheng et al., 2004). In fact, high levels of *PTCH1* and *HIP* expression correlate with high (8–10) Gleason scores (Sheng et al., 2004)where we have observed *Perlecan* expression. Furthermore, activation of the Sonic Hedgehog pathway by expression of *Gli* in the low metastatic potential rat AT2.1 cell line produced highly metastatic behavior, suggesting that high-level activation of the Sonic Hedgehog pathway determines metastatic behavior (Karhadkar et al., 2004). Finally, Sonic Hedgehog promotes the growth of LNCaP derived xenograft tumors in mice (Fan et al., 2004). We examined the potential of Perlecan to regulate Sonic Hedgehog signaling in tumors. The importance of heparan sulfate proteoglycans for Sonic Hedgehog signaling has been demonstrated in neural development, as mutations in the heparan sulfate binding site on Sonic Hedgehog causes decreased Sonic Hedgehog-driven proliferation (Rubin et al., 2002). In *Drosophila*, mutations in either Perlecan, or heparan sulfate synthesis or modification genes, greatly perturb Hedgehog signaling efficiency by affecting Hedgehog transport and binding (Bellaiche et al., 1998; Bornemann et al., 2004; Datta, 1995; Datta et al., 2006b)]. Here we extend these findings in development to neoplasia by demonstrating that Sonic Hedgehog both co-localizes and directly binds to Perlecan in tumors, and that Sonic

Hedgehog signaling occurs through Perlecan. This links Perlecan to the Sonic Hedgehog-Patched-Gli signaling pathway involved in prostate cancer (Datta and Datta, 2006), where Perlecan acts to modulate the effects of Sonic Hedgehog. As the Sonic Hedgehog signaling pathway has been linked to multiple tumor types including prostate, stomach, brain, and skin tumors (Datta and Datta, 2006) this evidence suggests a more general role for Perlecan in tumor regulation and tumorigenesis. We have surveyed a variety of tumor types and found SHH and Perlecan colocalization in a number of these, such as squamous cell carcinomas and adenocarcinomas of various origins along with tumors deriving from areas of normal *Perlecan* expression such as chondrosarcomas and osteosarcomas (data not shown).

*Perlecan in familial versus sporadic prostate cancers*

We have demonstrated a positive correlation between Perlecan immunostaining and prostate tumors, in particular for high Gleason score tumors (Table B-1). While genetic mapping studies make Perlecan an excellent candidate for the CAPB oncogene, our clinical validation has been performed on prostate samples without information regarding their familial prostate cancer history. Due to the rarity of families with familial brain and prostate tumors, it is most likely that the tumors studied do not represent CAPB kindreds. The suggested role of Perlecan in up-regulating Sonic Hedgehog signaling in sporadic prostate tumors, combined with its association with a prostate cancer genetic susceptibility locus, places Perlecan among a small group of genes with links to both familial and sporadic prostate cancers. This dual placement implies that

Perlecan is part of a common oncogenesis pathway that both familial and sporadic tumors may traverse during oncogenesis. Of note, other members of the Sonic Hedgehog pathway, namely *SU(FU)*, *GLI1* and *SMOH* also map to areas implicated in familial genetic studies (Datta and Datta, 2006)and are up-regulated in studies of sporadic prostate cancer tumors (Karhadkar et al., 2004; Sanchez et al., 2004; Sheng et al., 2004). Thus combining genetic analyses with evaluation of spontaneous tumors may allow us to identify the common pathways for carcinogenesis.

*Perlecan's role in prostate tumor growth: selective growth advantage for aggressive tumor cells under low androgen and/or growth factor conditions*

High levels of Perlecan protein correlate significantly with aggressive, highly proliferating prostate tumors in our tissue microarrays and are also up-regulated in aggressive tumors from individual patients. Yet Perlecan is not present or overexpressed in every tumor or even in every metastatic site of tumor spread. While this result is not surprising considering the heterogeneity of neoplasia, it does suggest that subsets of tumors may utilize Perlecan signaling in specific situations. This correlation is demonstrated in the varied responses of the LNCaP-derived prostate cancer cell lines under poor growth conditions. In these situations *Perlecan* expression is maintained in the C4, C4-2, and C4-2B cell lines capable of forming stromaindependent tumors while the LNCaP parental line requires stromal support to form tumors and cannot maintain the Perlecan specific growth advantage (Wu et al., 1994). This trait suggests a survival benefit to the more tumorigenic and metastatic tumor cells. Under poor growth

conditions where low androgen and growth factor concentrations are present, the increased presence of Perlecan and its ability to concentrate growth factors would provide a survival advantage for tumor cells until a more suitable microenvironment can be found. In fact, our studies show that relative up-regulation of Perlecan expression by the more metastatic lines during serum starvation allowed them to maintain their levels of SHH stimulation, while the relative down-regulation of Perlecan expression in LNCaP resulted in decreased SHH signaling activity. Even under normal growth conditions, the more metastatic cell lines were able to form more Perlecan-SHH complexes and obtain greater SHH stimulation. Thus in the changing tumor microenvironment the more metastatic tumor cells have a choice of pathways (androgen, Perlecan-SHH) that can be modified or modulated to maintain tumor growth. Heparan sulfate proteoglycans such as Perlecan have been shown to bind growth factors and may act as reservoirs or co-receptors for many growth factors (Wu et al., 1994). Thus increasing Perlecan levels under growth factor limiting conditions such as within an inadequately vascularized tumor would be beneficial to a tumor cell. We propose that Perlecan may sustain the growth of nutrient starved prostate cancer cells in rapidly spreading tumors by amplifying their sensitivity and response to SHH signaling. These findings are summarized in a model of Perlecan action (Figure B-6); in microenvironments with decreased growth factors and androgen, such as those encountered by rapidly growing tumors, Perlecan provides a secondary pathway for growth through SHH. This is used in both the androgen responsive and androgen insensitive aggressive tumor cells. Based on this model, one would hypothesize that

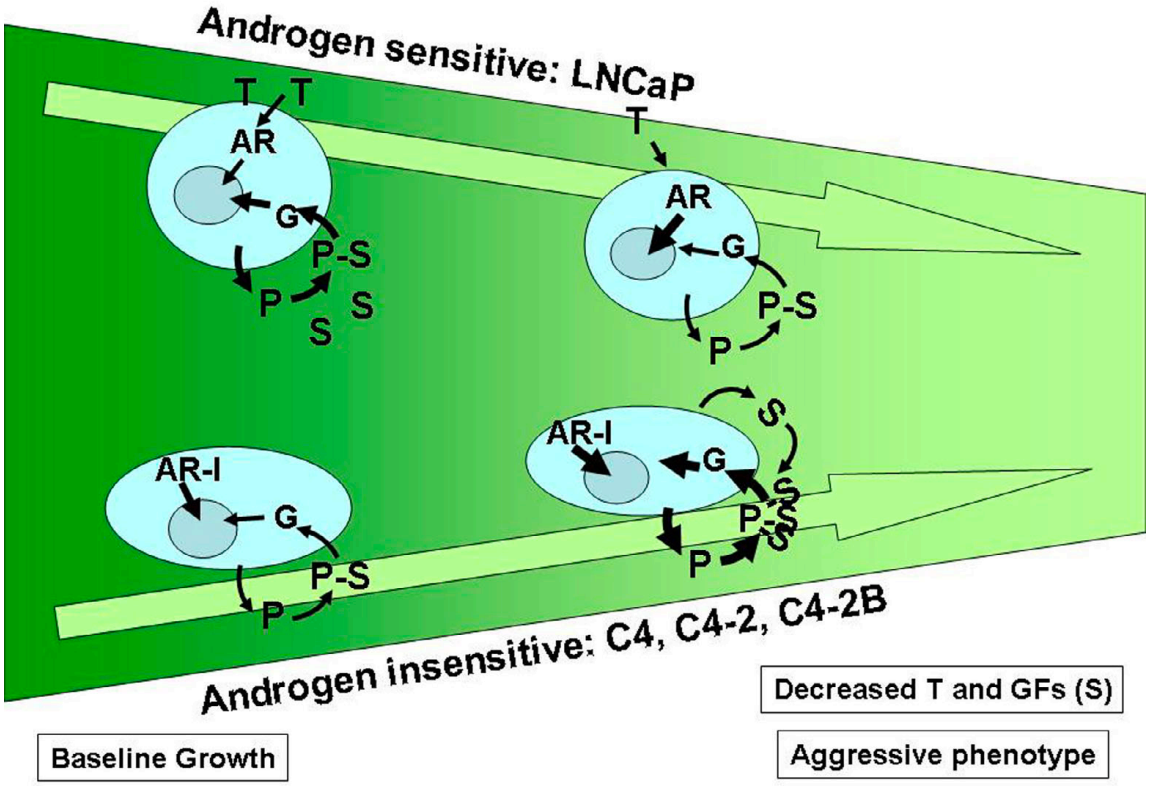


**Figure B-6. Modulation of androgen and Perlecan regulated Sonic Hedgehog signaling.** As changes occur to the tumor microenvironment, prostate cancer cells modulate their use of both androgen and Perlecan mediated Sonic Hedgehog signaling. The use of androgen (T) occurs via the androgen receptor (AR). Perlecan (P) is produced, binds Sonic Hedgehog (S) and signals through the Gli (G) proteins. The heaviness of each arrow indicates relative signaling strength (gene expression, complex formation). Androgen sensitive cells (LNCaP) utilize both androgen and Perlecan-SHH signaling under normal conditions, but decrease Perlecan-SHH signaling under poor growth conditions. In contrast aggressive androgen insensitive cells (C4, C4-2, C4-2B) utilize both pathways, and upregulate the Perlecan-SHH signaling under poor growth conditions. This may occur through increased SHH binding affinity to Perlecan.

chemotherapeutic treatments that simultaneously target both the androgen and the Perlecan-mediated Sonic Hedgehog pathways would provide the best control of androgen sensitive aggressive prostate cancer.

*Perlecan as a global regulator of growth factor action*

While we have demonstrated that Sonic Hedgehog is critical to Perlecan-dependent cancer cell growth, other growth factors may also be regulated through Perlecan at different times or in different clinical stages. Recent results (Savore et al., 2005) suggest that Perlecan may regulate the activity of different growth factors during metastasis to bone. Thus the true role of Perlecan may not be regulating a single growth factor, but its ability to allow the tumor cell to adapt to differing tumor microenvironments by facilitating the signaling of different growth factors. If this is shown to be true, Perlecan may be an excellent target for drug targeting, with tumor specific targeting achieved through the selective blocking of specific growth factor binding sites on Perlecan.

*Perlecan function in metastasis, a role in the bony matrix*

Perlecan is secreted by tumor cells, but is also present in specific stromal microenvironments in the body. This may affect a tumor's propensity to spread to specific sites. We have shown here that prostate cancer maintains Perlecan expression when it spreads to the lung or liver, but is less likely to do this in the soft tissue or lymph nodes. Maintaining or finding "Perlecan rich" sites may explain the propensity of tumors

to home to specific sites during metastatic spread. A specific example of a Perlecan rich site would be the bone extracellular matrix, a major site for prostate cancer metastasis. In these sites Perlecan plays a role in normal bone formation and regulation through the modulation of growth factors utilized by osteoblasts (Hassell et al., 2002; Hecht et al., 2002; van der Horst et al., 2003). Recent studies using the bone-targeted prostate cancer line C4-2B show that Perlecan is required for development of metastases through the modulation of growth factors, and leads to efficient tumor growth and vascularization (Savore et al., 2005). Thus it appears that the presence of Perlecan in the bony matrix may help explain the tropism of prostate cancer to the bony matrix. Use of Perlecan as a drug target may prove advantageous by blocking bone metastasis and its associated morbidity. Lastly, Perlecan, as a secreted protein, may prove to be a useful biomarker for metastatic prostate cancer as well as a marker of either the risk or detection of tumor metastasis to bone since it can be easily detected in urine or serum samples, respectively.

## METHODS

*Bioinformatics based analysis for candidate genes in the CAPB region*

The 1p36 region, as defined by the chromosomal basepair data present in the human genome build 16 from the UCSC Genome Browser datasets, was searched for defined genes as identified in the NCBI LocusLink database. This search identified 5,108 expressed exons comprising 659 identified transcripts and 619 defined genes. Using text mining we searched a dataset of 3,737 prostate cancer genes as defined by co localization of the gene name based on a hand annotated list from LocusLink and the

words "prostate cancer" in MEDLINE. From this dataset 14 genes in the 1p36 region had been described in prostate cancer studies. A second text-mining search we identified 15 genes in the CAPB region that also had been described in studies of the brain. None of the genes in the brain or prostate cancer text mining datasets were common. We then focused our examination on CAPB region genes with associated data in brain studies, and prostate and prostate cancer expression data from the Cancer Genome Anatomy Project (CGAP) along with cDNA microarray expression data generated in our laboratory for the prostate cancer cell lines LNCaP, DU-145, and PC3. A comparison of these datasets revealed three genes, EPHA2, HSGP2, and CAP2B, with data in both brain research studies and expression in the prostate cancer or the precancerous change high grade prostatic intraepithelial neoplasia. Of these three genes, HSPG2 also was contained within our prostate cancer cell line cDNA expression datasets, with increased levels of expression in the derived invasive sublines of PC3 when compared to a derived non-invasive subline.

*Prostate samples and tissue culture*

LNCaP, PC3 and DU-145 cell lines were obtained from ATCC and grown under standard conditions. The LNCaP series LNCaP, C4, C4-2 and C4-2B were obtained from Dr. L. Chung. All primary prostate tumors were obtained by MWD using approved protocols with informed consent on the part of the subjects.

*Real-time PCR on cell line RNA samples*

Total RNA isolated from cell lines using Trizol and then further purified using the RiboPure kit (Ambion). Purified RNA was digested with DNAse (Invitrogen), and analyzed using the SYBER Green system according to manufacturers protocols (Applied Biosystems) on an ABI Prism 7700 machine. Each sample was run in triplicate at three different concentrations. Primers were designed using Primer Express software and are available upon request. Fold increase/decrease comparisons were calculated using the delta-delta Ct method.

*Tissue microarray and immunohistochemistry*

Upon institutional review board approval, a tissue microarray was prepared from 288 radical prostatectomy cases present at the Medical College of Wisconsin. A second tissue microarray was prepared from samples collected under approved protocols at the University of Pittsburgh Medical Center. 0.6 mm cores were arrayed and 5 um sections processed. Benign tissue, high-grade prostatic intraepithelial neoplasia, or invasive tumor tissue were identified by MWD or RD by high molecular weight cytokeratin staining (CK903 Ab, DAKO). A third tissue microarray was prepared from samples collected under approved protocols as part of the rapid autopsy program at the University of Michigan. For microarray samples, a common antigen retrieval procedure was carried out. Slides were processed for Perlecan or SHH and developed with HRP conjugated secondary antibodies and DAB substrate. For a portion of the tissue microarray anonymous de-identified pathologic and outcomes data were available.

Individual cores were examined as duplicates and staining correlated using Chi-squared, Fisher's Exact or two-tailed ANOVA analyses.

*Transfection and proliferation assays*

Purified and desalted siRNAs were purchased from Ambion as a proprietary non-validated *Perlecan* siRNA and a scrambled siRNA control. SiRNA and *GLI1* expression vector transfections were carried out with Lipofectamine 2000 (Invitrogen) as described by the manufacturer and effects measured after 72 hours. Casodex was used in cell cultures as described previously. Immunocytochemistry on cell lines was carried out using with anti-BrdU (Research Diagnostics or Becton-Dickinson) and HRP-conjugated secondary antibodies (Boehringer Mannheim) using standard techniques.

*Protein extracts, Western blotting and immunoprecipitations*

Normal and tumor tissue from the same patients were obtained as described below following approved protocols. Sections were assessed pathologically by a urologic pathologist (MWD) to determine areas of normal and tumor tissue. Samples were microdissected and total protein isolated. Proteins were also isolated from cultured medium from cell lines grown under normal or serum starved conditions. Proteins were run on a 1.6% agarose gel, blotted and probed for Perlecan (Chemicon). Equal samples were loaded onto a standard SDS-PAGE gel, blotted and probed for GAPDH (Santa Cruz) as a loading control. Equal amounts of conditioned medium from equivalently confluent cell lines were immunoprecipitated with an anti- Perlecan or unrelated control

antibody, the resulting complex run on denaturing SDS-PAGE, and the presence of SHH verified by immunoblotting (Santa Cruz).

# VITA

Name: Andrea Lynn Barrett

Address: Department of Biochemistry and Biophysics, c/o Dr. Sumana Datta, Texas A&M University, College Station, TX 77843

Education: Ph.D., Biochemistry, Texas A&M University, College Station, TX 77843, 2007
B.S., Chemistry, Sam Houston State University, Huntsville, TX 77340, 2001

Publication: Datta, M.W., Hernandez, A.M., Schlicht, M.J., Kahler, A.J., DeGueme, A.M., Dhir, R., Shah, R.B., Farach-Carson, C., **Barrett, A.**, and Datta, S. (2006). *Perlecan*, a candidate gene for the CAPB locus, regulates prostate cancer cell growth via the Sonic Hedgehog pathway. *Molecular Cancer* **5**: 9.

Sanchez, P., Hernandez, A.M., Stecca, B., Kahler, A.J., DeGueme, A.M., **Barrett, A.**, Beyna, M., Datta, M.W., Datta, S., and Ruiz i Altaba, A. (2004). Inhibition of prostate cancer proliferation by interference with SONIC HEDGEHOG-GLI1 signaling. *PNAS* **101** (34), 12561-12566.